Aus dem Institut für Transfusionsmedizin und Immunologie
der Medizinischen Fakultät Mannheim
(Direktor: Prof. Dr. med. Harald Klüter)

Analysis of reactions of macrophages to titanium and biodegradable coating materials

Inauguraldissertation
zur Erlangung des Doctor scientiarum humanarum (Dr. sc. hum.)
der
Medizinischen Fakultät Mannheim
der Ruprecht-Karls-Universität
zu
Heidelberg

vorgelegt von
Alexandru Gudima

aus
Chișinău, Republik Moldau
2017

Dekan: Prof. Dr. Sergij Goerdt
Referentin: Prof. Dr. Julia Kzhyshkowska

TABLE OF CONTENTS

ABBREVIATION LIST

°C	degrees centigrade
µg	microgram
µl	microliter
µm	micrometer
µTi	titanium microbeads
AD	anno Domini
ANOVA	analysis of variance
APMA	4-aminophenylmercuric acetate
BC	before Christ
BCC	body-centered cubic
BGD	Brilliant Green dye
BGD1, BGD2, BGD3	PLA films embedded with BGD for 1, 2 and 3 hours respectively
BSA	bovine serum albumin
CAT	catestatin
CCL	chemokine (C-C motif) ligand
CCR	C-C chemokine receptor
CD	cluster of differentiation
CD14	CD14 positive macrophages
cDNA	complementary deoxyribonucleic acid
CHI3L1	chitinase-3-like protein 1
CHIT1	chitotriosidase
COX	cytochrome c oxidase
Cp Ti	commercially pure titanium
CR	complement receptor
Ct	threshold cycle
CXCL	C-X-C motif chemokine ligand
DAMP	damage-associated molecular pattern
ddH$_2$O	double distilled water
DEPC	diethyl pyrocarbonate
DMSO	dimethylsulfoxide
DNA	deoxyribonucleic acid
dNTPs	deoxyribonucleotides
EDTA	ethylene diamine tetra acetic acid
EGF	epidermal growth factor
ELISA	enzyme-linked immunosorbent assay
EM	emission
EMEM	Eagle's minimal essential medium
EU	European Union
EX	excitation
FACS	fluorescent activated cell sorting
Fc	fragment crystallisable
FCS	fetal calf serum
FcγR	Fc gamma receptor
FDR	false discovery rate
FPR	N-formyl peptide receptor
g	gram / relative centrifugal force
GAPDH	glyceraldehyde 3-phosphate dehydrogenase
GM-CSF	granulocyte-macrophage colony-stimulating factor
GPa	gigapascal
h	hour(s)
HA	hydroxyapatite
HA	hyaluronic acid
HCP	hexagonal close-packed
HMGB1	high mobility group box 1 protein
HRP	horseradish peroxidase
HSP	heat shock protein
IFNγ	interferon gamma

IgG	immunoglobulin G
IL	interleukin
IL-1Ra	Interleukin 1 receptor antagonist
iNOS	inducible nitric oxide synthase
JMFI	juxtacrine macrophage-fibroblast interaction
L	liter
LIF	leukemia inhibitory factor
LPS	lipopolysaccharide
LTA	lymphotoxin-alpha
M	molar concentration
M(Control)	non-stimulated macrophages
M(IFNγ)	macrophages activated with IFNγ
M(IL-4)	macrophages activated with IL-4
M1	classically activated macrophages
M2	alternatively activated macrophages
MACS	magnetic-activated cell sorting
MARCO	macrophage receptor with collagenous structure
M-CSF	macrophage colony-stimulating factor
MIF	macrophage migration inhibitory factor
min	minute(s)
ml	milliliter
mM	millimolar concentration
mm	millimeter
MMP	matrix metalloproteinase
MPa	megapascal
MRI	magnetic resonance imaging
mRNA	messenger RNA
N	equivalent concentration
NF-κB	nuclear factor kappa-light-chain-enhancer of activated B cells
ng	nanogram
NLRP3	NLR family pyrin domain containing 3
nm	nanometer
nTi	titanium nanoparticles
OPG	osteoprotegerin
PAR	polyarginine
PAR/HA	polyarginine-hyaluronic acid based coating
PBMC	peripheral blood mononuclear cell
PBMC-CD14	PMBC depleted of the CD14 positive monocytes
PBS	phosphate buffered saline
PCR	polymerase chain reaction
PDGF	platelet-derived growth factor
PEG	poly(ethylene-glycol)
PELA	ethylene oxide/lactic acid copolymer
PET	polyethylene terephthalate
PFA	paraformaldehyde
pg	picogram
PGE	prostaglandin E
PITPNM3	phosphatidylinositol transfer protein family member-associated 3
PLA	polylactic acid
PLGA	poly(lactide-co-glycolide)
PMFI	paracrine macrophage-fibroblast interaction
PMMA	polymethylmethacrylate
pmol	picomolar
PRR	pattern-recognition receptor
psi	pound per square inch
PVA	poly(vinyl-alcohol)
RANK	receptor activator of nuclear factor kappa B
RANKL	receptor activator of nuclear factor kappa-B ligand
RBC	red blood cells
RMA	Robust Multi-Array Average
RNA	ribonucleic acid
RNS	reactive nitrogen species

ROS	reactive oxygen species
rpm	revolutions per minute
RT	room temperature
RT-qPCR	reverse transcription real-time polymerase chain reaction
s	second(s)
SA	heat killed Staphylococcus aureus
SR	scavenger receptor
Std	standard
TAE	tris/Acetate/EDTA-buffer
TGF	transforming growth factor
TGFβR1	transforming growth factor, beta receptor I
TLR	toll-like receptor
TNFRSF	tumor necrosis factor receptor superfamily, member
TNFSF	tumor necrosis factor (ligand) superfamily, member
TNFα	tumor necrosis factor alpha
TRADD	tumor necrosis factor receptor type 1-associated DEATH domain protein
TRAP	tartrate-resistant acid phosphatase
U	conventional units
UHMWPE	ultra-high-molecular-weight polyethylene
UV	ultraviolet
V	volt(s)
VBA	Visual Basic for Applications
vs	versus
wt%	percentage by mass

1 INTRODUCTION

1.1 Implants and medical devices

Medical devices, prosthesis and implants were used in medicine since the dawn of civilization. The earliest records of medical tools describe the usage of flint scrapers and borers for trepanation as early as during the Neolithic age. Starting from the bronze age and during the Classical age the use of knives, needles, toothed forceps, bone elevators, dilators and other surgical instruments made of bronze and iron are described[1]. Early mentions of prosthesis can be found in the Vedas (between 3500 and 1800 BC) where a prosthetic iron leg was made for the Warrior-Queen Vishpla. There is also evidence of prosthetic use in ancient Egypt. A toe from an Egyptian mummy displayed in Cairo museum was replaced by a prosthesis made of wood and leather (circa 1500 BC)[2]. Ancient Egyptians are also known to employ gold wires for the stabilization of periodontally involved teeth (circa 2500 BC). Later, Etruscans developed teeth replacements from oxen bones, while Phoenicians carved teeth out of ivory and utilized gold wires to stabilize them and create a fixed bridge. Mayans are credited with the use of first dental implants which were made from shells to replace mandibular teeth (circa 600 AD)[3].

It is only natural that throughout the ages, in line with advances in technology, medical devices greatly evolved. From simple metal scalpels to μm precise laser scalpels, medical devices have seen great progress during the ages and therefore the definition of medical device also changed. Modern definitions of medical devices and implants are presented below.

Directive 2007/47/EC of the European Union defines a ***medical device*** as any instrument, apparatus, appliance, software, material or other article used for the purpose of:
- diagnosis, prevention, monitoring, treatment or alleviation of disease;
- diagnosis, monitoring, treatment, alleviation of or compensation for an injury or handicap;
- investigation, replacement or modification of the anatomy or of a physiological process;
- control of conception;

and which does not achieve its principal intended action in or on the human body by pharmacological, immunological or metabolic means, but which may be assisted in its function by such means[4].

Implants (implantable devices) are medical devices intended:
- to be partially or totally introduced in the human body by surgical intervention;
- to replace an epithelial surface or the surface of the eye;

and are intended (expected) to remain in place for at least 30 days after the procedure (Annex 9 directive 93/42/EEC)[5].

Nowadays millions of patients around the world improve their quality of life with the help of implants. In 2011, in the European Union alone, there were more than 44 million people with disabilities registered[6]. Some of them are able to restore the function of the disabled organs with implants. Surgeries for hip or knee replacement are very effective in relieving pain and restoring walking function, while cochlear implants greatly improve the hearing ability. For 2014, there were more than 1.5 million such procedures reported by European Union member states. Table 1 provides an overview

of surgeries related to hip or knee replacement and cochlear implantation performed by each member of the European Union[7].

Table 1. Number of surgeries performed for hip or knee replacement and cochlear implantation by the members of the European Union in 2014. (Data for Belgium, Bulgaria, Greece, Latvia and Netherlands are missing)

European Union member	Cochlear Implantation	Hip Replacement	Secondary Hip Replacement	Total Knee Replacement
Austria	336	23822	1781	18881
Croatia	85	6291	662	2355
Cyprus	10	412	5	380
Czech Republic		18425		12698
Denmark	304	13214	1431	9709
Estonia		1450		
Finland	151	13360	1921	10436
France	1461	158134	17310	103302
Germany	3805	237067	24682	159686
Hungary	175	12581	1089	7015
Ireland	143	5781	565	2107
Italy		101510	33446	65279
Lithuania	21	4718	364	2193
Luxembourg		1053	106	895
Malta	11	326	12	636
Poland	563	37152	1133	11780
Portugal		9101	4256	6111
Romania	110	12853	953	4604
Slovakia		6737	507	5456
Slovenia	30	3407	320	2178
Spain	895	51849	5572	56364
Sweden	353	22725	1886	12685
United Kingdom	1294	119802	9395	95909
Total	9747	861770	107396	590659

Implants are used to restore many other functions as well. From dental implants that help with mastication to cardiac pacemakers that preserve life, implants can be used in virtually all body organs to improve or restore their function. As implants come in direct contact with body tissues the study of implant-tissue interaction from an immunological point of view is of great importance and will constitute the main focus of this study.

1.1.1 Classification of medical devices and implants

The European Union recommends a classification of medical devices according to their safety and purpose. The medical devices are divided in 4 classes (I, IIa, IIb and III) with the low risk devices being included in class I and high risk devices in class III. Classification is done according to the rules listed in Directive 93/42/EEC (Annex IX) which take into account the degree of invasiveness, duration of contact with the body, the ability to biologically or chemically modify body liquids, etc[5]. Table 2 presents the classification of medical devices according to the EU directive with some examples[8].

Table 2. Classification of medical devices according to The Directive 93/42/EEC. Adapted from Journal of the Royal Society of Medicine, volume 105, Suppl 1:S22-8, Elaine French-Mowat, Joanne Burnett, How are medical devices regulated in the European Union?, Copyright (2012), with permission from SAGE publishing.

Class	Associated risk	Description	Examples
I *Is (sterile)* *Im (measuring)*	low	Most non-invasive devices	hospital beds, sterile plasters, bandaging, thermometers,
IIa	medium	Exchange energy with a patient in a non-hazardous way. Invasive but limited to natural orifices	hearing aids, ultrasonic diagnostic devices, tooth crowns, contact lenses,
IIb	medium	Exchange energy with a patient in a potential hazardous way. Invasive devices partially or totally implanted in the body.	infusion pumps, surgical lasers, defibrillators, dialysis devices, dental implants
III	high	Support and sustain human life. Connects directly to the central nervous system or to the central circulatory system	heart catheters, heart valves, endoprosthesis, breast implants, implanted cerebella stimulators

According to this classification implants fall under the classes IIb and III, because they present a medium to high risk for the health of patients. Implants can be further classified according to the medical field in which they are used: orthopedic, cardiovascular, neurological and sensory, respiratory, gastrointestinal, urogenital and cosmetic implants. Table 3 gives an overview of this classification and provides some examples[9-14].

Table 3. Classification of Implants according to the field of use.

Medical Field	Examples	
Orthopedic	Knee replacements Hip replacements Elbow implants Shoulder implants Ankle implants	Thoracolumbar implants Intervertebral spacers Implantable spinal stimulators Internal fixation devices Craniomaxillofacial implants
Cardiovascular	Implantable cardioverter-defibrillators Cardiac pacemakers Coronary stents	Tissue heart valves Ventricular assist devices Implantable heart monitors
Neurological and sensory	Neurostimulators Intraocular lenses Glaucoma and other lenses	Tympanostomy tube Cochlear implants
Respiratory	Artificial larynx Artificial trachea	Diaphragm implants
Gastrointestinal	LINX Reflux Management System Gastric bands	Gastric electrical stimulators Biliary stents
Urogenital	Soft tissue repair Intrauterine devices	Penile implants Artificial urinary sphincter
Cosmetic	Dental implants Breast implants Nose prosthesis	Soft tissue fillers Gluteal implants
Other	Hormonal implants Implantable drug pumps	Brachytherapy products

1.1.2 Types of implant materials

One of the most important decisions made during the design of an implant is the choice of its material. First of all, it has to be biocompatible, meaning that it performs with an appropriate host response in a specific application[15]. Since materials have different properties, the same material cannot be used for all applications. Mechanical properties (hardness, elasticity, brittleness, malleability, etc.) are one of the most important factors taken into account when selecting the implant material. Strong mechanical properties of metals make them ideal for the use in orthopedics where strength and stiffness are needed for the replacement of hard tissue, while the flexibility of polyesters make them ideal for artificial vascular graft, sutures and meshes[11]. Other properties that influence the selection of the implant material are biodegradability, ease of fabrication, conductibility (electrical, light, sound), thermal properties, surface properties and adhesion, resistance to corrosion, shelf life and price[11, 14, 16].

Currently there are numerous types of different materials used for fabrication of implants. They can all be grouped in 5 classes: metals, ceramics, polymers, composite and biologic materials[11, 17]. Each class has its advantages and disadvantages which also play a role in their selection for a specific application. For example, metals are strong, tough, possess electrical conductivity and are ductile, making them suitable for joint replacement, bone screws and plates, pacers and wires. Their drawback is that they are dense, may corrode and are difficult to make. Ceramics are very biocompatible, but also brittle, weak in tension and not resilient. They are mostly used in dental and orthopedic implants. Polymers are resilient and easy to fabricate and are used for sutures, blood vessels, ear and nose implants. Their disadvantage is that they deform with time, are not strong and may degrade. Composites are strong and can be tailor-made, but are difficult to produce. They are used in bone cement and dental resins[14]. Table 4 illustrates the 5 classes of materials along with some examples from each class[9, 11, 14, 16, 17].

Table 4. Types of implant materials. (PMMA, polymethylmethacrylate; HA, hydroxyapatite; UHMWPE, ultra-high-molecular-weight polyethylene; PELA, ethylene oxide/lactic acid copolymer).

| Class	Subclass	Examples	
Metals		Stainless Steel Co-Cr alloys Ti and Ti alloys Commercially pure Ta	Gold Dental amalgam Platinum group (Pt, Pd, Rh, Ir, Ru, and Os)
Ceramics	*Non-absorbable*	Alumina (Al_2O_3) Zirconia (ZrO_2)	Carbons
	Biodegradable	Calcium Phosphate Coralline Tricalcium Phosphate	Aluminium-Calcium-Phosphate Ferric–Calcium–Phosphorous-Oxide Ceramics
	Bioactive	Bioactive glasses	Ceravital
Polymers	*Non-absorbable*	Polyethylene Polypropylene Polyamides Polyurethanes	Polymethylmethacrylate Polyesters Silicone Cyanoacrylates
	Biodegradable	Polyglycolic acid (PGA) Polydioxanone	Polylactic acid (PLA) Poly(Lactide-co-Glycolide)(PLGA)
Composite materials	*Particulate*	Dental composite resins Polyethylene/HA	PMMA/HA Starch/HA
	Fibrous	Graphite-epoxy PELA /Polyurethane	Carbon fiber reinforced UHMWPE PMMA/UHMWPE
Biologic materials		Collagen Silk	AlloDerm

1.2 Titanium as an implantable material

Titanium (Ti) is a widely used material in implantation, either in pure form or in the form of alloys. It is a member of transition metals and is located in the 4th period and the 4th group of the periodic table of elements. Titanium is the ninth most abundant element in the earth's crust and can be found in nature within a number of minerals, the most common being ilmenite ($FeTiO_3$), which has black or brownish-black opaque crystals, and rutile (TiO_2), which can be reddish-brown, red, yellow, or black in color. Titanium has an atomic number of 22 and its electron configuration is $[Ar]3d^24s^2$. There are 5 naturally occurring isotopes of titanium, ^{46}Ti (8.25%), ^{47}Ti (7.44%), ^{48}Ti (73.72%), ^{49}Ti (5.41%) and ^{50}Ti (5,18%) and it exists in 2 allotropic states (α and β)[18, 19].

Titanium exists mostly in the "+4" oxidation state and exhibits limited reactivity in "+2" and "+3" oxidation states. It has high affinity for oxygen and depending on the oxidation state forms the following oxides TiO, Ti_2O_3 and TiO_2. Additionally, in the "+2" oxidation state titanium forms titanium dichloride ($TiCl_2$), while in the "+3" oxidation state it forms titanous trichloride ($TiCl_3$), titanous hydroxide ($Ti[OH]_3$) and can also exist as the titanous ion (Ti^{3+}) [19, 20].

TiO_2 is the most common oxide of titanium. In nature it is usually found in the form of rutile, but can also exist in 2 other polymorphs: anatase and brookite[19, 21]. Although both anatase and rutile have tetragonal structures, formed by chains of distorted TiO_6 octahedra, their structure is slightly different. In anatase each octahedron is in contact with 8 neighbor octahedrons, while in rutile each octahedron is in contact with 10 neighbors[22]. TiO_2 is white and has been extensively used in cosmetic and painting industries[23, 24]. Due to its excellent photocatalytic properties, it has also been used for hydrogen production under UV and water clean-up procedures where halogens and hydrocarbon contamination is found[25-27].

Titanium's low density (4.506 g/cm^3) together with low thermal conductivity and structural stability at high temperatures has made it ideal for aerospace industry. Combined with steel it is used to make strong alloys, which are lighter and also corrosion resistant[28]. At high temperatures, exceeding 883°C, titanium undergoes an allotropic transformation from α state to β. In α state its structure is hexagonal close-packed (HCP), whereas in β state it is transformed into a body-centered cubic (BCC) crystal structure (Figure 1)[19, 29].

hexagonal close-packed (hcp)   body-centered cubic (bcc)
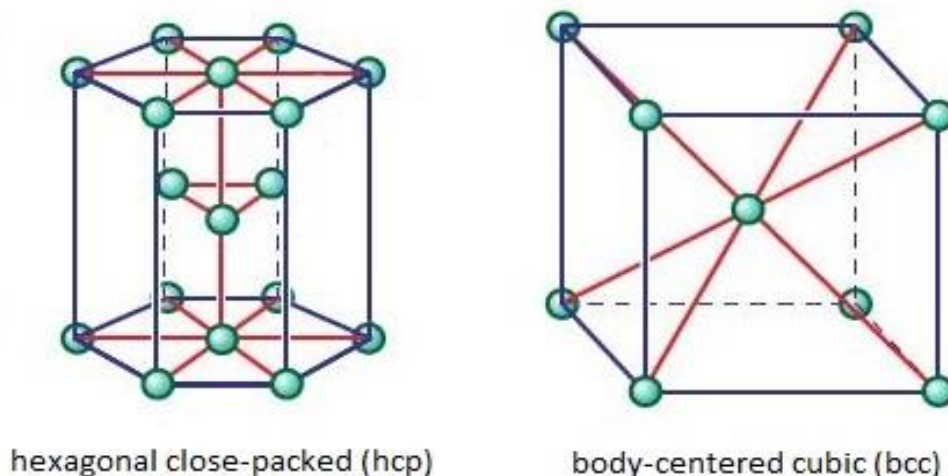
© 2011 Encyclopædia Britannica, Inc.

Figure 1. Allotropic states of titanium. Crystal structure of α state (left) and β state (right) of titanium. Adapted with permission from (Encyclopedia Britannica, 2011), Copyright Encyclopedia Britannica Inc.

Each state has its advantages and disadvantages and alloys are made taking into account their physical properties. To preserve the good weldability of α state, elements that raise the α to β transition temperature (α stabilizers), are added during alloy fabrication. These are aluminum, oxygen, gallium, germanium, calcium, and nitrogen. On the other hand, β stabilizers, like vanadium and molybdenum, lower the α to β transition temperature, in this way preserving its superior strength. Some alloys are fabricated with a combination of α and β stabilizers, thus obtaining a material with mixed properties. In this context titanium alloys are divided into 4 classes: α, near α, α–β and β alloys[9, 11, 14, 19].

1.2.1 Mechanical properties of titanium and titanium alloys

Currently there are a number of titanium alloys specifically made for biomedical applications. For dental implants 5 grades of titanium and titanium alloys are being used. Grades 1-4 are unalloyed and are made of commercially pure titanium (Cp Ti) with traces of nitrogen (0.03-0.05%), carbon (0.1%), hydrogen (0.015%), iron (0.2-0.5%) and oxygen (0.18-0.4%). Variation in these elemental compositions confers different properties to the titanium implant. The strength of the material increases with its grade, whereas elongation (change in physical shape without breaking) decreases[14, 30].

Grade 5 (Ti-6Al-4V) is an α–β alloy with 6% aluminum (α stabilizer) and 4% vanadium (β stabilizer) and is one of the most used titanium alloys in biomedical applications. Higher strength compared to Cp Ti has made Ti-6Al-4V the material of choice for applications such as total joint replacement, where superior mechanical properties are needed[31]. When compared to other materials like 316 stainless steel or Co-based alloys, Ti-6Al-4V possesses higher specific strength (tensile strength per density). However, due to poor shear strength it is not suitable for bone screws or plates[11, 14].

Although Ti-6Al-4V is the most used biomedical titanium alloy, its mechanical properties for long-term orthopedic implants are still not ideal. The elastic modulus of human cortical bones and cancellous bones are 4-30GPa and 0.2-2GPa respectively. In comparison to bones, metallic implants have a much higher elastic modulus which can result in bone resorption in the connection part[32]. The big difference between elastic modulus of bones and implants has been shown to result in stress shielding of human bones[33]. This phenomenon is characterized by reabsorption of bone tissue, due to the distribution of the load stress to the implant[34]. When elastic modulus is considered, Ti-6Al-4V (110GPa) is superior to its metallic counterparts, like 316 stainless steel (210GPa) or Co-Cr (240GPa) alloys, however it is still higher than that of human bones[35]. For this reason, other titanium alloys with lower elastic modulus are being developed. In this aspect, of particular interest are β alloys, since BCC crystal structure has a lower elastic modulus than HCP crystal structure. Titanium alloys containing niobium (Nb), zirconium (Zr), molybdenum (Mo) and tantalum (Ta) have been extensively studied in recent years. Additionally, low cost elements such as iron (Fe), chromium (Cr), manganese (Mn) and tin (Sn) are also used to reduce the cost of alloy making. Table 5 gives an overview of mechanical properties of titanium and its alloys designed for biomedical applications[32].

Table 5. Mechanical properties of titanium and its alloys designed for biomedical applications. Adapted from Materials, volume 7, Li et al., New Developments of Ti-Based Alloys for Biomedical Applications, distributed under the Creative Commons Attribution License (CC BY 3.0).

Alloy Designation (wt%)	Tensile Strength (MPa)	Yield Strength (MPa)	Elongation (%)	Elastic Modulus (GPa)
α-type				
CP Ti grade 1 (annealed)	240	170	24	102.7
CP Ti grade 2 (annealed)	345	275	20	102.7
CP Ti grade 3 (annealed)	450	380	18	103.4
CP Ti grade 4 (annealed)	550	485	15	104.1
α+β-type				
Ti-6Al-4V ELI (annealed)	860–965	795–875	10–15	101–110
Ti-6Al-4V (annealed)	895–930	825–869	6–10	110–114
Ti-6Al-7Nb (wrought)	900–1050	880–950	8.1–15	114
Ti-5Al-2.5Fe (cast)	1020	895	15	112
β-type				
Ti-13Nb-13Zr (aged)	973–1037	836–908	10–16	79–84
Ti-12Mo-6Zr-2Fe (annealed)	1060–1100	1000–1060	18–22	74–85
Ti-15Mo (annealed)	874	544	21	78
Ti-15Mo-5Zr-3Al (solution treated/aged)	852–1100	838–1060	18–25	80
Ti-35Nb-7Zr-5Ta (annealed)	597	547	19	55
Ti-16Nb-10Hf (aged)	851	736	10	81
Ti-29Nb-13Ta-4.6Zr (aged)	911	864	13.2	80
Ti-15Mo-2.8Nb-0.2Si (annealed)	979–999	945–987	16–18	83
Ti-24Nb-4Zr-7.9Sn (hot-rolled)	830	700	15	46
Ti-24Nb-4Zr-7.9Sn (hot-forged)	755	570	13	55
Ti-24Nb-4Zr-7.9Sn (selective laser melting)	665	563	14	53
Ti-35Nb-7Zr-5Ta-0.4O (annealed)	1010	976	19	66
Ti$_{65.5}$Nb$_{22.3}$Zr$_{4.6}$Ta$_{1.6}$Fe$_6$ (sintering/960 °C/0 min)	–	2425	6.91	52

In clinical settings, surgeons have been raising concerns regarding springback (capacity of an elastic material to return to its original form) from materials with a low elastic modulus. On the other hand, patients need materials with low elastic modulus in order to avoid stress shielding. For this reason, titanium alloys with self-adjusting elastic modulus are being developed[36]. Although there is a tendency to make the implant as close as possible to its natural counterpart, it should be taken into account that natural tissue has the advantage of adaptability to new conditions, a quality that no artificial implant possesses[14].

1.2.2 Biomedical applications of titanium

One of the reasons for choosing titanium over other metals for implants is its biocompatibility. Titanium has the ability to form, spontaneously in contact with air, an ultrathin (10nm) film of TiO_2 on its surface in a process called passivation. Therefore, at the implant-tissue interface the material which comes into contact with cells is usually TiO_2. The TiO_2 layer is self-adherent and very stable providing titanium with corrosion resistance[11]. Additionally, it is biopassive, meaning it does not readily react with body fluids and their components. However, when titanium alloys are used for implantation, other oxides also form. In the most used titanium alloy, Ti-6Al-4V, the

stable oxides formed are TiO_2, Al_2O_3, V_2O_5 and V_2O_4. While TiO_2 exhibits inertness, Al_2O_3, V_2O_5 and V_2O_4 display toxicity and can lead to necrosis around the implant[37]. For this reason, there is a need to design new titanium alloys and the biocompatibility of the introduced elements has to be considered. It has been shown that elements such as Nb, Ta, Zr, Si, Mo, Sn, Pd, In, Sr, B, Ca, and Mg do not exhibit cytotoxicity, while elements such as Be, Al, V, Cr, Mn, Fe, Co, Ni, Cu, Zn, and Ag possess cytotoxic effects and therefore should not be used in titanium alloy fabrication for biomedical applications[38].

Although nickel displays some cytotoxic effects it has been alloyed with titanium and successfully used for biomedical applications for a long time. TiNi alloys possess unusual properties: if the material is plastically deformed, it can revert to its initial shape upon increase in temperature. This effect is called the shape memory effect. The TiNi alloy used in biomedical applications is commercially known as Nitinol and displays the shape memory effect near room temperature. Such properties are useful in applications like orthodontic archwires, aneurism clips, vascular stents and vena cava filters[11].

Titanium's low magnetic susceptibility is another rationale for using it in biomedical applications. Since magnetic resonance imaging (MRI) has become an indispensable diagnostic tool in recent years, it is necessary to choose an implant material that produces smaller artifacts on MRI images. In this regard, titanium is superior to stainless steel, having a smaller magnetic susceptibility by an order of magnitude (2.3×10^{-4} and 3.0×10^{-3} respectively). In spinal surgery, where the position of the implant has to be adjusted in relation to the bones and adjacent soft tissues, and where MRI images are used for follow up, titanium is the material of choice[37].

The first records of the use of titanium in implantation came in the late 1930s, describing good tolerability of titanium in animal models[14]. Nowadays titanium is used in a variety of biomedical applications, ranging from cosmetic applications like dental implants to life-saving applications like cardiovascular stents. Commercially pure titanium, due to its corrosion resistance and biocompatibility, has been used in dental implants, maxillofacial and craniofacial implants, screws and staples for spinal injury, pacemaker cases, housings for ventricular assist devices and implantable infusion drug pumps. In applications where higher strength is needed, titanium alloys are used. These include femoral hip stems, fracture fixation plates, spinal components, fasteners and intramedullary nails. An overview of titanium and its alloys use in biomedical application is presented in Table 6 [9, 13, 30, 31, 37, 39-41].

Table 6. Uses of titanium and its alloys in biomedical application.

Medical Field	Examples	
Orthopedic implants	Femoral hip stems	Spinal components
	Metal backed acetabular shell	Intramedullary nails
	Fracture fixation screws and plates	Maxillofacial implants
Cardiovascular implants	Prosthetic heart valves	Annuloplasty ring
	Pacemakers and defibrillators	Left Ventricular Assist Devices
	Vascular access port	Vascular stents
	Vena cava filters	Vessel clips
Dental applications	Dental implants	Dental cast metal framework
	Zygomatic implants	Titanium copings
	Brackets	Orthodontic archwires
Neurological and sensory implants	Bone-anchored hearing device	
	Neurostimulators	
Respiratory implants	Artificial larynx	
	Nasal septal reparation	
Gastrointestinal implants	LINX Reflux Management System	
Other implants	Implantable infusion drug pumps	

1.3 Foreign body reaction

Nowadays many medical conditions can be solved with the help of implants and biomedical devices. Although the materials for implant manufacturing are chosen to be highly biocompatible, still, occasionally adverse immune reactions to implant materials occur. These can result in excessive inflammation at the implant-tissue interface, generate pain and sometimes even implant rejection. Consequently, this leads to an additional surgery procedure, higher costs and deteriorated quality of life[42]. The recognition of the implanted materials by immune cells is part of the foreign body reaction mechanism.

Mosby's medical dictionary defines foreign bodies as any object or substance that is introduced from outside in any organ or tissue in which it does not belong under normal circumstances[43]. There are two ways through which foreign bodies can be introduced in the organism, either through body's natural orifices (mouth, nostrils, ear canals, etc.) or by penetrating the skin. By far the most common way of introduction of foreign bodies in the organism is through ingestion. They do not always have negative effects, as food can also be considered to be a foreign body. In 80% of cases of foreign body ingestion children up to the age of 6 are involved. The most common ingested objects are coins and batteries. In older children and adults, food boluses are the most frequent foreign bodies retained in the gastrointestinal tract. In adults this usually happens in context of underlying pathologies such as strictures, malignancy, esophageal rings or achalasia. However, up to 80% of cases of foreign body ingestion do not require any medical intervention[44, 45].

Implants and biomedical devices are inserted into the body through medical procedures, and usually need to pass through the skin. In this case the body's first barrier of defense against foreign bodies is penetrated. There are also other defense mechanisms against foreign bodies such as cilia in the respiratory epithelium, peristalsis in the gastrointestinal tract, tears or cerumen. When these defense barriers are breached the body's immune system is involved and inflammation is initiated[45]. From this point, there are three scenarios that can develop: i) failure to resolve the acute phase of inflammation can lead to chronic inflammation and peri-implantitis; ii) if the healing process successfully resolves the inflammation, homeostasis is achieved; iii) a pathological healing process can lead to encapsulation and fibrosis. Therefore, in order to obtain homeostasis, a balance needs to be reached between inflammatory and healing processes[42, 46].

1.3.1 Macrophages as main regulators of the foreign body reaction

The primary role in initiating and regulating the foreign body reaction is attributed to macrophages. They are the cells responsible for the recognition and phagocytosis of the foreign body as well as for the initiation of the inflammatory reaction associated with it[45]. Moreover, due to their high level of plasticity, macrophages are able to also start the repair and healing process which can lead to the reinstatement of homeostasis[46]. For these reasons, in recent years a lot of attention has been paid to macrophages in terms of their interaction with biomaterials and numerous studies have used macrophages as models for assessing the biocompatibility of biomaterials[47].

Macrophages are cells of the immune system present in virtually all tissues. They originate from three sources: embryonic yolk sac, fetal liver monocytes, and adult bone marrow-derived monocytes. In different tissues they originate from different main sources: in brain from yolk sac, in liver and lung from fetal liver monocytes, while in the skin, heart and gut from adult bone marrow-derived monocytes. Macrophage origin

and localization plays an important role in their response to stress signals. Tissue-specific environmental cues as well as ontogeny related signals influence macrophage activation. Thus the same activation signal can result in different outcomes in macrophages from distinct tissues and ontogeny[48].

An important aspect of macrophage physiology is their plasticity. Depending on the environmental cues macrophage can adopt different phenotypes and consequently secrete a distinct set of cytokines. For a long time, macrophage activation model depicted two groups of macrophages: classically activated macrophages and alternatively activated macrophages. Classically activated macrophages, also called M1, are known to be activated by IFNγ or TLR ligands and exert a pro-inflammatory function by secreting pro-inflammatory cytokines such as TNFα, IL-1β, IL-6, and IL-12. Alternatively activated macrophages, or M2 macrophages, are induced by IL-4, IL-13, immune complexes in combination with IL-1β or LPS, IL-10, TGFβ or glucocorticoids. They play a role in resolution of the inflammation and wound healing and secrete anti-inflammatory cytokines such as IL-1Ra, IL-10 and TGFβ. Alternatively activated macrophages were further subdivided into 3 subsets: M2a (activated by IL-4 or IL-13), M2b (by ligation of Fc receptors in combination with IL-1β or LPS) and M2c (induced by IL-10, TGFβ or glucocorticoids)[49]. Additionally, studies have shown that activated macrophages, upon a change in environmental signals, can undergo a transformation into the opposite phenotype from M1→M2 and vice versa, hence the term plasticity[50]. However, recent studies, based on transcriptional profiling, suggest that macrophage physiology is much more complex, with experts in the field distancing themselves from the M1/M2 dichotomy as the new macrophage activation model is presented as a spectrum of activation states[51, 52].

Studies regarding implants show macrophages skewed towards a pro-inflammatory state. As implantation is associated with a local injury caused by surgery, the release of damage-associated molecular patterns (DAMPs) will activate macrophages along with the activation of blood coagulation cascades and complement system. When a foreign body enters the organism macrophages are able to directly recognize it or to recognize the adsorbed protein layer on its surface. The protein layer is usually composed of extracellular matrix proteins, albumins, immunoglobulins and components of the complement system. Macrophages are able to recognize them via pattern-recognition receptors (PRRs) and opsonic receptors initiating an inflammatory reaction[45, 53]. A list of receptors and their ligands involved in recognition of biomaterials and the adsorbed protein layer is presented in Table 7.

Table 7. Macrophage receptors involved in foreign body recognition. Adapted from Vrana et al., Cell and Material Interface: Advances in Tissue Engineering, Biosensor, Implant, and Imaging Technologies, Copyright (2015), with permission from CRC Press.

Receptor	Ligand
FcγRI (CD64)	IgG1, IgG3, IgG4
FcγRIIa (CD32a)	IgG3, IgG1, IgG2
FcγRIIc (CD32c)	IgG
FcγRIIIa (CD16a)	IgG
CR1 (CD35)	Mannan-binding lectin, C1q, C4b, C3b
CR3 (αMβ2, CD11b/CD18, Mac-1)	iC3b
CR4 (αXβ2, CD11c/CD18)	iC3b
α5β1	Fibronectin, Vitronectin
αvβ3	Vitronectin
αvβ5	Vitronectin
TLR1/2	Gram-positive bacteria, HSP60, HSP70, HMGB1
TLR4	LPS, HSP60, HSP70, HMGB1, fibronectin EDA, fibrinogen
SR-AI/II	TiO2 particles
MARCO	TiO2 particles, silica

If the initial inflammation is resolved, implantation is considered successful and the implant can stay in place for years. However, with time, due to long-term mechanical stress (material fatigue), wear particles (microscopic wear debris) are released at the implant-tissue interface. These particles induce activation of macrophages either via recognition through the aforementioned receptors or via phagocytosis[42]. This is characterized by activation of several signaling pathways in macrophages, most notably NF-κB[54]. As a result, macrophages release a range of pro-inflammatory cytokines and growth factors such as TNFα, IL-1α, IL-1β, IL-6, IL-8, IL-11, IL-15, TGFα, GM-CSF, M-CSF, PDGF and EGF[55]. The pro-inflammatory environment promotes osteoclast formation via RANKL/RANK/OPG pathway, thus inducing osteolysis[56].

The size of the wear particles also plays a role in macrophage response to them. If the particle size is bigger than 10μm, macrophages are unable to engulf them. However, in certain conditions, in the presence of soluble factors such as IL-4, CCL2, fibronectin and osteopontin macrophages can fuse together to form foreign body giant cells. These cells are able to engulf particles bigger than 10μm and also take part in the phenomenon of frustrated phagocytosis, which is characterized by a release of a wide array of mediators of degradation that can ultimately lead to device failure. Furthermore, macrophages recruit additional immune cells to the periprosthetic tissue by secreting pro-inflammatory chemokines such as CCL2, CCL4, CCL8, CCL13 and CCL22. Accumulation of immune cells at the implant-tissue interface enhances the acute inflammatory phase. Failure to resolve the acute phase of inflammation leads to chronic inflammation, generation of foreign body giant cells and fibrous encapsulation of the implant[57].

1.3.2 Other cells involved in foreign body reaction

It is well established that the foreign body reaction is initiated and coordinated by macrophages; however osteoclasts, osteoblasts, lymphocytes, fibroblasts and thrombocytes are also involved[42]. One of the first cell types able to reach and interact with implanted biomaterials are thrombocytes. As part of their involvement in the wound healing process they can deposit more than 300 proteins in the periprosthetic tissue. These proteins take part in the provisional matrix formation around the implant and are also recognized by macrophages. In response, macrophages up-regulate the expression of pro-inflammatory genes such as TNF, IL1A, IL1B, and CCL1 and down-regulate the expression of anti-inflammatory genes like IL10, CXCL12 and CXCL13[58].

The main cells responsible for bone resorption and osteolysis are osteoclasts. Osteoclasts are multinucleated cells of monocyte-macrophage lineage that increase in number in the periprosthetic tissue as levels of CCL2 and CCL4 rise[42]. The release of pro-inflammatory cytokines in response to wear particles, activates osteoclasts through RANKL/RANK/OPG pathway. This is potentiated by inhibition of anti-osteoclastogenic signaling through IL-6 and IFNγ[59]. As a result, there is an increase in number of activated osteoclasts at the implant-bone interface which promote osteolysis and consequently lead to aseptic loosening[60].

Bone homeostasis is achieved only when there is a balance between bone resorption mediated by osteoclasts and bone formation mediated by osteoblasts. In inflammatory settings, such as those achieved during a foreign body reaction, the balance is tilted towards bone resorption[61]. Osteoblasts, when stimulated by wear particles, secrete osteoclastogenesis factors RANKL and M-CSF, thus promoting osteolysis[62]. Additionally, their ability to secrete osteoid and collagen I is impaired. Moreover, osteoblasts release an array of pro-inflammatory mediators like IL-1, IL-6, IL-8, TNFα, CCL2 and MMP-1 that enhance the inflammatory reaction and recruit immune cells to the periprosthetic tissue[63, 64].

The current model of the interaction of macrophages with osteoblasts and osteoclasts in implantation settings is illustrated in Figure 2. Macrophages initiate the foreign body reaction either as a result of direct recognition of titanium, by contact with the adsorbed protein layer, bacteria, damage-associated molecular patterns (DAMP), or by phagocytosis of wear particles. These events activate macrophages and trigger the secretion of pro-inflammatory cytokines and chemokines, which in turn activate osteoblasts. Activated osteoblasts initiate the production of inflammatory cytokines and chemokines, thus enhancing the inflammation. Additionally, wear particles induce apoptosis in osteoblast and consequently the bone deposition decreases. Chemokines released by osteoblasts and macrophages recruit additional immune cells to the site of inflammation. Synergistic effect of wear particle-induced anti-osteoclastogenic signaling and osteoblast expression of RANKL, M-CSF and CCL2 increases the number of osteoclasts at the implant-tissue interface. Finally, macrophage inflammatory cytokines activate osteoclasts leading to increased osteolysis.
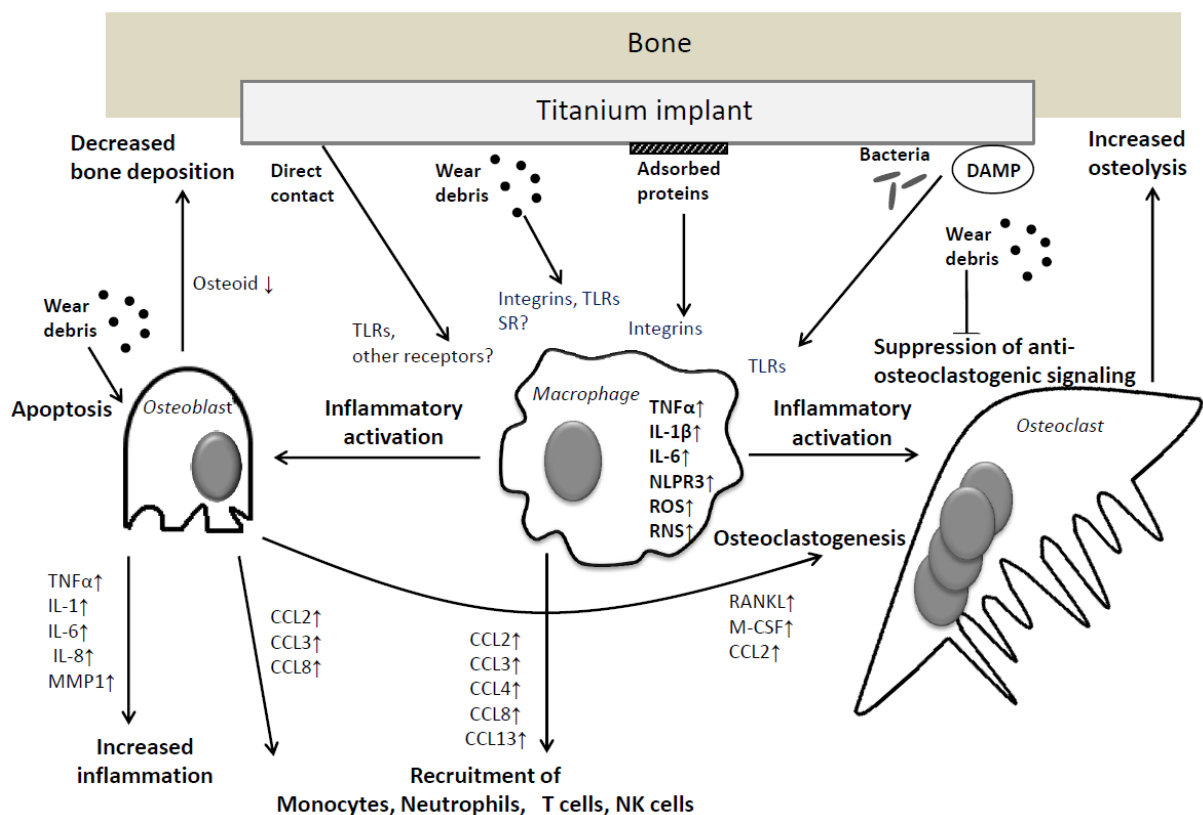

Figure 2. Interaction between macrophages, osteoblasts and osteoclasts at the tissue-implant interface. DAMP - damage-associated molecular pattern molecules, TLRs – toll-like receptors, SR – scavenger receptors, ROS – reactive oxygen species, RNS – reactive nitrogen species. Adapted from Kzhyshkowska et al., Macrophage responses to implants: prospects for personalized medicine, Copyright (2015), with permission from Society for Leukocyte Biology.

Lymphocytes and fibroblasts are also involved in foreign body reaction. Upon wear particle stimulation, fibroblasts promote osteoclastogenesis by secreting pro-inflammatory cytokines and growth factors such as IL-1β, IL-6, IL-8, CCL2, MMP1, COX-1, COX-2, LIF, TGFβ1 and TGFβR1[65]. Lymphocytes, on the other hand, do not take part in osteolysis. Their role in foreign body reaction is to mediate the type IV delayed hypersensitivity response by interacting with macrophages through IL-15, IL-15Rα and IL-2Rβ. Type IV delayed hypersensitivity response is sometimes found in patients with hypersensitivity to metal ions. When wear particles activate fibroblasts

they are able to attract and activate macrophages via secretion of IL-3, GM-CSF, IFNγ, LTA and MIF. In response, macrophages secrete IL-2 and activate more T helper cells, thus enhancing the reaction[55, 56].

1.3.3 Macrophage-driven immune response to titanium

Titanium has been used in biomedical applications mainly due to its high biocompatibility, good mechanical properties, excellent corrosion resistance and low magnetic susceptibility. However, micromotion and friction between articulating surfaces under high mechanical stress may result in release of microscopic wear debris[11]. Immune cells recognize the released wear particles as foreign bodies and consequently will initiate an inflammatory reaction[42]. Numerous studies have tried to determine immune response to titanium by analyzing macrophage responses. The most common cellular models for in vitro testing are RAW264.7 cells (mouse leukemic monocyte-macrophage cell line), THP-1 cells (human monocytic leukaemia cell line) and mouse bone-marrow derived macrophages. When culturing macrophages with titanium nano- and microparticles, increased gene expression and secretion of TNFα, IL-1β and IL-6 was observed[66-68]. Furthermore, titanium up-regulates the expression of inflammatory chemokines like CCL2 and CCL3, which can recruit additional macrophages and neutrophils to the periprosthetic tissue[69]. Inflammasome protein, NLRP3, responsible for IL-1β and IL-18 activation, is also up-regulated in macrophages by titanium[70, 71]. Additionally, it was shown that titanium particles induce oxidative stress in macrophages, characterized by an increase in production of reactive oxygen species (ROS), NO and iNOS, factors known to be involved in osteolysis[69, 72, 73].

In vivo studies corroborate the findings from cell culture experiments. Insertion of titanium particles, pins, rods and screws in tibia, femur, maxilla and calvaria are frequently used to model implantation settings. In these models, titanium was able to induce up-regulation of cytokines such as TNFα, IL-1β and IL-6 and chemokines like CCL2 and CCL3[74-76]. Moreover, inflammasome protein NLRP3 as well as ROS and reactive nitrogen species (RNS) are also up-regulated in the areas adjacent to titanium[77, 78]. In vivo models also provide valuable information regarding titanium influence on osteolysis. Thus, it was found that in the proximity of the titanium implant there is an up-regulation of RANKL and TRAP (tartrate-resistant acid phosphatase) expression, which are common markers for osteoclasts[74, 79]. Previously it was shown that osteoclastogenesis in response to wear particles is highly reliant on RANKL[80]. In cellular models, RANKL expression was up-regulated by titanium particles in human osteoblasts[62, 81]. Therefore, titanium promotes osteolysis by employing macrophages and osteoblasts into secreting a range of pro-inflammatory cytokines and factors of osteoclastogenesis.

The size and surface pattern of titanium also influences the inflammatory reactions towards it. In a comparative study between titanium particles and titanium discs, THP-1 cells exhibited increased expression of cytokines such as TNFα, CCL2, CCL3 and IL-1Ra when cultured on discs[82]. When altering the surface of titanium, it was found that hydrophilic surfaces reduce the expression of pro-inflammatory cytokines like TNFα, IL-1α, IL-1β, IL-6 and CCL2 as well as increase the expression of anti-inflammatory cytokines like IL-4 and IL-10, suggesting better biocompatibility properties. These effects were true for both macrophages and osteoblasts[83-85].

1.4 Advanced solutions to overcome foreign body reaction in implantation

Advances in medicine and technology have led to the use of implants as solutions for a variety of medical conditions. While implants can be lifesaving devices, they still carry a certain amount of risk, thus are classified as class II and III medical devices. The surgical procedure needed for the insertion of implants carries the usual perioperative risks like infection, excessive pain, hemorrhage, wound dehiscence, etc. However, the majority of implants fail long after the surgery was performed. This is due to long-term mechanical stress, release of wear particles and development of chronic inflammation. Some examples of implant failures associated with inflammation are presented in Table 8[42].

Table 8. Examples of implant failures associated with inflammation. Reproduced from Kzhyshkowska et al., Macrophage responses to implants: prospects for personalized medicine, Copyright (2015), with permission from Society for Leukocyte Biology.

Type of implant	Commonly used material	Cause for implantation	Reasons for failure
Teeth	• Titanium • Zirconium • Ti-Ni alloy	Tooth loss	Periimplantitis, Osteolysis, Fibrosis at the implant-bone interface
Knee	• Co-Cr alloy • Polyethylene • Titanium alloys • Stainless steel	Osteoarthritis, Rheumatoid arthritis	Aseptic loosening, Infection, Periprosthetic fracture, Arthrofibrosis
Hip	• Co-Cr alloy • Polyethylene • Titanium alloy • Ceramic • Stainless steel	Osteoarthritis, Osteonecrosis, Inflammatory arthritis	Aseptic loosening, Infection, Periprosthetic fracture
Spine	• Titanium • Stainless steel • Plastic	Spinal deformity, Scoliosis, Osteoporosis	Pseudoarthrosis, Infection, Pain
Left ventricular assist device	• Titanium	End-stage heart failure	Coagulation disorders, Wound infections, Stroke

To reduce the rate of implant failure there is a need for a more biocompatible implant material. The ideal implant material should produce no foreign body reaction, should not support the growth of microorganisms and should be nontoxic, nonallergic and noncarcinogenic. Additionally, it should possess adequate mechanical properties (strength, stiffness, fatigue, etc.), adequate optical properties and density and should be sterilizable, easy to manufacture and have a long shelf-life[11, 16]. Unfortunately, together, all these properties are not found in any implant material. Titanium possesses most of these properties; however, to overcome some of the deficiencies, different techniques to modify titanium implants are being developed.

1.4.1 Porous materials

Today, even the best β-type titanium alloys possess an elastic modulus higher than that of bones (Table 5). This may result in bone resorption through stress shielding. To reduce the elastic modulus to values close to those of cortical and cancellous bones, porous alloys were introduced. Porous alloys reduce the amount of material supporting

a cross section, when compared to bulk alloys, ensuring that under mechanical stress, the deformation is larger, while stiffness is smaller[32]. Additionally it was shown that porous materials allow for greater osseointegration, by providing cells with the necessary space to grow inside the implant[86].

When designing a porous implant, several features such as porosity, pore size and the interconnectivity network need to be taken into account. Porosity (void fraction) needs to be higher than 50% in order to promote adequate osseointegration, while the minimum pore size has to be 100µm. The optimal pore size however, has to be higher than 300µm in order to promote not only attachment, differentiation and growth of osteoblasts but also to promote capillary formation to supply the new bone tissue with blood[87]. An open interconnectivity network provides space for bone tissue ingrowth and capillary formation. While porosity increases osseointegration, it also reduces mechanical properties of the material. Therefore, porosity and pore size have to be designed in such a way that the mechanical requirements for a specific application are met[32].

1.4.2 Surface modifications

The biocompatibility of an implant material is mainly determined by its surface. Some materials have better mechanical properties than others, however suffer from biocompatibility issues. To preserve the mechanical properties and at the same time increase a material's biocompatibility, surface modification techniques are used. For titanium, there are a number of methods used to modify the surface, which can be broadly grouped into mechanical, physical and chemical methods. Mechanical methods such as machining, grinding, polishing or blasting are used to remove surface contamination, improve adhesion in subsequent bonding steps and to produce specific nano or micro patterns on the surface of the implant, which consequently alters the roughness of the surface[88]. Surface roughness has a significant influence on cell behavior, as it was demonstrated that an increase in surface roughness can boost cell attachment and proliferation[89]. Additionally, surface topography is known to influence macrophage activation state, which, as previously explained, play a pivotal role in the initiation and coordination of the foreign body reaction[90].

Physical methods such as thermal spray (flame spray, plasma spray), physical vapor deposition and ion implantation and deposition can be used to improve corrosion and wear resistance as well as increase biocompatibility. Glow discharge plasma treatment is applied to remove the native oxide layer or to sterilize, oxide or nitride the surface. With chemical methods like alkaline treatment, hydrogen peroxide treatment and sol-gel method titanium implant biocompatibility, bioactivity and bone conductivity can be improved. Acidic treatment can be used to remove contamination or oxide scales. Chemical vapor deposition and anodic oxidation are applied to improve wear and corrosion resistance and increase biocompatibility[37, 88].

In general surface modification methods are used to achieve the following outcomes[37]:
- ➢ cleaning or removal of the native surface layers
- ➢ modification of the surface structure and topography
- ➢ modification of the composition and structure of oxide layer
- ➢ controlled formation of a new surface layer

Controlled formation of a new surface layer is primarily used to generate a thin biomaterial coating on the surface of the implant. It is a promising approach to preserve the bulk properties of the implant and at the same time achieve higher biocompatibility[42]. By immobilizing certain peptides, proteins or growth factors on the surface of the implant specific cell and tissue responses can be obtained[88]. Coatings

can also change the hydrophilicity of the surface, as it is known that hydrophilic surfaces closely interact with biological fluid, promoting protein adsorption and, consequently, cell receptor activation[91]. Additionally, surface hydrophilicity can alter macrophage phenotype, and thus their inflammatory response to the implant material[92]. Moreover, implants with special surface coatings can decrease the inflammatory response, thus reducing the chance of complications. For coating purposes, various natural polymers such as alginate, chitosan, collagen, dextran and hyaluronic acid are used. The advantage of natural polymers is that they offer better integration chances, however they can be immunogenic and are thermolabile, which makes the manufacturing process more complicated. An alternative approach is to use synthetic polymers such as polylactic-acid (PLA), poly(lactide-co-glycolide) (PLGA), poly(ethylene-glycol) (PEG) and poly(vinyl-alcohol) (PVA)[93]. Synthetic polymers used for coatings besides being highly hydrophilic, can also provide resistance to biofilm (a thin layer of microorganisms) formation[94].

Common implant coating structures are hydrogels and polyelectrolyte multilayers. Hydrogels are three-dimensional networks of polymers, which absorb high amounts of water (can consist up to 90% of water) and are permeable to small bioactive molecules. Their advantages are that their mechanical properties are similar to those of soft tissues and they can be pre-loaded with drugs, growth factors or other bioactive substances that are gradually released in the adjacent tissue. The release rate can be adjusted by controlling the degree of crosslinking[42, 93]. Some proof of concept experiments show promising results in vivo, with extracellular matrix-based hydrogel coatings promoting an anti-inflammatory phenotype of macrophages[95]. The disadvantages of hydrogels are that they have a poor adhesion to the substrate, the mechanical strength can be inadequate for some applications and sometimes they have biocompatibility issues[93].

Polyelectrolyte multilayers are implant coatings obtained using layer by layer (LbL) alternated deposition of polyanions and polycations. These structures can also be loaded with bioactive molecules that are slowly released into the tissue. Polyelectrolyte multilayers can be fabricated with nanoscale precision, varying thickness, porosity, charge density and viscoelasticity[96]. Moreover they can be designed to possess anti-microbial and immunomodulatory properties, a very attractive feature in implantation[97]. However, some drawbacks such as degradation under physiological conditions and difficulties in controlling the release rate of the bioactive molecule still need to be addressed[42].

1.5 Aim and objectives

Despite broad application of titanium as an implant material, the molecular and cellular mechanisms of detrimental inflammatory responses and implant failure still have to be elucidated. Macrophages are key innate immune cells that mediate recognition of foreign body and orchestrate local tissue inflammatory reactions. However, the knowledge about the molecular profile of the responses of different subtypes of macrophages to titanium surface as well as to implant coatings is limited.

The aim of the thesis project was to study the reactions of human primary macrophage subtypes to titanium and biodegradable implant coating materials.

The specific objectives were:

1. To identify cytokine and transcriptional profile of human primary macrophages to titanium surfaces by ELISA, Affymetrix microarray analysis and RT-qPCR.

2. To compare reactions of macrophages to titanium of different size. (titanium discs, microbeads and nanoparticles) using ELISA and RT-qPCR.

3. To analyze the combined effects of bacteria (Staphylococcus aureus) and titanium on macrophage cytokine secretion.

4. To analyze how fibroblasts or PBMC may alter inflammatory reactions of macrophages to titanium.

5. To identify inflammatory reactions of macrophages to biodegradable implant coating materials.

2 MATERIALS AND METHODS

This work was written under the operating system *Windows 10* with the text processing program *Microsoft Office Word 2016*. The presented pictures, as well as numerous reports, have been processed using the programs *Microsoft Office Excel 2016*, *GraphPad Prism 6*, *Corel Draw Graphics Suite X6* and *Adobe Photoshop CS6.*

2.1 Chemicals, reagents and kits

Table 9. Chemicals and reagents.

Product	Company
0.05% Trypsin/EDTA solution	Biochrom
10✗ Earle's Balanced Salt Solution (EBSS)	Sigma Aldrich
10x Incomplete PCR buffer	BIORON
Acetic Acid	Merck
Agarose	Roth
AlamarBlue®	Invitrogen
Biocoll solution	Biochrom
Bovine Serum Albumin (BSA)	Sigma Aldrich
CD14 MicroBeads	Miltenyi Biotec
D-(+)-Glucose solution 10%	Sigma Aldrich
Deoxyribonucleotides (dNTPs) 10M	Fermentas
DEPC Water	Thermo Fisher Scientific
Dexamethasone	Sigma Aldrich
Dimethylsulfoxide (DMSO)	Sigma Aldrich
DNase Buffer(10x)	Thermo Fisher Scientific
DNase I RNase free 1U/µl solution	Fermentas
EMEM medium	ATCC
Ethanol	Roth
FcR Blocking Reagent, human	Miltenyi Biotec
Fetal calf serum (FCS)	Biochrom
GelRed Nucleic Acid Gel Stain, 10,000x	Biotium
GeneRuler DNA ladder	Fermentas
Glycerol	Sigma Aldrich
Heat Killed Staphyloccocus aureus	Invivogen
Loading dye 6x	Fermentas
Macrophage-SFM (serum-free medium)	Life Technologies
MEM Spinner modification	Sigma Aldrich
$MgCl_2$	Sigma Aldrich
Oligo(dT) primer	Thermo Fisher Scientific
PBS Dulbecco, w/o Ca $^{2+}$, Mg $^{2+}$	Biochrom
PCR primers (designed in the lab)	Eurofins MWG Operon
PCR probes (designed in the lab)	Eurofins MWG Operon
PCR ready-made mixes	Life Technologies
Penicillin / Streptomycin	Biochrom

Product	Company
Percoll	GE Healthcare Life Sciences
Phosphate buffered saline (D-PBS), sterile 1x	Invitrogen
Recombinant Human IFN-γ	Peprotech
Recombinant Human IL-4	Peprotech
Recombinant Human M-CSF	Peprotech
Sensimix II Probe kit	Bioline
Sodium Azide	Alfa Aesar
SytoxRed	Invitrogen
Triton X-100	Sigma Aldrich
Trypan blue solution	Sigma Aldrich
Tween 20	Sigma Aldrich
UltraPure™ 0.5M EDTA	Invitrogen
β-Mercaptoethanol	Sigma Aldrich

Table 10. Kits.

Product	Company
Chitotriosidase (Human) Custom ELISA Kit	RayBiotech
E.Z.N.A. total RNA kit I	Omega bio-tek
Human CCL18 DuoSet ELISA kit	R&D systems
Human Chitinase 3-like 1 DuoSet ELISA kit	R&D systems
Human IL-1beta DuoSet ELISA kit	R&D systems
Human IL-1ra DuoSet ELISA kit	R&D systems
Human IL-6 DuoSet ELISA kit	R&D systems
Human IL-8 DuoSet ELISA kit	R&D systems
Human LIGHT/TNFSF14 DuoSet ELISA kit	R&D systems
Human MMP-7 activity assay	Quickzyme Biosciences
Human MMP-9 activity assay	Quickzyme Biosciences
Human TNF-alpha DuoSet ELISA kit	R&D systems
Human Total MMP-7 DuoSet ELISA kit	R&D systems
Human Total MMP-9 DuoSet ELISA kit	R&D systems
RevertAid H Minus First Strand Synthesis Kit	Fermentas
RNeasy mini kit	Qiagen

2.2 Consumables

Table 11. Consumables.

Product	Company
22µm filters	Fisherbrand
22x22mm coverslips	Marienfeld
CASYcups	Omni Life Sciences
Cell culture plates	Greiner
Cryovials	Nunc
Elisa plate sealers	R&D systems
Elisa Plates	R&D systems
GeneChip® Human Gene 1.0 ST Array	Affymetrix
LS columns	Miltenyi Biotec
Parafilm	American National Can
PCR tubes	Star Labs
Petri dishes	Nunc
Pipette tips	Eppendorf

Product	Company
Pipettes	Gilson, Eppendorf
Plastic wrap	Toppits
qPCR plate sealers	Axon Labortechnik
qPCR plates	Axon Labortechnik
Safe-Lock Eppendorf Tubes, 1.5ml	Eppendorf
Scalpel	Feather
Sterile pipette tips	Avantguard, Star Labs, Nerbeplus
TiO_2 15nm nanoparticles	NanoAmor Europe
Transwell inserts (0.4µm pore size)	Sigma
Tubes	Falcon

2.3 Equipment

Table 12. Equipment.

Product	Company
Autoclave VX-95	Systec
BD FACSCanto II	BD Biosciences
CASY Cell counter	Schärfe System
Centrifugal vacuum concentrator 5301	Eppendorf
Centrifuge 5415 D	Eppendorf
Centrifuge 5804R	Eppendorf
Centrifuge Rotina 420	Hettich
Centrifuge Rotina 420R	Hettich
Centrifuge Universal 320	Hettich
Cryo freezing container	Nalgene
Deep freezer (-80°C)	Sanyo
ENDURO Electrophoresis comb	Labnet
ENDURO Electrophoresis power supply	Labnet
Freezer (-20°C)	Liebherr
HydroFlex ELISA microplate washer	Tecan
Ice machine	Scotsman AF100
Incubator 37°C	Edmund Bühler GmbH
Inverted microscope	Leica
Laminar flow hood	Thermo
LightCycler 480	Roche
Magnetic stirrer MR3000	Heidolph
Microwave oven	Sharp
MultiDoc-It™ Imaging System	UVP
Neubauer haemocytometer	Assistent
Pipette Controller	Accu Jet Pro, Brand
Roller	Ortho Diagnostic Systems
Rotator	Neolab
Shaker KS 260 basic	IKA
Tecan Infinite 200 PRO	Tecan
Thermocycler DNA Engine	Bio-Rad
Thermomixer 5436	Eppendorf

Product	Company
Thermomixer comfort	Eppendorf
Tweezers	Neolab
Vortex Genie 2	Scientific Industries
Water bath	Memmert

2.4 Buffers and solutions

2.4.1 Running buffer for electrophoresis

50xTAE buffer
> 242g of Tris free base and 18.61g of Disodium EDTA were added to 700ml ddH$_2$O and stirred until they dissolved. 57.1ml Glacial Acetic Acid was added and the volume was adjusted to 1L.

1xTAE buffer
> 20ml of 50xTAE buffer was added to 980ml of ddH$_2$O.

2.4.2 Solutions for immunological methods

Wash buffer for ELISA (0.05% Tween 20 in PBS)
> 500µl of Tween 20 was pipetted into 1L of PBS. The beaker was stirred on a magnetic stirrer for 30min and the solution was stored at RT.

FACS buffer (0.4% BSA, 0.02% Sodium Azide):
> 4g of BSA and 2ml of 10% Sodium Azide solution were dissolved in 1L of PBS. The solution was adjusted to pH 7.4 and sterile filtered with a 0.22µm filter.

Red blood cell lysis buffer (RBC-lysis buffer):
> For a 10xRBC-lysis buffer 82,91g of NH$_4$Cl (1.55M), 7.91g of NH$_4$HCO$_3$ (0.1M) and 0.29g of EDTA (1mM) were dissolved in 1L of ddH$_2$O.
> 1x RBC-lysis buffer was prepared by adding 100ml of 10xRBC-lysis buffer to 900ml of ddH$_2$O.

2.4.3 Solutions for monocyte isolation

Percoll gradient:
> Every 30ml of Percoll gradient solution was prepared in a 50ml Falcon tube with 13.5ml Percoll, 15ml Minimal Essential Medium Eagle Spinner modification and 1.5ml of 10xEarle's Balanced Salt Solution.

MACS buffer (0.5% BSA, 2mM EDTA):
> 2.5g of BSA was dissolved in 500ml PBS. 2ml of 0,5M EDTA was added and the mixture was filtered to a sterile flask.

2.5 Molecular biology techniques

2.5.1 Primers

Table 13: List of primers designed in the lab. F: forward, R: reverse, Pr: probe. All primers and probes were ordered from Eurofins MWG Operon.

Primer name	Target gene	Sequence (5'-3' direction)
F848	GAPDH	CATCCATGACAACTTTGGTATCGT
R848	GAPDH	CAGTCTTCTGGGTGGCAGTGA
Pr849	GAPDH	AAGGACTCATGACCACAGTCCATGCC
F2229	MMP7	CTTCCTGTATGCTGCAACTCA
R2229	MMP7	GGGATCTCCATTTCCATAGG
Pr2229	MMP7	TCCCATACCCAAAGAATGGCCAA
F2020	CCL18	ATACCTCCTGGCAGATTCCAC
R2020	CCL18	GCTGATGTATTTCTGGACCCAC
Pr2020	CCL18	CAAGCCAGGTGTCATCCTCCTAACCAAGAGAG
F896	TNF	TCTTCTCGAACCCCGAGTGA
F896	TNF	AGCTGCCCCTCAGCTTGA
Pr896	TNF	AAGCCTGTAGCCCATGTTGTAGCAAACC

Table 14: List of ready-made mixes. All ready-made mixes were ordered from Life Technologies.

Assay code	Target Gene
Hs00234646_m1	CCL13
Hs00270756_m1	CCL23
Hs04187715_m1	CCL8
Hs00609691_m1	CHI3L1
Hs00185753_m1	CHIT1
Hs00174164_m1	CSF1
Hs00218889_m1	IL17RB
Hs01029060_m1	MMP8
Hs00234579_m1	MMP9
Hs01560899_m1	TNFRSF21
Hs00542477_m1	TNFSF14

2.5.2 Isolation of total RNA

E.Z.N.A. total RNA kit I from Omega was used for RNA isolation. The lysis buffer was prepared by adding 20µl of β-mercaptoethanol to each 1ml of the TRK buffer.

1. *For cells*: 350µl of lysis buffer was added to $3\text{-}5\times10^6$ cells, which were completely disrupted by passing through a needle fitted to a syringe for 10-15 times.
2. 350µl of 70% ethanol were added to the lysate and vortexed briefly. The sample was added to a HiBind RNA spin column placed into a 2ml collection tube.
3. After centrifuging for 1min at 10000g the flow-through was discarded. The column was washed once with 500µl wash buffer I.
4. The column was centrifuged at 10000g followed by washing twice in 500µl wash buffer II (each wash was followed by a centrifugation step at 10000g).
5. The final flow-through was discarded and a new 2ml collection tube was placed under the column which was centrifuged for 2min at maximum speed.

6. The column was placed in a fresh 1.5ml RNase free Eppendorf tube and RNA was eluted with 40µl of DEPC-treated water and incubated for 5min. Samples were centrifuged at maximum speed for 1min.
7. The elution step was repeated with the eluate to increase RNA concentration as recommended by the manufacturer.
8. The RNA concentration was determined by measuring the absorption peak at 260nm wavelength with Tecan Infinite 200 PRO.
9. The quality of RNA samples was determined by running the RNA on 1% agarose gel. RNA samples were stored at –80°C for later application.

2.5.3 First strand cDNA synthesis

For cDNA synthesis RevertAid H Minus First Strand Synthesis Kit from Fermentas was used.
1. RNA samples were digested with DNase I to remove possible contamination of isolated RNA with fragments of genomic DNA. For this the following components were used:

Total RNA	5µl (up to 1µg)
10x DNase I buffer with MgCl2 (Fermentas)	1µl
RNase free DNase I (Fermentas)	1µl
Distilled water (RNase free)	3µl

2. The samples were incubated at 37°C for 40min (DNA digestion step) in a Thermomixer followed by enzyme inactivation at 70°C for 10min.
3. For primer annealing 1µl of Oligo (dT) primer and 1µl of water was added to each sample and incubated at 70°C for 5min. The samples were placed on ice.
4. For cDNA synthesis the following components were added and mixed well:

5x Reaction Buffer	4µl
Ribolock RNase inhibitor	1µl
10M dNTP mix	2µl
RevertAid H minus reverse transcriptase	1µl

5. The samples were incubated at 42°C for 1h in a Thermomixer. Afterwards, the enzymatic activity was stopped by incubation at 70°C for 10min.
6. The cDNA samples were diluted 10 times with ddH$_2$O and stored at -20°C for later use.

2.5.4 RNA preparation for Affymetrix microarray analysis

Total RNA was prepared using E.Z.N.A. total RNA kit I as described above.
1. The volume of RNA sample was adjusted with DEPC-treated water to 100µl. 12µl of 10x DNase I buffer with MgCl$_2$ (Fermentas) and 10µl of RNase free DNase I (Fermentas) were added to sample and mixed well by pipetting.
2. DNA digestion was done at 37°C for 40min in a Thermomixer.
3. For RNA cleanup procedure RNeasy kit from Qiagen was used. 350µl of RLT buffer were added to the samples and the samples were vortexed.
4. 250µl of 100% ethanol were added to the samples and mixed by pipetting.
5. The samples were added to RNeasy mini column, placed in a 2ml collection

tube and centrifuged at 10000g for 1min.

6. The flow through was discarded and columns were washed two times with 500µl of RPE buffer (each wash was followed by a centrifugation step at 10000g).

7. The collection tubes were changed and the samples were centrifuged at maximum speed for 2min.

8. The columns were placed in fresh 1.5ml RNase free Eppendorf tube and RNA was eluted with 40µl of DEPC-treated water and incubated for 5min. Samples were centrifuged at maximum speed for 1min.

9. The elution step was repeated with the eluate to increase RNA concentration as recommended by the manufacturer.

10. The RNA concentration was determined by measuring the absorption peak at 260nm wavelength with Tecan Infinite 200 PRO

11. If the concentration of RNA was lower than 30ng/µl, the samples were concentrated using Eppendorf centrifugal vacuum concentrator 5301.

2.5.5 Hybridization of gene chip microarray data

RNA was tested by capillary electrophoresis on an Agilent 2100 bioanalyzer (Agilent) and high quality was confirmed. Hybridization of probes was done using arrays of human HuGene-1_0-st-type from Affymetrix. Biotinylated antisense cRNA was then prepared according to the Affymetrix standard labelling protocol with the GeneChip® WT Plus Reagent Kit and the GeneChip® Hybridization, Wash and Stain Kit (both from Affymetrix, Santa Clara, USA). Afterwards, the hybridization on the chip was performed on a GeneChip Hybridization oven 640, then dyed in the GeneChip Fluidics Station 450 and thereafter scanned with a GeneChip Scanner 3000. All of the equipment used was from the Affymetrix-Company (Affymetrix, High Wycombe, UK). All the necessary procedures needed for hybridization and scanning of chips were performed by technical assistants Ms. Maria Muciek and Ms. Carolina De La Torre in the Affymetrix Core Facility of Medical Research Center, Medical Faculty Mannheim.

2.5.6 Polymerase chain reaction (PCR)

Genes were amplified from cDNA templates using primers specific to the gene of interest.

1. The following reagents were added to a 1.5ml Eppendorf tube to make a master mix for the number of samples:

Reagent	Amount/sample (µl)
ddH$_2$O	18.3
Buffer (w/o +Mg^{2+}) 10x	2.5
dNTPs (10 mM)	0.5
MgCl$_2$ (100 mM)	0.4
Taq polymerase (5 U/µl)	0.3
Forward primer (10 pmol/µl)	1
Reverse primer (10 pmol/µl)	1

2. The master mix was divided amongst PCR tubes and 1µl of cDNA template was added to each tube and mixed by pipetting.

3. Amplification was performed using Thermocycler DNA Engine from Biorad and the following program was used:

95°C	3min
95°C	30s
60°C	30s
72°C	1min
72°C	10min
12°C	forever

35 cycles (covering the 95°C 30s, 60°C 30s, 72°C 1min steps)

*PCR products were visualized using agarose gel electrophoresis.

2.5.7 Real-time PCR with Taqman probe

Genes were amplified from cDNA templates using primers specific to the gene of interest.

1. A master mix for all the samples was prepared in a 1.5ml Eppendorf tube containing:

Reagent	Amount (µl) / sample
Sensimix II	5
Reference Primer	0.5
Target Primer	0.5
ddH$_2$O	3

2. The master mix was divided amongst 1.5ml Eppendorf tubes. As each sample was run in triplicates, 3µl of cDNA template was added to each tube and mixed by pipetting
3. Amplification was performed using LightCycler 480 from Roche and the following program was used:

95°C	10min
95°C	15s
60°C	1min
37°C	2min

50 cycles (covering the 95°C 15s, 60°C 1min steps)

Dual-labeled probes for target genes contained FAM on 5' end and BHQ1 quencher at 3' end of sequence. In all experiments GAPDH was used as the reference gene. The probe for GAPDH contained JOE on 5' end and BHQ1 quencher at 3' end of sequence.

2.5.8 Agarose gel electrophoresis

1. 2g of agarose was mixed with 100ml of 1xTAE electrophoresis buffer to obtain a 2% agarose gel mixture (used for detecting DNA fragments less than 200bp). The mixture was heated in a microwave until completely dissolved.
2. The solution was allowed to cool down to 50-60°C and 10µl of GelRed Nucleic Acid Gel Stain (10000x) was added to the solution.
3. The solution was poured into a gel tray equipped with a comb and allowed to solidify (approximately 30min).

4. The comb was removed and the gel was placed into the electrophoresis unit filled with 1xTAE buffer.
5. To verify the size of the target fragments 3µl of GeneRuler DNA Ladder was added to the first lane.
6. The samples were prepared as follows: 2µl of sample + 8µl of ddH$_2$O + 2µl of loading dye.
7. Electrophoresis was carried out at 130 V for 45 min. The results were visualized by UV illumination and captured using MultiDoc-It™ Imaging System.

2.6 Cell culture techniques

2.6.1 Cultivation of cell lines and primary cells

Table 15. Cultivation conditions of cell lines and primary cells.

Cell line / primary cell	Growth medium	Growth conditions	Morphology	Cell type
BJ	EMEM + 10% FCS + 100µg/ml penicillin/ streptomycin	5% CO$_2$	adherent	Human fibroblasts from skin, foreskin
Primary human monocytes	Macrophage-SFM + 10^{-8}M Dexamethasone + 1ng/ml M-CSF Optional: cytokines as indicated in Section 2.6.8	7.5% CO$_2$	suspension	Human peripheral blood monocytes
PBMC	Macrophage-SFM + 10^{-8}M Dexamethasone + 1ng/ml M-CSF Optional: cytokines as indicated in Section 2.6.8	7.5% CO$_2$	suspension	Human peripheral blood mononuclear cells

2.6.2 Thawing of fibroblasts

1. A T25 flask was prepared with 5ml medium.
2. The vial with the frozen cells was thawed at 37°C in a water bath.
3. The cell suspension was added to 9ml of PBS in a 15ml Falcon tube and centrifuged for 8min at 1200rpm.
4. The supernatant was discarded and the pellet was resuspended in 1ml of medium.
5. The cells were added to the flask.
6. The flask was put into the 37°C incubator with 5% CO$_2$ and 95% humidity.
7. At 80-90% confluence the cells were split and cultivated further in T75 flasks.

2.6.3 Splitting of fibroblasts

Cells were cultivated in T75 flasks and were split when their confluence reached 80-90%.

1. A 15ml Falcon tube was prepared for each flask.
2. The medium was aspirated from the flasks and the cells were washed with 10ml of PBS. PBS was added carefully on the side and then aspirated.
3. 3ml of warm (37°C) Trypsin/EDTA solution was added to each flask and the flasks were incubated at 37°C for 3min.
4. To stop the enzymatic reaction 2ml of medium was added to each flask.

5. 10ml of PBS was vigorously added to each flask to wash and detach the cells.
6. The cell suspension of each flask was added to its corresponding Falcon tube and the tubes were centrifuged for 8min at 1200rpm.
7. The supernatant was aspirated and the pellets were resuspended in 1ml of medium.
8. New T75 flasks were prepared with 10ml medium. 0.5ml of the cell suspension was added to each new T75 flask.
9. The plates were incubated at 37°C with 5% CO_2 and 95% humidity.

2.6.4 Cryopreservation of fibroblasts

1. A 15ml Falcon tube was prepared for each flask.
2. The medium was aspirated and the cells were washed with 10ml of PBS. PBS was added carefully on the side and then aspirated.
3. 3ml of warm (37°C) Trypsin/EDTA solution was added to each flask and the flasks were incubated at 37°C for 3min.
4. To stop the enzymatic reaction 2ml of medium was added to each flask.
5. 10ml of PBS was vigorously added to each flask to wash and detach the cells.
6. The cell suspension of each flask was added to its corresponding Falcon tube and the tubes were centrifuged for 8min at 1200rpm.
7. The supernatant was aspirated and the pellets were resuspended in 1ml of freezing medium (EMEM + 20% FCS + 10% DMSO).
8. The suspension was put into cryovials and transferred into a cryo freezing container with 250ml of isopropanol. The container was placed into a -80°C freezer.
9. The next day, the samples were transferred to liquid nitrogen tanks.

2.6.5 Isolation of CD14+ monocytes from human peripheral blood (buffy coats)

1. Buffy coats with 20-50ml of blood were received from the German Red Cross blood bank. A unique donor number was given to each Buffy Coat.
2. Blood was transferred from the plastic bag to a T75 flask, diluted 1:1 with PBS (without Ca^{2+} and Mg^{2+}) and mixed by pipetting up and down.
3. For each 30ml of diluted blood a 50ml Falcon tube with 15ml Biocoll separating solution was prepared.
4. 30ml of diluted blood was carefully layered (against the tube wall) on top of Biocoll solution. The tubes were centrifuged at 420g, for 30min without break.
5. PBMC (the second layer) were collected with a sterile Pasteur pipet and transferred into a new 50ml Falcon tube (cells from each tube were transferred into a new one).
6. The mixture was added up to 50ml with PBS and the tubes were centrifuged at 420g for 10min with break.
7. The supernatant was discarded and the cell pellets from each donor were resuspended with 5ml PBS and collected in one 50ml Falcon tube for each donor (tubes from the same donor were combined in this step).
8. The cells were washed with 50ml PBS and centrifuged at 420g for 10min with break. The supernatant was discarded.
9. Percoll gradient (30ml) was prepared with 13.5ml Percoll, 15ml of MEM Spinner modification and 1.5ml 10x Earle's Balanced Salt Solution.

10. The cells were resuspended with 3ml PBS and carefully layered (against the tube wall) on top of the Percoll gradient.
11. The old tube was washed with 4ml of PBS and the content was added to the Percoll gradient tube. Cells were centrifuged at 420g, for 30min without break.
12. The upper phase (PBS) and second phase (cells enriched for monocytes) were collected into a 50ml Falcon tube.
13. The solution was mixed well, filled up to 50ml with PBS and centrifuged at 420g, for 10 min with break. The supernatant was discarded.
14. The cell pellets were resuspended with 3ml PBS and transferred into a 15ml Falcon tube. The 50ml tube was washed with 4ml of PBS. The solution was added into the 15ml tube and filled up to 10ml.
15. Cells were counted and the rest of them were centrifuged at 420g, for 10 min with break. Cell counting was performed on CASY Cell counter.
16. The cell pellet was resuspended in CD14+ microbeads and MACS buffer according to the formula: 5µl CD14 beads and 95µl MACS buffer per $1x10^7$ cells.
17. The cells were incubated for 20 minutes on a rotator at 4°C.
18. The tubes were filled up to 10ml with MACS buffer and centrifuged at 420g, for 10min.
19. During this time, LS columns were attached to the magnetic stand (One column is maximal for $1x10^8$ cells) and 15ml Falcon tubes were placed under columns. The columns were washed with 3ml of MACS buffer.
20. The cell pellet was resuspended in 1ml MACS buffer and then added to each column. The column was washed 3 times with MACS buffer, each time 3ml.
21. The column was removed from the magnetic separation unit and placed on top of a fresh 15ml Falcon tube. CD14+ monocytes were eluted from the column with 10ml MACS buffer.
22. Cells were counted and centrifuged at 420g, for 10min. The cell pellet was resuspended in 1ml of Macrophage-SFM medium and cultured according to the experimental plan.

2.6.6 Isolation of PBMC and generation of CD14+ and PBMC-CD14 fractions from human peripheral blood (buffy coats)

Steps 1-7 are identical to those from the protocol for isolation of CD14+ monocytes from human peripheral blood (section 2.6.5).

8. The 50ml Falcon tubes were filled up to 50ml with PBS and a sample of cell suspension was taken for counting. The rest were centrifuged at 420g for 10min with break. Counting was done on a CASY cell counter.
9. Cell pellets were resuspended in 5ml of PBS and $20x10^6$ PBMC were taken out and placed on ice until cultured.
10. The remaining cells were washed with 50ml PBS and centrifuged at 420g for 10min.
11. The cell pellet was resuspended in CD14+ microbeads and MACS buffer according to the formula: 10µl CD14 beads and 90µl MACS buffer per $1x10^7$ cells.
12. The cells were incubated for 20min on a rotator at 4°C.
13. The tubes were filled up to 10ml with MACS buffer and centrifuged at 420g, for 10min.

14. During this time, LS columns were attached to the magnetic stand (One column is maximal for 1×10^8 cells) and 15ml Falcon tubes were placed under columns. The columns were washed with 3ml of MACS buffer.
15. The cell pellet was resuspended in 1ml MACS buffer and then added to each column. The column was washed 3 times with MACS buffer, each time 3ml.
16. The column was removed from the magnetic separation unit and placed on top of a fresh 15ml Falcon tube. CD14+ monocytes were eluted from the column with 10ml MACS buffer.
17. Cells from both the tubes containing CD14+ monocytes and those containing PBMC-CD14+ monocytes (flow-through) were counted and centrifuged at 420g, for 10min. The cell pellet was resuspended in 1ml of Macrophage-SFM medium and cultured according to the experimental plan.

2.6.7 Cell counting

Monocyte and PBMC cell counting was performed on a CASY cell counter from Schärfe System.
1. 10µl of sample was added to 10ml of CASYton solution in a CASYcup.
2. The CASYcup was placed under the CASY capillary and the appropriate program for PBMC was chosen.
3. After each measurement 3 cycles of cleaning procedure were performed.
4. Only the viable cell number was used for further calculations.

Fibroblasts were counted using a Neubauer hemocytometer.
1. 20µl of cells were mixed with 20µl of Trypan blue solution in a 1.5ml Eppendorf tube.
2. 10µl of the mixture was pipetted into the hemocytometer chamber via capillary action.
3. The number of cells in the four marked squares which did not take up Trypan blue were counted using a microscope.
4. Cells overlapping the top and left boundaries were counted while cells overlapping the bottom and right boundaries were not.
5. The number of cells per ml was calculated using the following formula: number of cells in the 4 corners/4 x 10^4 x dilution factor

2.6.8 Specific conditions used for primary human monocytes and PBMC

Isolated primary human monocytes and PBMC were cultured in Macrophage-SFM medium supplemented with 10^{-8}M Dexamethasone and 1ng/ml M-CSF. The concentration of cells was 1×10^6/ml for coating materials and 2×10^6/ml for titanium experiments. For coating experiments the medium was additionally supplemented with 5mM Glucose. Cells were seeded in 24-well plates, 1.5ml/well. Three subtypes of monocytes were obtained by stimulation: M(Control) - no additional stimulation; M(IFNγ) - stimulated with 100ng/ml IFNγ; M(IL-4) - stimulated with 10ng/ml IL-4. The same stimulations were used for PBMC and PMBC depleted of CD14+ monocytes (PBMC-CD14). Cells were cultured for 6 days.

2.6.9 Co-culturing of primary human monocytes and BJ Fibroblasts

To preserve the same conditions in all experiments, isolated primary human monocytes and BJ Fibroblasts were co-cultured in Macrophage-SFM medium supplemented with 10^{-8}M Dexamethasone and 1ng/ml M-CSF. The concentration of cells was 1×10^6/ml for monocytes and 1×10^5/ml for fibroblasts. Cells were seeded in 24-well plates, 1ml/well. Monocytes were co-cultured with BJ Fibroblasts either directly in the same well (cell-cell contact) or in a transwell system (0.4µm pores). When co-cultured in transwell system, 1ml of monocyte suspension was added outside the transwell insert (0.4µm pore size with PET track-etched membrane), while 10^5 fibroblasts were seeded inside the transwell supplemented with 200µl of culture medium. As controls, both monocytes and fibroblasts alone were cultured. Additional stimulation with IFNγ and IL-4 was done as described in section 2.6.8. Cells were cultured for 6 days.

2.6.10 Activation of macrophages with heat killed Staphylococcus aureus.

Isolated primary human monocytes were cultured in Macrophage-SFM medium supplemented with 10^{-8}M Dexamethasone and 1ng/ml M-CSF. Cells were seeded 24-well plates, 1.5ml/well (2×10^6 cells/ml). Three subtypes of monocytes were obtained by stimulation: M(Control) - no additional stimulation; M(IFNγ) - stimulated with 100ng/ml IFNγ; M(IL-4) - stimulated with 10ng/ml IL-4. Cells were cultured in total for 7 days. 10^7 heat killed Staphylococcus aureus cells per ml was used to additionally activate monocytes either immediately on day 0 or on the 6th day.

2.6.11 Analysis of macrophage cell viability with Alamar Blue

1. 0.5ml of supernatants from each well was removed, leaving 1ml of supernatant inside.
2. 100µl of Alamar Blue was added to each well, and the plate was incubated at 37°C for 3h.
3. Three times 100µl of supernatant from each well (triplicates) was collected and transferred into a 96-well plate for measuring.
4. Measurement was done on with Tecan Infinite 200 PRO using 560EX nm/590EM nm filter settings.

2.6.12 Preparation of biomaterials for cell culture

Titanium discs
Medical grade titanium discs of 13.7x2mm size (both polished and porous) were provided by our collaborators from Protip Medical in the frames of EU FP7 IMMODGEL project. The discs were autoclaved at 121°C for 20 min at 18psi.

Titanium microbeads
Medical grade titanium microbeads (125-200µm in size) were provided by our collaborators from Protip Medical in the frames of EU FP7 IMMODGEL project.
1. 45mg of microbeads were weighted in 1.5 Eppendorf tubes. This amount of beads was sufficient to cover up to ¾ of the area of a well (24-well plate).
2. 200µl of 70% Ethanol was added to each tube and incubated for 1h.
3. The beads were carefully washed twice with 400µl sterile PBS.
4. The beads were placed in the appropriate wells and the plate was further sterilized under UV light for 1h.

TiO₂ nanoparticles

TiO_2 nanoparticles of 15nm size were purchased from NanoAmor Europe. Prior to use, they were sterilized under UV light for 1h. nTi particles were added in 0.0025wt% per well.

PLA films

PLA films were sterilized with ethylene oxide. PLA films were provided by Dr. Sergei I. Tverdokhlebov from Tomsk Polytechnic University.

PAR/HA and PAR/HA+CAT coatings

PAR/HA and PAR/HA+CAT coatings were provided as coatings on coverslips by Dr. Philippe Lavalle from Strasbourg University. The coverslips were sterilized under UV light for 1h.

2.7 Immunological methods

2.7.1 Antibodies

Table 16. List of primary antibodies.

Antibody	Company	Catalog number	Species	Application	Working concentration; dilution
Anti-Human CD14 FITC	eBioscience	11-0149-42	Mouse	FACS	10µg/ml 1:20
IgG1 K Isotype Control	eBioscience	11-4714-42	Mouse	FACS	10µg/ml 1:20

2.7.2 Flow cytometry

Flow cytometry was used to verify the purity of CD14+ monocytes after isolation. Additionally, it was used to determine the depletion of CD14+ monocytes in the PBMC-CD14 fraction of PBMC. All procedures were performed in FACS tubes.

1. After monocyte or PBMC isolation $1x10^6$ cells were taken for FACS staining.
2. The cells were divided into two fractions ($0.5x10^6$ cells) and possible contamination with erythrocytes was removed with addition of 2ml of RBC-lysis buffer. Cells were incubated for 10min at RT.
3. Cells were centrifuged for 4min at 400g with break, at RT.
4. Cells were resuspended in 100µl FACS buffer.
5. 10µl of FcR Blocking Reagent was added and incubated with cells for 5min at 4°C.
6. Antibodies (conjugated with fluorochrome) were added (0,2-1µg per tube according to manufacturer instructions) to each sample. The cells were briefly vortexed and incubated for 30min at 4°C.
7. Cells were washed 2 times with 500µl FACS buffer. Each wash was followed by a centrifugation step (4min at 400g with break, at RT)

8. Cells were resuspended in 200µl FACS buffer before measurement. Staining was analyzed using BD FACS Canto II.

2.8 Protein-related techniques

2.8.1 Enzyme-linked Immunosorbent Assay (ELISA)

Protocol for ELISA kits from R&D systems.
All procedures were performed at RT unless stated otherwise. ELISA was performed according to the manufacturer's instructions.

1. The Capture Antibody was diluted to working concentration according to manufacturer instruction in PBS without carrier protein.
2. A 96-well micro plate was immediately coated with 100µl per well of Capture Antibody. The plate was sealed and incubated overnight.
3. The plate was washed with HydroFlex ELISA microplate washer (350µl wash buffer 4 times).
4. Each well was filled with 100µl of Reagent Diluent (1% BSA in PBS) to block unspecific binding sites. Incubate 1 hour.
5. The Reagent Diluent was aspirated from the wells and 100µl of fresh Reagent Diluent was added to the wells designated for standards and 50µl of Reagent Diluent was added to the wells designated for samples.
6. 50µl of sample or 100µl of standards diluted in Reagent Diluent was added per well. The plate was covered with an adhesive strip and incubated for 2 hours.
7. The plate was washed with HydroFlex ELISA microplate washer (350µl wash buffer 4 times).
8. The Detection Antibody was diluted to working concentration according to manufacturer instruction in Reagent Diluent. 100µl of Detection Antibodies were pipetted into each well and the plate was incubated for 2 hours.
9. The plate was washed with HydroFlex ELISA microplate washer (350µl wash buffer 4 times).
10. Streptavidin-HRP was diluted to working concentration according to manufacturer instruction in Reagent Diluent. 100µl of Streptavidin-HRP was added to each well and the plate was incubated for 20 minutes in the dark.
11. The plate was washed with HydroFlex ELISA microplate washer (350µl wash buffer 4 times).
12. Substrate Solution was prepared by mixing 5ml of Reagent A with 5ml of Reagent B. 100µl of Substrate Solution was added to each well and the plate was incubated for 20 minutes in the dark.
13. 50µl of Stop Solution (2N H_2SO_4) was added to each well. The absorbance at 450nm was read on a Tecan Infinite 200 PRO reader.
14. To determine each sample's concentration a standard curve was drawn by plotting the mean absorbance for each standard on the y-axis against the concentration on the x-axis. Individual sample absorbance values were then compared to the standards values and the concentration was calculated according to the polynomial equation that describes the curve. In diluted samples, the concentration read from the standard curve was multiplied by the dilution factor. The sample's concentration was extrapolated if the absorbance values were below the lowest standard and above blank.

Protocol for ELISA kits from RayBiotech
All procedures were performed at RT unless stated otherwise. ELISA was performed according to the manufacturer's instructions.

1. Assay Diluent (Item E2), Wash buffer (Item B), TMB One-step Substrate Reagent (Item H) and Stop solution (Item I) were thawed approximately 1h.
2. 1xAssay Diluent (Item E2) was prepared to a working concentration by dilution 1:5 in ddH_2O.
3. The samples and standard was prepared by dilution with 1xAssay Diluent (Item E2).
   Standard (std) preparation: 400µl of 1xAssay Diluent (Item E2) was added to the standard vial (Item C) to get stock concentration of 10ng/ml.
   Standards were prepared in seven 1.5ml Eppendorf tubes. For highest standard concentration 100µl of stock standard solution was added to 400µl of 1xAssay Diluent (Item E2). In the other 6 tubes 300µl of 1xAssay Diluent (Item E2) was added. 200µl of concentrated standard solution was used for preparing serial dilutions.

	Std1	Std2	Std3	Std4	Std5	Std6	Std7	Blank
Diluent volume + higher standard	400µl + 100µl std	300µl + 200µl std1	300µl + 200µl std2	300µl + 200µl std3	300µl + 200µl std4	300µl + 200µl std5	300µl + 200µl std6	400µl
Concentration (pg/ml)	2000	800	320	128	51.20	20.48	8.19	0

4. Samples and standards were incubated for 2.5h.
5. Detection Antibody (Item F) was prepared by adding 100µl of 1xAssay Diluent (Item E2). Detection Antibody (Item F) was adjusted to a working concentration by 1:80 dilution in 1xAssay Diluent (Item E2).
6. Wash buffer (Item B) was diluted 1:20 to a working concentration in ddH_2O. The plate was washed 4 times with 300µl of 1xWash buffer (Item B).
7. 100µl of 1xDetection Antibody (Item F) was added to each well and incubated for 1h.
8. The plate was washed 4 times with 300µl of 1xWash buffer (Item B).
9. Working concentration of Streptavidin-HRP was prepared by dilution 1:400 in 1xAssay Diluent (Item E2). 100µl of Streptavidin-HRP was added to each well and incubated for 45min.
10. The plate was washed 4 times with 300µl of 1xWash buffer (Item B).
11. 100µl of TMB One-step Substrate Reagent (Item H) was added to each well and incubated for 30min in the dark with gentle shaking.
12. 50µl of Stop solution (Item I) was added to each well. The absorbance at 450nm was read on a Tecan Infinite 200 PRO reader.
13. To determine each sample's concentration a standard curve was drawn by plotting the mean absorbance for each standard on the y-axis against the concentration on the x-axis. Individual sample absorbance values were then compared to the standards values and the concentration was calculated according to the polynomial equation that describes the curve. In diluted samples, the concentration read from the standard curve was multiplied by the dilution factor. The sample's concentration was extrapolated if the absorbance values were below the lowest standard and above blank.

2.8.2 MMP-7 and MMP-9 activity assays

The concentration of active MMP-7 and MMP-9 was measured using MMP activity assays from Quickzyme Biosciences. MMP activity assays were performed according to the manufacturer's instructions. All procedures were performed at RT unless stated otherwise.
1. Assay Buffer and Wash Buffer were thawed for 2h.
2. Wash Buffer was prepared by repeated washing with distilled water and collected in a 500ml bottle.

Steps 3 to 5 were done only for MMP-7 activity assay

3. MMP-7 antibody dilution was thawed and prepared as follows: 100µl in 10ml Assay Buffer.
4. The plate was covered with 100µl of MMP-7 antibody and incubated at 37°C for 2h.
5. The plate was washed 4 times.
6. The standard was prepared by adding 950µl Assay Buffer to the standard vial (C = 32ng/ml).
7. Standards were prepared in twelve 1.5ml Eppendorf tubes. First 250 µl of Assay Buffer was added to each tube and then 250µl of concentrated standard was added to the first tube. After this 250µl of solution from the first tube was transferred to the next one and so on (serial dilution).
8. 100µl of standards and samples were added to the appropriate wells. Plate was incubated overnight at 4°C.
9. APMA stock solution was prepared by adding 50µl DMSO to the APMA vial.
10. 10µl of stock APMA was added to 10ml of Assay buffer to prepare ready-to-use APMA solution.
11. The plate was washed 4 times.
12. 50µl of ready-to-use APMA solution was added to the standards and Blank and 50µl of Assay Buffer to the wells in which endogenous MMP activity is analyzed.

Step 13 was done only for MMP-9 activity assay
13. The plate was incubated for 1.5h at 37°C.
14. The Detection Reagent was prepared by adding 550µl of Detection Enzyme and 880µl of Substrate Solution to 4070µl of Assay Buffer.
15. 50µl of Detection Reagent was added to each well.
16. The plate was incubated at 37°C and MMP activity was read at 405nm with 20s shaking on Tecan Infinite 200 PRO at the following time points: 0h, 3h, 6h, 24h.
17. To determine the active concentration in each sample, a standard curve was drawn by plotting the mean absorbance for each standard on the y-axis against the concentration on the x-axis. Individual sample absorbance values were then compared to the standards values and the concentration was calculated according to the polynomial equation that describes the curve. In diluted samples, the concentration read from the standard curve was multiplied by the dilution factor. The sample's concentration was extrapolated if the absorbance values were below the lowest standard and above blank.

2.9 Statistical analysis

2.9.1 Statistical analysis of ELISA and RT-qPCR data

The significance of difference between groups of experimental data in ELISA and RT-qPCR analysis was determined using Wilcoxon matched-pairs rank test or Student's paired t-test. A P-value less than 0.05 was considered statistically significant. All statistical analysis was performed in GraphPad Prism 6.

2.9.2 Statistical analysis of Affymetrix microarrays

Statistical analysis of microarray data was done by Dr. Carsten Sticht from the Affymetrix Core Facility of Medical Research Center, Medical Faculty Mannheim. A Custom CDF Version 19 with ENTREZ based gene definitions was used to annotate the arrays[98]. The Raw fluorescence intensity values were normalized applying quantile normalization and RMA background correction. One-way-ANOVA was performed to identify differential expressed genes using a commercial software package SAS JMP10 Genomics, version 6, from SAS (SAS Institute, Cary, NC, USA). A false positive rate of a=0.05 with FDR correction was taken as the level of significance. Plots (3D Scatterplots and Venn diagrams) are made with JMP.

Further analysis of gene expression data was done in Microsoft Excel with self-made VBA scripts. Heat maps were generated in Morpheus application from Broad Institute. Gene families were selected from the Molecular Signatures Database from Broad Institute.

3   RESULTS

3.1   Experimental design

Titanium is a widely used material for implant fabrication. This is due to its superior mechanical properties and excellent biocompatibility. However, the development of chronic inflammation at the implant-tissue interface often leads to implant failure. High mechanical stress and friction between articulating surfaces causes the release of wear particles, which are recognized by the immune system as foreign bodies. Since macrophages are the key initiators of the foreign body reaction and orchestrators of inflammation, their reaction to titanium was tested.

To determine the reaction of macrophages to titanium an in vitro test system based on human peripheral blood-derived monocytes was developed. Monocytes were isolated from buffy coats and were cultured on titanium discs with a polished surface or on cell culture plastic for control. The size of titanium discs was optimized (13.7x2mm) to cover maximum surface in a well of a 24-well plate. To maximize the contact with titanium and increase RNA yield, $3x10^6$ cells ($2x10^6$ cells/ml) were seeded in each well. In order to mimic physiological conditions Macrophage-SFM medium was supplemented with 10^{-8}M Dexamethasone and 1ng/ml M-CSF. To simulate distinct activation states of macrophages, the cells were stimulated either with IFNγ or with IL-4. The experimental design is illustrated in Figure 3. In order to isolate high quality RNA for further microarray analysis cells were seeded in triplicates per stimulation. Supernatants and RNA were collected after 6 days of culture.
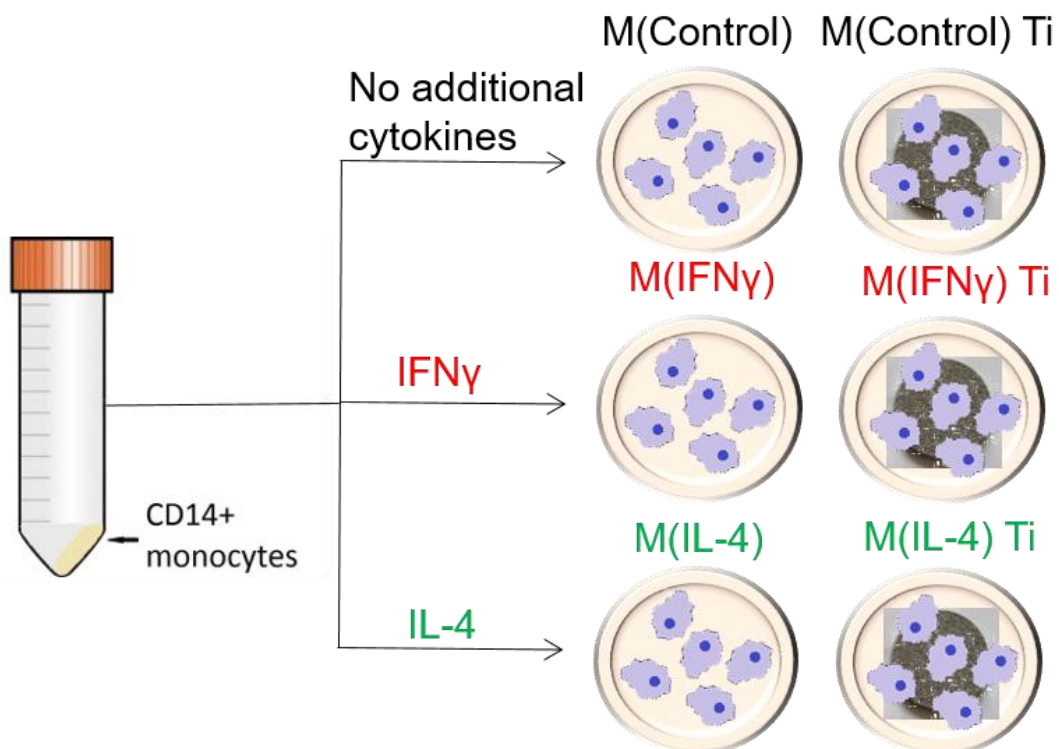
Figure 3. Schematic representation of the experimental design. Human peripheral blood monocytes were isolated from buffy coats by magnetic cell sorting using CD14 beads. M(IFNγ) and M(IL-4) macrophages have been generated by stimulating human monocytes with IFNγ and IL-4, correspondingly, for 6 days in serum-free medium. In this study the new nomenclature for designating macrophage activation and polarization will be used[52].

3.2 Analysis of macrophage reaction to polished titanium discs

3.2.1 Analysis of macrophage cytokine secretion induced by polished titanium

Macrophages control both acute inflammatory reactions and healing processes. IFNγ induces a pro-inflammatory cytokine profile in macrophages, while IL-4 is responsible for the activation of healing activities of macrophages. To determine if titanium is able to induce secretion of pro-inflammatory or anti-inflammatory cytokines, supernatants from macrophages cultured on polished titanium discs were analyzed by ELISA. As members of pro-inflammatory cytokines TNFα, IL-1β and IL-6 were chosen, while CCL18 was selected as a cytokine that displays anti-inflammatory properties.
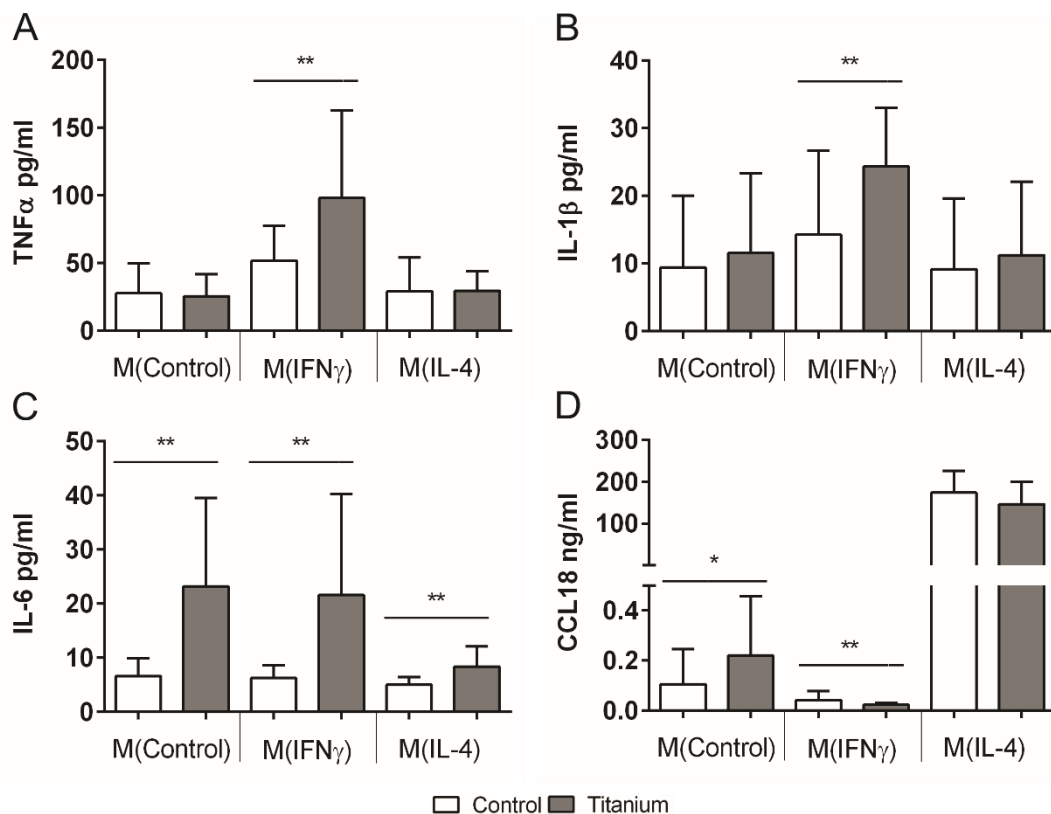
Figure 4. Macrophage cytokine secretion in response to polished titanium determined by ELISA. A. TNFα secretion; **B.** IL-1β secretion; **C.** IL-6 secretion; **D.** CCL18 secretion. All graphs represent mean values from 8 individual donors with standard deviations. For statistical analysis Wilcoxon matched-pairs rank test was used (* p < 0.05; ** p < 0.01).

Figure 4A illustrates the secretion of TNFα by macrophages in response to titanium. TNFα was significantly up-regulated by titanium in macrophages activated by IFNγ (98.2 ± 64.6pg/ml vs 51.9 ± 25.7pg/ml), while no difference was found in other activation states. Similar results were obtained when analyzing IL-1β secretion (Figure 4B), with up-regulated secretion in response to titanium in IFNγ stimulated macrophages (24.3 ± 8.6pg/ml vs 14.3 ± 12.4pg/ml). IL-6 (Figure 4C) was up-regulated by titanium regardless of the activation state, with the highest values in M(Control) (23.2 ± 16.3pg/ml vs 6.7 ± 3.2pg/ml) and M(IFNγ) (21.6 ± 18.7pg/ml vs 6.25 ± 2.4pg/ml). As expected, CCL18 was highest in M(IL-4). It was slightly down-regulated by titanium (146.6 ± 53.3ng/ml vs 173.9 ± 52.3ng/ml), however not statistically significant (Figure 4D). In M(IFNγ) titanium induces down-regulation of CCL18 (23.7 ± 7.3pg/ml vs 42.9 ± 34.8pg/ml), while in M(Control) up-regulation of CCL18 was detected (220 ±

236.2pg/ml vs 105.8 ± 139.8pg/ml). In summary, these data suggest that titanium induces the secretion of pro-inflammatory cytokines and, at the same time, inhibits the secretion of anti-inflammatory cytokines, thus promoting a pro-inflammatory state of macrophages.

3.2.2 Microarray gene expression analysis of macrophages stimulated by polished titanium

In order to analyze the effect of polished titanium on the gene expression in macrophages, peripheral blood CD14+ monocytes from 8 donors were cultured on polished titanium discs. On day 6 cells were harvested and used for RNA isolation. Based on RNA integrity number and concentration, RNA from 6 of them was chosen for microarray analysis. For each donor 6 different groups of macrophages were analyzed: M(Control), M(IFNγ), M(IL-4), M(Control) Ti, M(IFNγ) Ti and M(IL-4) Ti (Figure 3). The summary of microarray analysis of macrophage gene expression in response to polished titanium is presented in Figure 5.
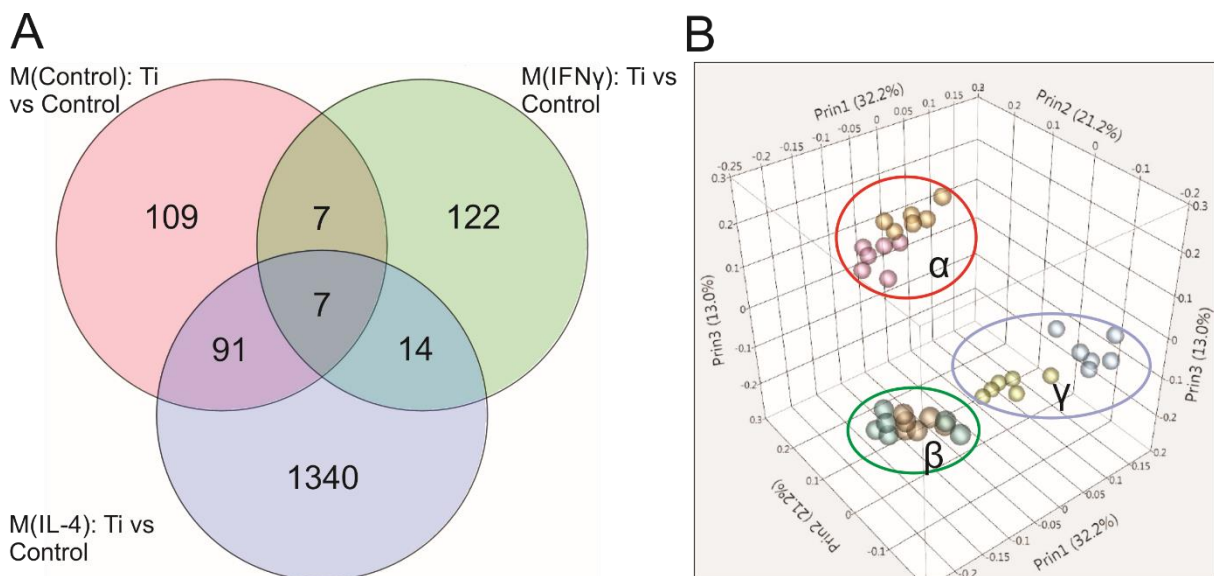
Figure 5: Summary of microarray analysis of gene expression in macrophages cultured on polished titanium discs. A. Venn's diagramm of differentially expressed genes in macrophages cultured with polished titanium vs control. Each number represents the number of genes differentially expressed in response to titanium. Each circle represents a population of macrophages with a different stimulation (Red – Control, Green – IFNγ, Blue - IL-4). Intersecting points represent the number of genes differentially regulated by polished titanium in 2 or more stimulations. **B.** Clustering of the microarray data in a 3D scatterplot. Each sphere represents genes from one donor. α - clustering of data from M(Control) (pink – Control; orange - Titanium); β - clustering of data from M(IFNγ) (green – Control; brown - Titanium); γ - clustering of data from M(IL-4) (yellow – Control; cyan - Titanium).

A total of 1690 genes were differentially regulated by polished titanium (Figure 5A). Whereof, 1452 genes were found statistically significant up- or down-regulated in M(IL-4), 214 genes in M(Control) and 150 genes in M(IFNγ). The 3D scatterplot confirmed these findings and revealed that polished titanium has the most pronounced effect on M(IL-4), while M(Control) and M(IFNγ) have more homogeneous populations (Figure 5B). The analysis also showed that titanium induces differential regulation of 14 common genes for both M(Control) and M(IFNγ), 98 common genes for M(Control)

and M(IL-4), 21 common genes for M(IFNγ) and M(IL-4), and 7 common genes across all 3 macrophage activation states (Figure 5A).

A number of gene families were found to be differentially regulated in macrophages cultured with polished titanium (Table 17). These included: metallothioneins (9 members), matrix metalloproteinases (6 members), cytokine-cytokine receptors (44 members), zinc fingers C2-H2 type (52 members), immunoglobulin-like domain containing (23 members) and endogenous ligands (25 members).

Table 17. Gene families that are differentially expressed in macrophages cultured on polished titanium discs.

Gene Family	No. of genes up/down-regulated	Biological function	Prominent Member
Metallothioneins	9	Metal binding and transport; control of oxidative stress	MT2A > 7 fold change
Matrix metalloproteinase	6	Breakdown of extracellular matrix	MMP9 > 6 fold change
Cytokine-cytokine receptor family	44	Role in cell signaling, inflammation and immunomodulation, hematopoiesis	TNFSF14 > 4 fold change
Zinc Fingers, C2-H2 type	52	Interaction modules that bind DNA, RNA, proteins	EGR1 > 5 fold change
Immunoglobulin-like domain containing	23	Receptors, co-receptors, co-stimulatory molecules, cell adhesion	TIE1 > 6 fold change
Endogenous ligands	25	Signal transduction	SPP1 > 5 fold change

To narrow down the number of genes, whose expression changed in response to polished titanium discs, a stimulation-specific gene profile based on Affymetrix microarray data was computed. For each stimulation, additionally to the statistical threshold ($p<0.05$), an arbitrary cut-off was introduced. Thus, only the genes in which the difference in signal intensity between control and titanium was higher than 1 were taken into profile. This cut-off corresponds to a 2-fold change in gene expression and is commonly used for microarray analysis[99]. Following this algorithm, the number of genes that are more biologically meaningful (in contrast to only statistically significant) up- or down-regulated in response to polished titanium stimulation was determined. Thus, in M(Control) titanium induced significant up-regulation of 36 genes, in M(IFNγ) up-regulation of 10 genes and down-regulation of 5 genes, while in M(IL-4) up-regulation of 164 genes and down-regulation of 10 genes. A list of genes that are most up-regulated and down-regulated in macrophages cultured on polished titanium discs vs control is presented in Figure 6. To obtain a better overview of the most affected genes, the gene list was divided into 4 groups: genes affected by titanium regardless of activation state (4 genes); genes from the cytokine-cytokine receptor family (10 genes); genes involved in extracellular matrix degradation (3 genes); other genes with at least a 3-fold change (51 genes). The analysis of microarray data using the algorithm for the identification of biologically meaningful differentially regulated genes in response to titanium, reinforced the previous findings and revealed that the highest number of affected genes were in M(IL-4) macrophages. Thus, macrophage activation state significantly influences the response to polished titanium.
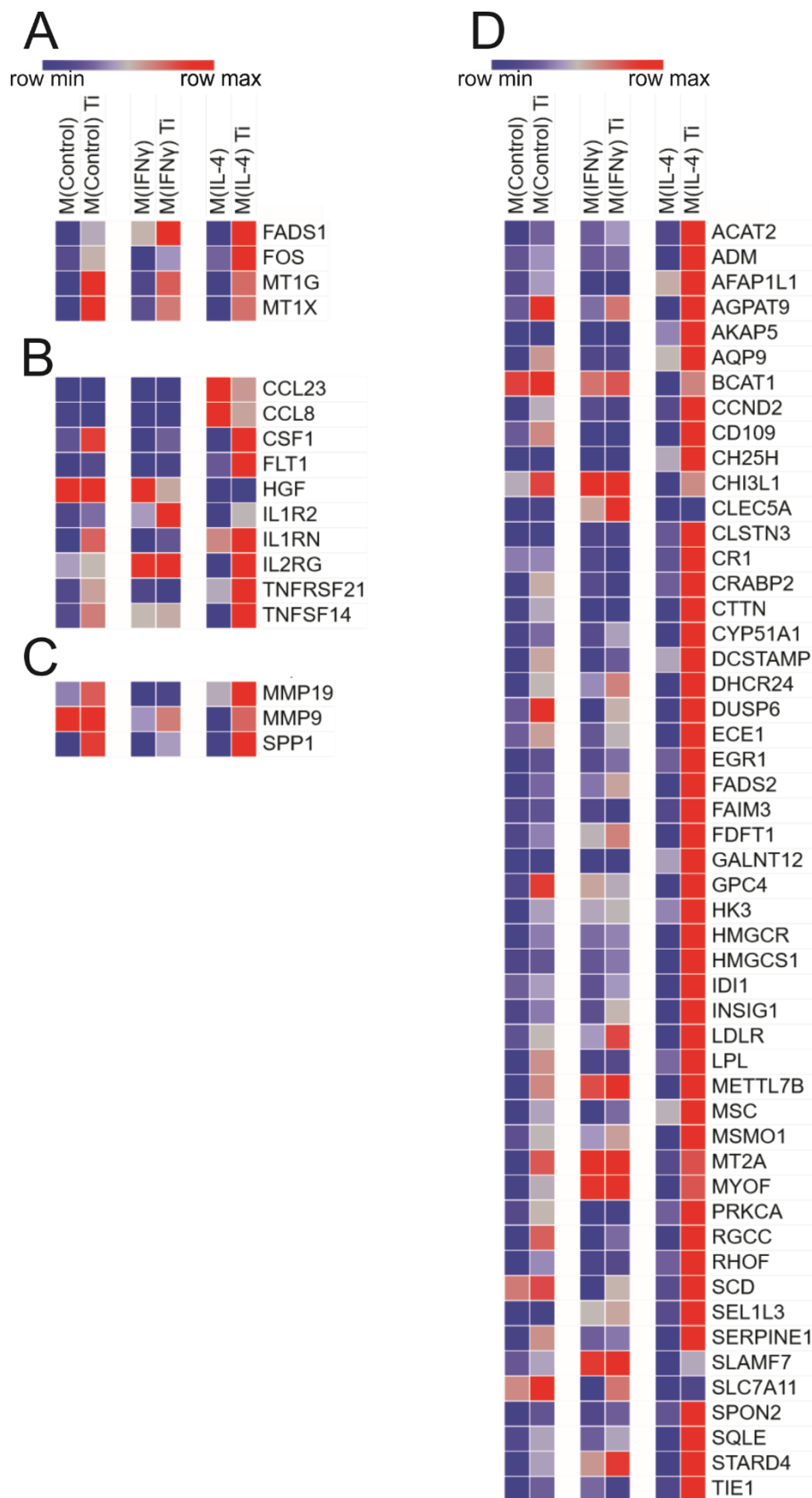
Figure 6. List of the most differentially regulated genes in macrophages cultured on polished titanium discs. A. Common genes for all activation states; **B.** Genes from cytokine-cytokine receptor family; **C.** Genes involved in extracellular matrix degradation; **D.** Genes with a 3-fold change. Colors indicate relative expression of each gene between different stimulations in the presence or absence of titanium. Genes are presented in alphabetical order.

3.2.3 Validation of microarray data obtained from macrophages cultured on polished titanium

Members of cytokine-cytokine receptors family and mediators of extracellular matrix degradation are key factors that control local level of inflammation and tissue remodeling. These are essential processes that define implant related complications. Therefore, several prominent members of these gene families were primarily selected from the microarray data for RT-qPCR validation (Figure 6). The following genes from cytokine-cytokine receptor family were analyzed: CSF1, CCL8, CCL23, TNFRSF21 and TNFSF14 (Figure 7). Additionally, the expression of three other members of the family (CCL13, CCL18 and IL17RB), for which titanium-induced differential expression was close to the selection criteria, were also analyzed due to their involvement in inflammation and implant related complications[100-102].
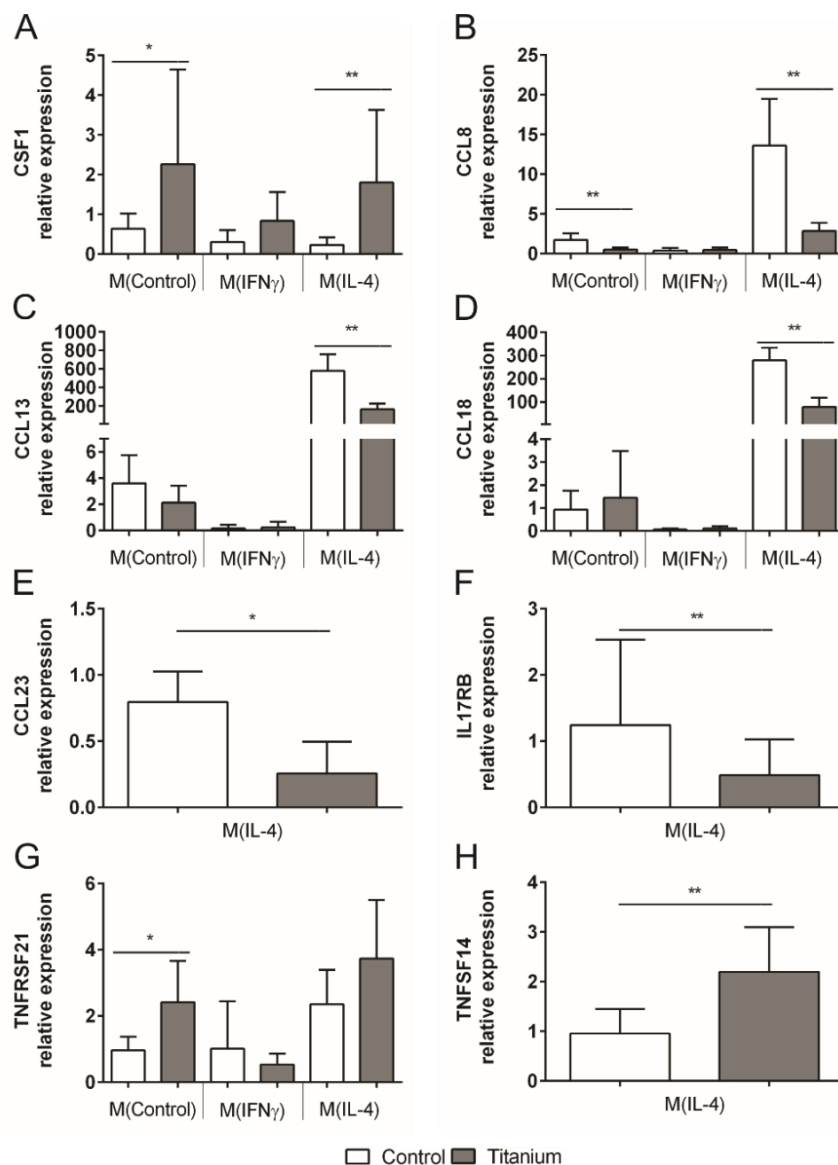
Figure 7. RT-qPCR analysis of expression of cytokine-cytokine receptor family genes in macrophages cultured on polished titanium discs. A. CSF1 expression; **B.** CCL8 expression; **C.** CCL13 expression; **D.** CCL18 expression; **E.** CCL23 expression; **F.** IL17RB expression; **G.** TNFRSF21 expression; **H.** TNFSF14 expression. All graphs represent mean values from 8 individual donors with standard deviations. In **E**, **F** and **H** only data for M(IL-4) is shown due to very low expression in other activation states (Ct > 40). For statistical analysis Wilcoxon matched-pairs rank test was used (* $p < 0.05$; ** $p < 0.01$).

CSF1 expression was significantly up-regulated by polished titanium in M(Control) (3.5 times) and in M(IL-4) (8 times) (Figure 7A). Similar findings were observed in the expression of TNFRSF21 and TNFSF14, with titanium up-regulating TNFRSF21 in M(Control) (2.5 times) and TNFSF14 in M(IL-4) (2.3 times) (Figures 7G and 7H). A different pattern was noted in the expression of CCL8, CCL13, CCL18, CCL23 and IL17RB. Titanium induced down-regulation of CCL8 expression in M(Control) (3.2 times) and in M(IL-4) (4.8 times) (Figure 7B). Likewise, titanium induced down-regulation of CCL13, CCL18, CCL23 and IL17RB expression in M(IL-4) (CCL13 – 3.5 times; CCL18 – 3.6 times; CCL23 – 3.1 times; IL17RB – 2.5 times) (Figures 7C, 7D, 7E and 7F).

Based on the stimulation-specific gene profile computed from the microarray data, two other genes (CHI3L1 and MMP9) were selected for RT-qPCR validation (Figure 8). CHI3L1 and MMP9 are involved in inflammation and tissue remodeling and, thus, potentially play a role in implant related complications[103, 104]. Additionally, the expression of two related genes (CHIT1 and MMP8), for which titanium-induced differential expression was close to the selection criteria, was also analyzed due to their involvement in implant related complications[105, 106]. CHIT1 and MMP8 expression was not significantly influenced by polished titanium stimulation, regardless of the activation state (Figures 8A and 8C). In contrast, CHI3L1 expression was up-regulated by polished titanium in all activation states: in M(Control) (2 times) in M(IFNγ) (1.8 times) and in M(IL-4) (3.3 times) (Figure 8B). While the highest expression levels for MMP9 were found in M(Control), MMP9 expression was stimulated by titanium only in M(IL-4) (5.1 times) (Figure 8D).
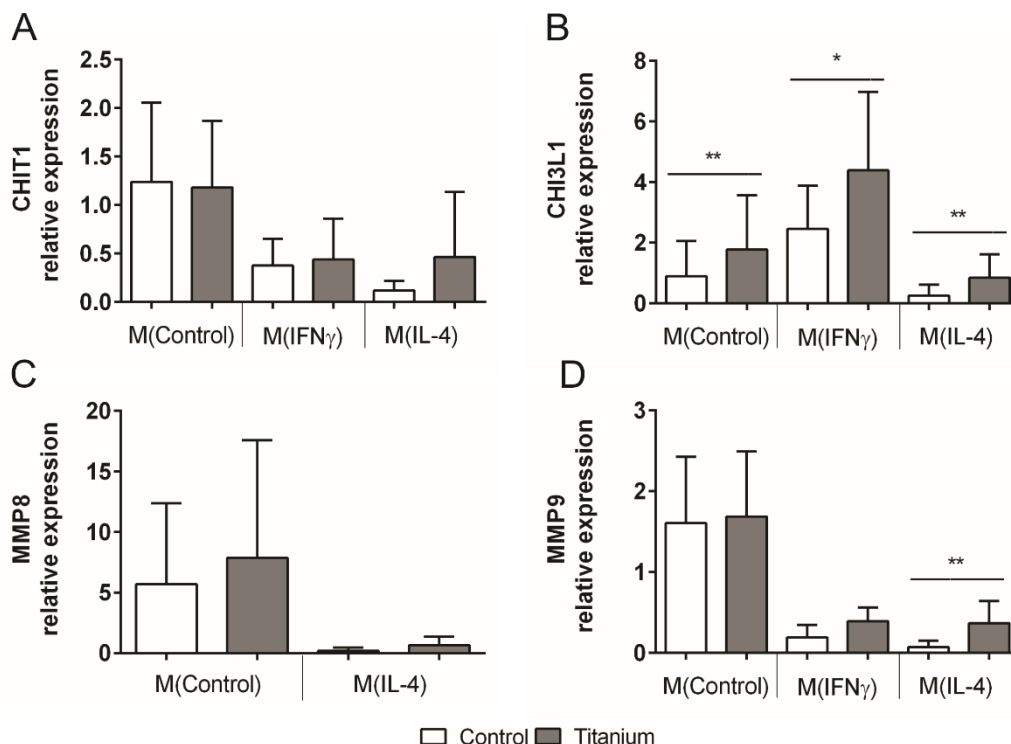
Figure 8. RT-qPCR analysis of expression of CHIT1, CHI3L1, MMP8 and MMP9 in macrophages cultured on polished titanium discs. A. CHIT1 expression; **B.** CHI3L1 expression; **C.** MMP8 expression; **D.** MMP9 expression. All graphs represent mean values from 8 individual donors with standard deviations. In **C** only data for M(Control) and M(IL-4) is shown due to very low expression in M(IFNγ) (Ct > 40). For statistical analysis Wilcoxon matched-pairs rank test was used (* $p < 0.05$; ** $p < 0.01$).

To determine if the same patterns of expression can be observed on the protein level, secretion of chitotriosidase, CHI3L1 (YKL-40), MMP-9 and TNFSF14 (LIGHT) was analyzed by ELISA. The secretion levels of chitotriosidase mirrors the results from RT-qPCR and was not statistically significantly changed under stimulation with polished titanium, although increased secretion in M(IL-4) was observed (32.3 ± 64.4ng/ml vs 0.7 ± 1.4ng/ml) (Figure 9A). Secretion of CHI3L1 maintained the same tendency observed on RT-qPCR (up-regulation upon titanium stimulation), however the changes were not statistically significant (Figure 9B). The biggest difference was noted in M(IL-4) where titanium increased CHI3L1 secretion to 60.5 ± 59.9ng/ml vs 1.3 ± 1.7ng/ml. MMP-9 secretion was significantly increased under polished titanium stimulation in M(Control) (156.9 ± 61.5ng/ml vs 73.1 ± 38.6ng/ml) and in M(IL-4) (133.4 ± 138.4ng/ml vs 1.4 ± 0.9ng/ml), while in M(IFNγ) no significant change was observed (Figure 9C). For TNFSF14, in contrast with data from RT-qPCR, there was no significant change on protein level, however the tendency for higher secretion in M(IL-4) under titanium stimulation (213.6 ± 210.9pg/ml vs 98.3 ± 13.5pg/ml) was maintained (Figure 9D).
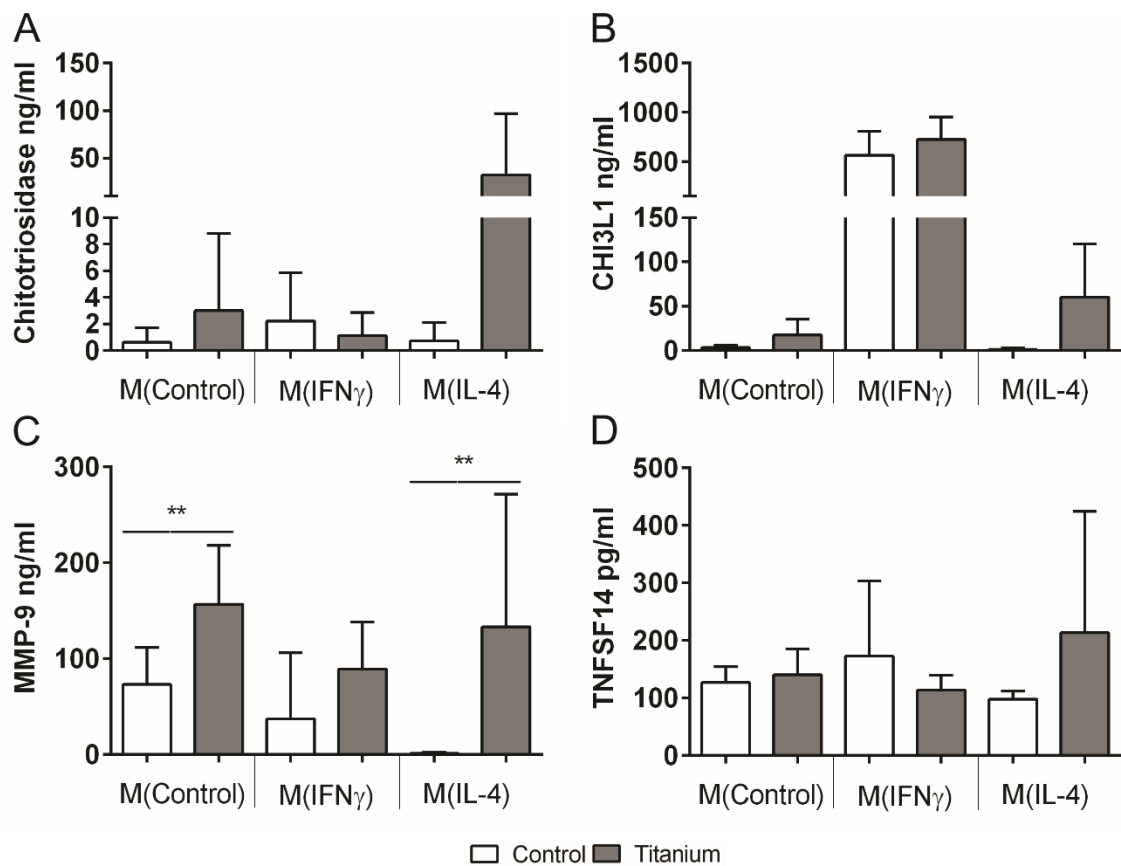
Figure 9. Secretion of chitotriosidase, CHI3L1, MMP-9 and TNFSF14 in macrophages cultured on polished titanium discs determined by ELISA. A. chitotriosidase secretion; **B.** CHI3L1 secretion; **C.** MMP-9 secretion; **D.** TNFSF14 secretion. All graphs represent mean values from 4 individual donors with standard deviations (except **C** – 8 donors). For statistical analysis Student's paired T test was used (* $p < 0.05$; ** $p < 0.01$).

In summary, RT-qPCR analysis provided a confirmation of microarray data. On protein level similar tendencies in expression patterns were observed. Altogether these results indicated that polished titanium is able to induce significant changes in the expression profile of genes involved in inflammation and extracellular matrix remodeling.

3.3 Analysis of macrophage reaction to porous titanium discs

3.3.1 Analysis of macrophage cytokine secretion induced by porous titanium

Since porous materials have been shown to promote osseointegration[86], it is reasonable to assume that these materials also display higher biocompatibility, and thus do not elicit a strong inflammatory reaction. In order to test this hypothesis, primary human macrophages were cultivated on porous titanium discs and cytokine production was analyzed by ELISA. TNFα was chosen as a pro-inflammatory cytokine, while CCL18 was selected as a cytokine that displays anti-inflammatory properties. Previous results have demonstrated that polished titanium significantly up-regulates MMP-9 secretion (section 3.2.3). To determine whether porous titanium also increases MMP-9 secretion, it was analyzed by ELISA.
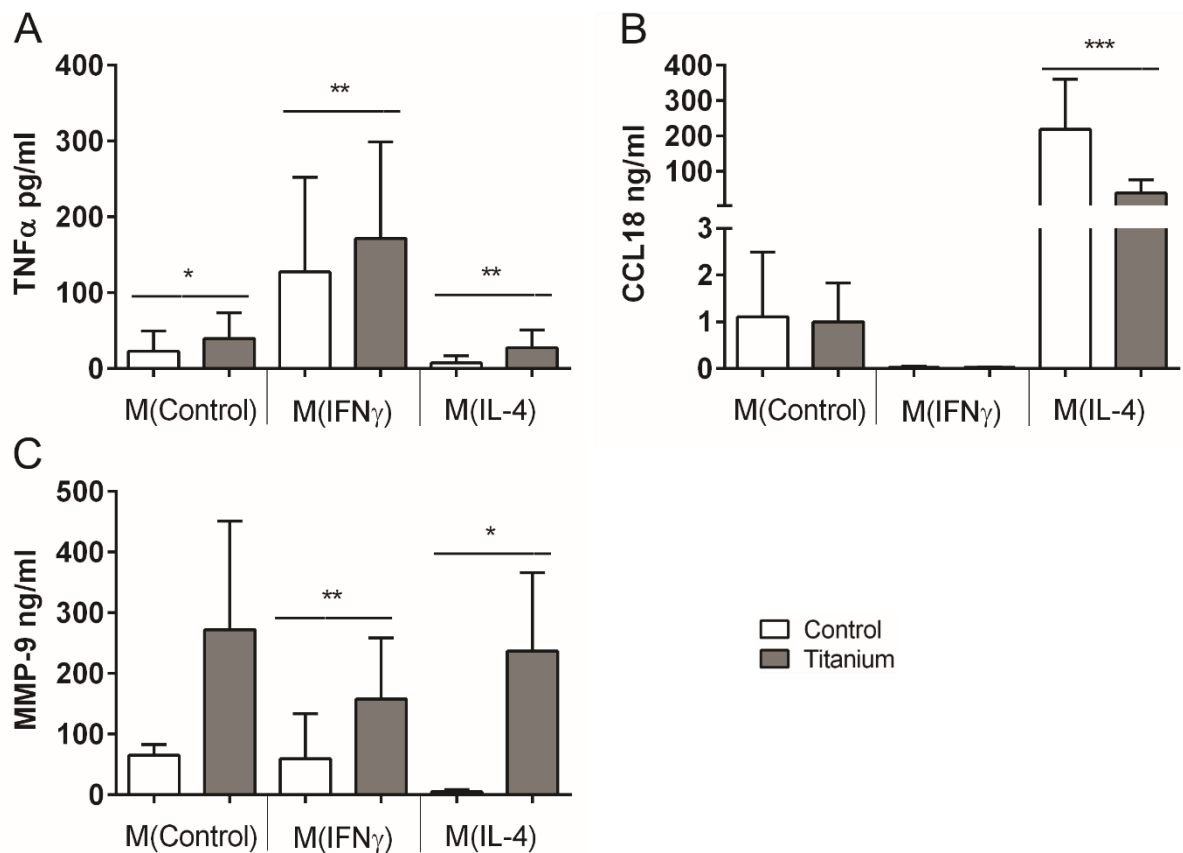
Figure 10. Secretion of TNFα, CCL18 and MMP-9 in macrophages cultured on porous titanium discs determined by ELISA. A. TNFα secretion; **B.** CCL18 secretion; **C.** MMP-9 secretion. **A** and **B** represent mean values with standard deviation from 11 individual donors, **C** from 4 donors. For statistical analysis Student's paired T test was used (* $p < 0.05$; ** $p < 0.01$; *** $p < 0.001$).

Figure 10A illustrates the secretion of TNFα by macrophages in response to porous titanium stimulation. TNFα was significantly up-regulated by titanium in all activation states: in M(Control) (39.9 ± 34pg/ml vs 22.8 ± 27.2pg/ml), in M(IFNγ) (171.9 ± 127.3pg/ml vs 127.6 ± 124.6pg/ml) and in M(IL-4) (27.6 ± 23.2pg/ml vs 7.4 ± 9.8pg/ml). In contrast porous titanium induced down-regulation of CCL18 only in M(IL-4) (38.6 ± 37.7ng/ml vs 218.9 ± 142.4ng/ml), while no difference was found in other activation states (Figure 10B). Secretion of MMP-9 was significantly up-regulated by porous titanium in M(IFNγ) (157.9 ± 100.5ng/ml vs 59.6 ± 73.9ng/ml) and M(IL-4) (237

± 129ng/ml vs 5.1 ± 3.5ng/ml). A tendency for higher secretion of MMP-9 was noted also in M(Control) (272.1 ± 178.8ng/ml vs 65.2 ± 17.7ng/ml), however the difference was not statistically significant (Figure 10C). Contrary to our initial hypothesis, these data indicate that porous titanium is able to induce the secretion of pro-inflammatory cytokines and matrix metalloproteinases and, at the same time, to inhibit the secretion of cytokines with anti-inflammatory properties, thus promoting both inflammation and matrix remodeling.

3.3.2 Microarray gene expression analysis of macrophages stimulated by porous titanium

Analysis of the secretion of TNFα, CCL18 and MMP-9 suggested that porous titanium induces similar changes in activation of pro-inflammatory and matrix remodeling activities of macrophages as those observed under polished titanium stimulation. In order to analyze the effect of porous titanium on the gene expression in macrophages, an Affymetrix microarray analysis was performed. To this end, RNA from macrophages cultured on porous titanium discs was isolated and samples from 8 donors out of 11 were chosen (based on RNA integrity number and concentration) for microarray analysis. For each donor 6 different groups of macrophages were analyzed: M(Control), M(IFNγ), M(IL-4), M(Control) Ti, M(IFNγ) Ti and M(IL-4) Ti (Figure 3). The summary of microarray analysis of macrophage gene expression in response to porous titanium is presented in Figure 11.
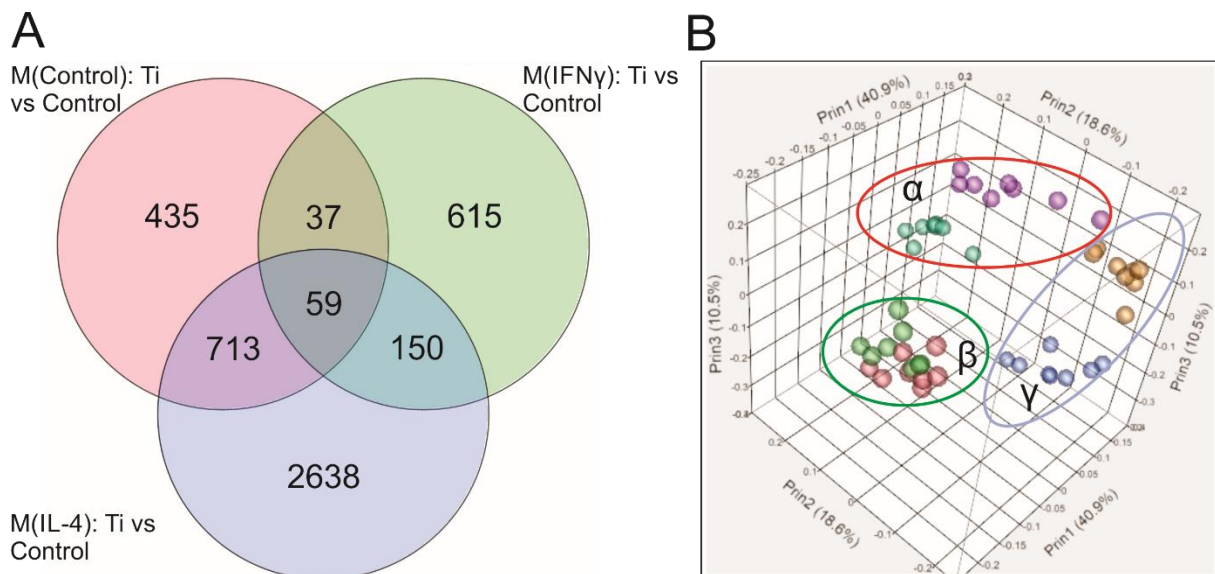
Figure 11. Summary of microarray analysis of gene expression in macrophages cultured on porous titanium discs. A. Venn's diagramm of differentially expressed genes in macrophages cultured with porous titanium vs control. Each number represents the number of genes differentially expressed in response to titanium. Each circle represents a population of macrophages with a different stimulation (Red – Control, Green – IFNγ, Blue - IL-4). Intersecting points represent the number of genes differentially regulated by porous titanium in 2 or more stimulations. **B.** Clustering of the microarray data in a 3D scatterplot. Each sphere represents genes from one donor. α - clustering of data from M(Control) (dark green – Control; violet - Titanium); β - clustering of data from M(IFNγ) (red – Control; green - Titanium); γ - clustering of data from M(IL-4) (blue – Control; orange - Titanium).

A total of 4648 genes were differentially regulated by porous titanium. Whereof, 1244 genes were found statistically significant up- or down-regulated in M(Control),

861 genes in M(IFNγ) and 3560 genes in M(IL-4). Microarray analysis also revealed that porous titanium induced differential regulation of 37 common genes for both M(Control) and M(IFNγ), 713 common genes for M(Control) and M(IL-4), 150 common genes for M(IFNγ) and M(IL-4), and 59 common genes across all 3 activation states of macrophages (Figure 11A). The 3D scatterplot confirmed these findings and showed that porous titanium has the most pronounced effect on M(IL-4) and M(Control), while M(IFNγ) have a more homogeneous population (Figure 11B).

Under stimulation with porous titanium a number of gene families were found to be differentially regulated in macrophages (Table 18). These are: metallothioneins (15 members), matrix metalloproteinases (6 members), cytokine-cytokine receptors (65 members), solute carrier family (92 members), chitinase-like proteins (3 members), integrins (19 members) and purinergic receptors (7 members).

Table 18. Gene families that are differentially expressed in macrophages cultured on porous titanium discs.

Gene Family	No. of genes diff. regulated	Biological function	Prominent Member
Metallothioneins	15	Metal binding and transport; control of oxidative stress	MT2A >5 fold change
Matrix metalloproteinase	6	Breakdown of extracellular matrix	MMP7 > 7 fold change
Cytokine-cytokine receptor family	65	Role in cell signaling, inflammation and immunomodulation, hematopoiesis	CSF1 > 2 fold change
Solute carrier family	92	Transmembrane transporters	SLC28A3 > 5 fold change
Chitinase-like proteins	3	Role in inflammation, angiogenesis	CHIT1 > 5 fold change
Integrins	19	Cell attachment, signal transduction	ITGA3 > 3 fold change
Purinergic receptors	7	Proliferation, migration, vascular reactivity, apoptosis, cytokine secretion	P2RY14 > 12 fold change

To narrow down the number of genes, whose expression changed in response to porous titanium discs, the algorithm described in section 3.2.2 was employed. Thus, a stimulation-specific gene profile based on Affymetrix microarray data, similar to the one used for polished titanium discs, was computed. Following this algorithm, the number of genes that are more biologically meaningful (in contrast to only statistically significant) up- or down-regulated in response to porous titanium stimulation was determined. In M(Control) porous titanium induced significant up-regulation of 74 genes and down-regulation of 4 genes, in M(IFNγ) up-regulation of 7 genes and down-regulation of 22 genes, while in M(IL-4) up-regulation of 121 genes and down-regulation of 49 genes. A list of genes that are most up-regulated and down-regulated in macrophages cultured on porous titanium discs vs control is presented in Figure 12. To obtain a better overview of the most affected genes, the gene list was divided into 4 groups: genes affected by porous titanium regardless of the activation state (9 genes); genes from the cytokine-cytokine receptor family (14 genes); genes involved in extracellular matrix degradation (6 genes); other genes with at least a 3-fold change (54 genes). The analysis of microarray data using the algorithm for the identification of biologically meaningful differentially regulated genes revealed that the highest number

of genes affected by porous titanium were in M(IL-4) macrophages. Thus, macrophage activation state significantly influences the response to porous titanium.
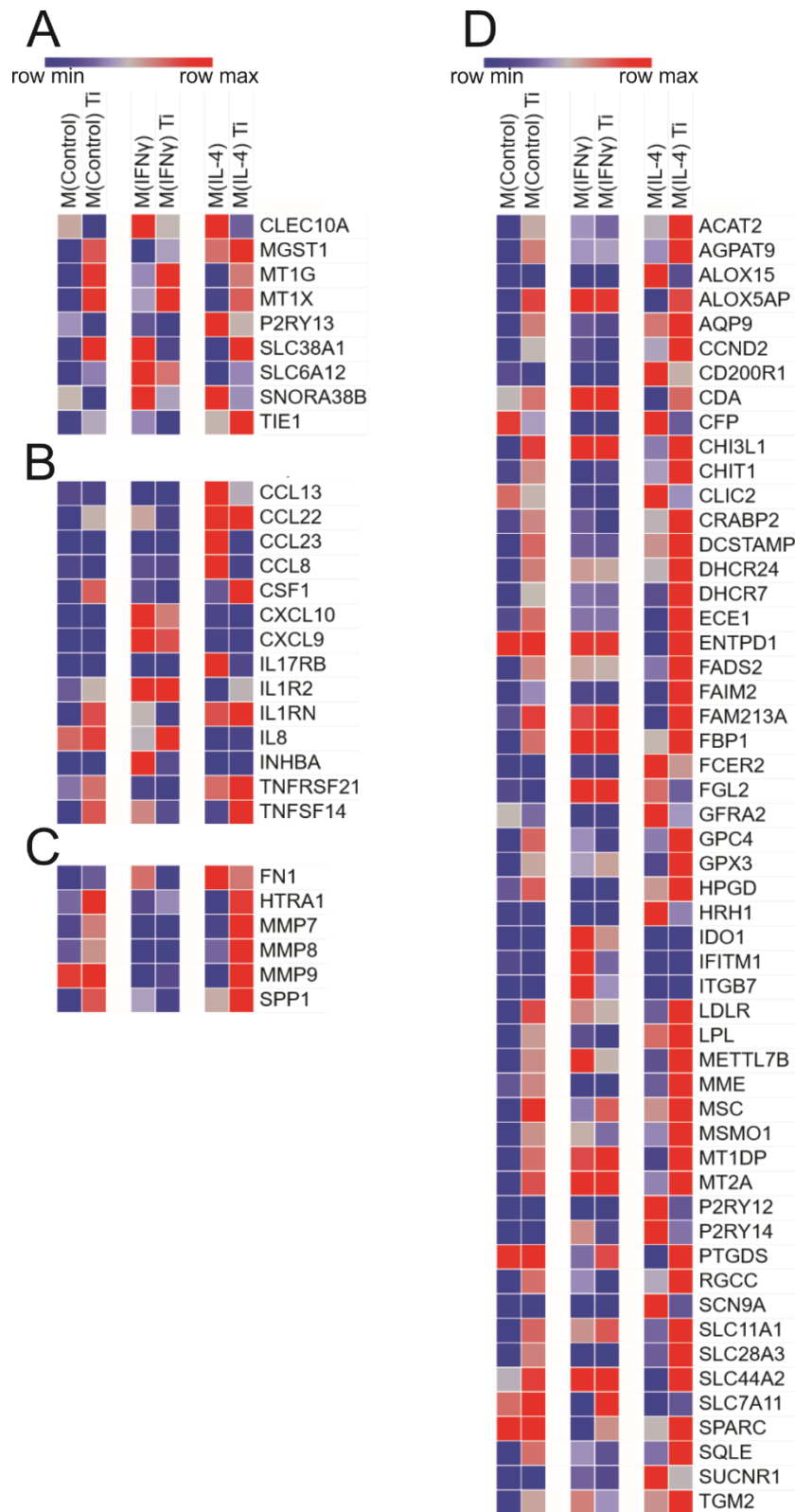

Figure 12. List of the most differentially regulated genes in macrophages cultured on porous titanium discs. A. Common genes for all activation states; **B.** Genes from cytokine-cytokine receptor family; **C.** Genes involved in extracellular matrix degradation; **D.** Genes with at least a 3-fold change. Colors indicate relative expression of each gene between different stimulations in the presence or absence of titanium. Genes are presented in alphabetical order.

3.3.3 Validation of microarray data obtained from macrophages cultured on porous titanium

Mediators of inflammation and matrix remodeling play an important role in implant related complications[107]. To confirm the results obtained by microarray analysis, several genes from the cytokine-cytokine receptor family were selected for RT-qPCR validation, namely: CSF1, CCL8, CCL13, CCL18, CCL23, IL17RB, TNFRSF21 and TNFSF14 (Figure 13).
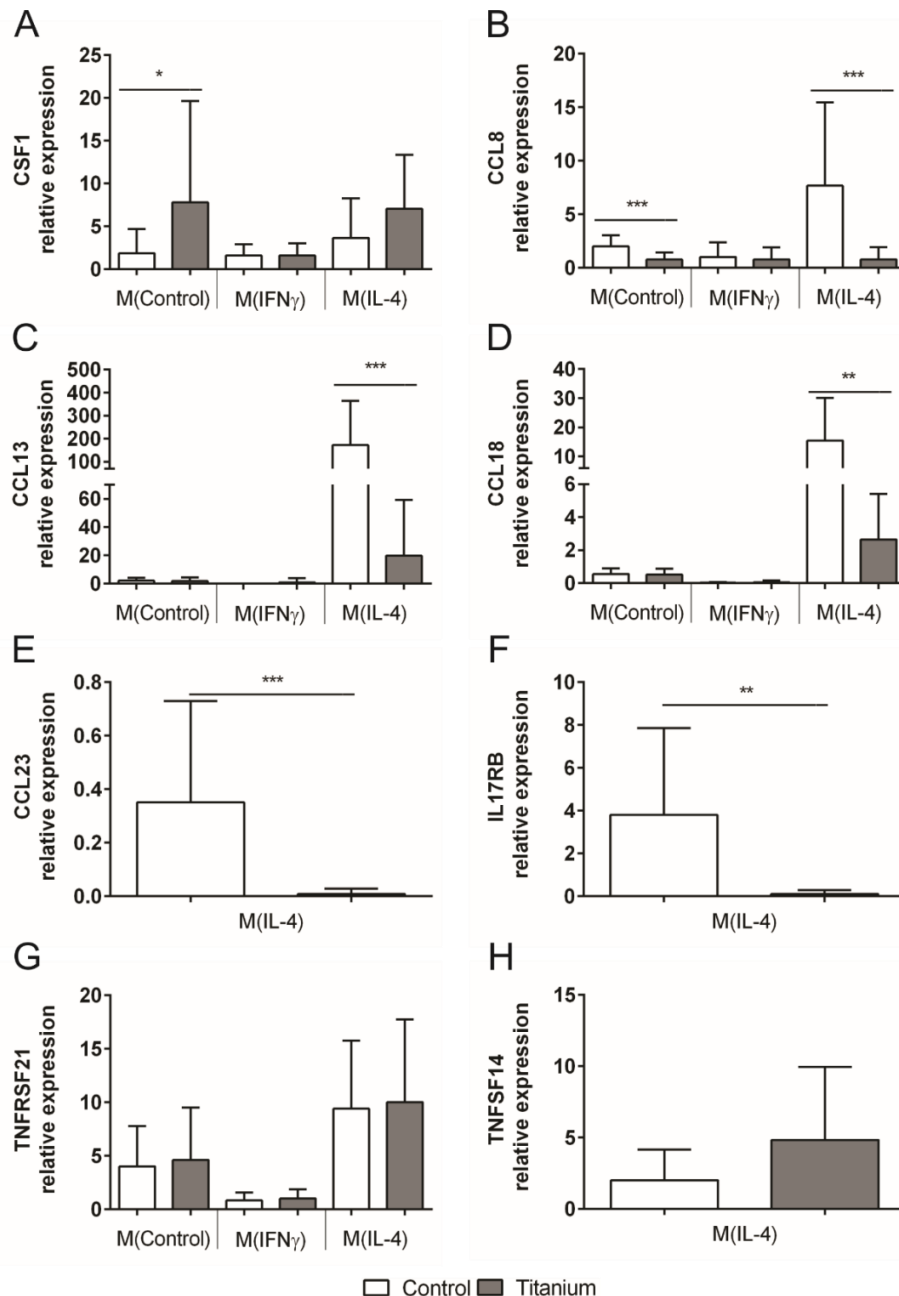
Figure 13. RT-qPCR analysis of expression of genes from cytokine-cytokine receptor family in macrophages cultured on porous titanium discs. A. CSF1 expression; **B.** CCL8 expression; **C.** CCL13 expression; **D.** CCL18 expression; **E.** CCL23 expression; **F.** IL17RB expression; **G.** TNFRSF21 expression; **H.** TNFSF14 expression. Graphs **A**, **B**, **C**, **E**, **G**, **H** represent mean values with standard deviations from 11 individual donors, **D** – from 9 donors, **F** – from 10 donors. In **E**, **F** and **H** only data for M(IL-4) is shown due to very low expression in other activation states (Ct > 40). For statistical analysis Wilcoxon matched-pairs rank test was used (* $p < 0.05$; ** $p < 0.01$; *** $p < 0.001$).

CSF1 expression was significantly up-regulated by porous titanium in M(Control) (4.2 times). A tendency for higher CSF1 expression upon titanium stimulation was noted in M(IL-4), however it was not statistically significant (Figure 13A). The expression pattern of CCL8 showed a clear down-regulation in macrophages cultured on porous titanium in M(Control) (2.6 times) and in M(IL-4) (9.7 times) (Figure 13B). Similar results were observed in the analysis of CCL13, CCL18, CCL23 and IL17RB expression, where porous titanium induced down-regulation of gene expression in M(IL-4) (CCL13 – 8.7 times; CCL18 – 5.8 times; CCL23 – 38.9 times; IL17RB – 32.6 times) (Figures 13C, 13D, 13E and 13F). In contrast, TNFRSF21 and TNFSF14 expression was not significantly influenced by porous titanium (Figures 13G and 13H). Although a tendency for higher TNFSF14 expression in titanium samples in M(IL-4) was observed, the difference was not statistically significant (Figure 13H).

Additionally, several genes (CHIT1, CHI3L1, MMP8 and MMP9), with potential role in implant related complications, due to their involvement in inflammation and tissue remodeling, were selected for RT-qPCR validation (Figure 14). Thus, it was noted that porous titanium induces up-regulation in CHIT1 expression regardless of the activation state: in M(Control) (4 times), in M(IFNγ) (1.4 times) and in M(IL-4) (4.4 times) (Figure 14A). Similarly, CHI3L1 expression was up-regulated by titanium in M(Control) (3.5 times) and in M(IL-4) (2.5 times) (Figure 14B). Expression of MMP8 and MMP9 was also up-regulated by titanium in M(IL-4) (MMP8 – 4.7 times; MMP9 – 3 times), with tendencies of higher expression observed in M(Control) (Figures 14C and 14D).
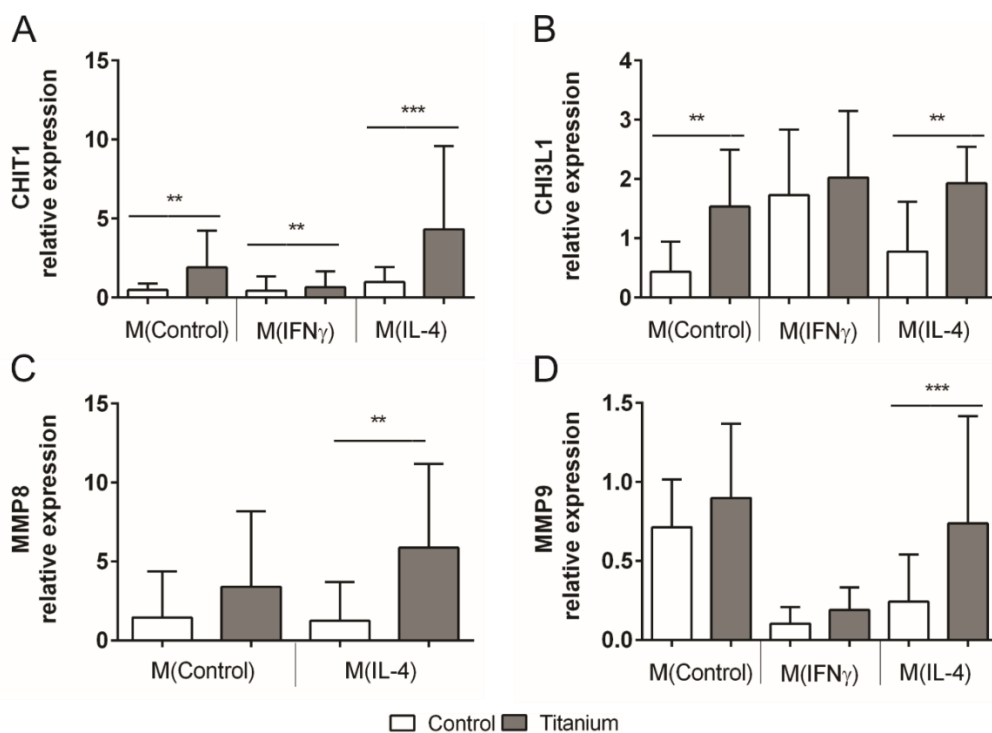
Figure 14. RT-qPCR analysis of expression of CHIT1, CHI3L1, MMP8 and MMP9 in macrophages cultured on porous titanium discs. A. CHIT1 expression; **B.** CHI3L1 expression; **C.** MMP8 expression; **D.** MMP9 expression. All graphs represent mean values from 11 individual donors with standard deviations. In **C** only data for M(Control) and M(IL-4) is shown due to very low expression in M(IFNγ) (Ct > 40). For statistical analysis Wilcoxon matched-pairs rank test was used (* p < 0.05; ** p < 0.01).

In summary these results indicate that porous titanium, similarly to polished titanium, is able to induce significant changes in the expression of genes involved in inflammation and extracellular matrix remodeling, especially in M(IL-4) activation state.

3.4 Comparison of macrophage reactions to Ti discs, Ti microbeads and Ti nanoparticles

It was reported that THP-1 cells have a slightly different cytokine release pattern when exposed to titanium discs in comparison to titanium particles, suggesting that the size of titanium also influences the immune reaction[82]. To determine if human peripheral blood-derived monocytes exhibit similar properties, an experiment involving polished titanium discs, titanium microbeads (µTi) and titanium nanoparticles (nTi) was designed. The previously described experimental setup (Figure 3) was used with the addition of the new materials.

In order to study if the size of titanium is able to alter the secretion of inflammatory or anti-inflammatory cytokines, supernatants from macrophages cultured on polished titanium discs, µTi and nTi were analyzed by ELISA. TNFα was chosen as a model of pro-inflammatory cytokines, while CCL18 was selected as a cytokine that displays anti-inflammatory properties.

In contrast to previous results, there was no significant change in secretion of TNFα induced by any type of titanium regardless of the activation state (Figure 15A). However, CCL18 secretion was down-regulated upon stimulation with any type of titanium in M(IL-4), with a significant difference in secretion between µTi and nTi (192.6 ± 113.7ng/ml vs 40.9 ± 36.5ng/ml) (Figure 15B).
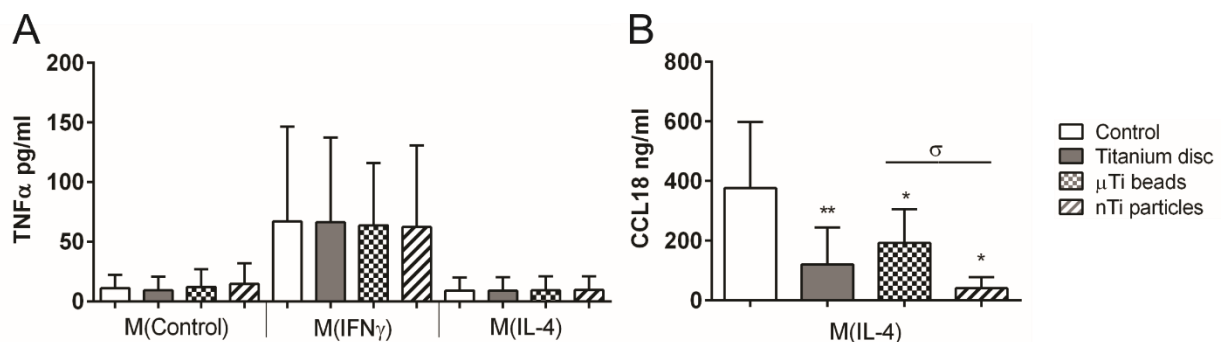
Figure 15. Effect of Ti discs, Ti microbeads and Ti nanoparticles on macrophage secretion of TNFα and CCL18. Cytokine secretion was determined by ELISA. **A.** TNFα secretion; **B.** CCL18 secretion. **A.** represents mean values with standard deviation from 4 individual donors, **B.** from 5 individual donors. In **B** only data for M(IL-4) is shown due to very low secretion levels in other activation states. For statistical analysis Student's paired T test was used. * denotes statistical significance between titanium and control of the respective activation state, while σ denotes statistical significance between different types of titanium (* p < 0.05; ** p < 0.01; σ p < 0.05).

Previous results revealed that titanium is able to alter the expression of several genes from cytokine-cytokine receptor family. To analyze whether titanium µTi and nTi induce a different expression pattern of CSF1, CCL8, CCL13, CCL23, IL17RB and TNFSF14 in comparison to polished titanium discs, RT-qPCR was performed (Figure 16). The expression of CSF1 correlated with previous data. In both M(Control) and M(IL-4) polished Ti discs and nTi up-regulated the expression of CSF1 compared to control, while no significant effect was observed in µTi samples. Additionally, nTi significantly up-regulated CSF1 expression compared to both Ti discs (3.9 times) and µTi (5.6 times). Similar results were observed in M(IFNγ) where nTi induced higher expression of CSF1 compared to Ti discs (6.9 times). In M(IL-4) both Ti discs and nTi up-regulated CSF1 expression compare to µTi (5.2 times and 3.3 times respectively) (Figure 16A). A different expression pattern was observed for CCL8. In M(Control) and

M(IL-4) all types of titanium down-regulated CCL8 expression, while no changes were noted in M(IFNγ). There was a significant difference in CCL8 expression between nTi and µTi (2.2 times) in M(Control). In M(IL-4) both Ti discs and µTi expressed higher levels of CCL8 compared to nTi (5.5 times and 7.1 respectively) (Figure 16B).
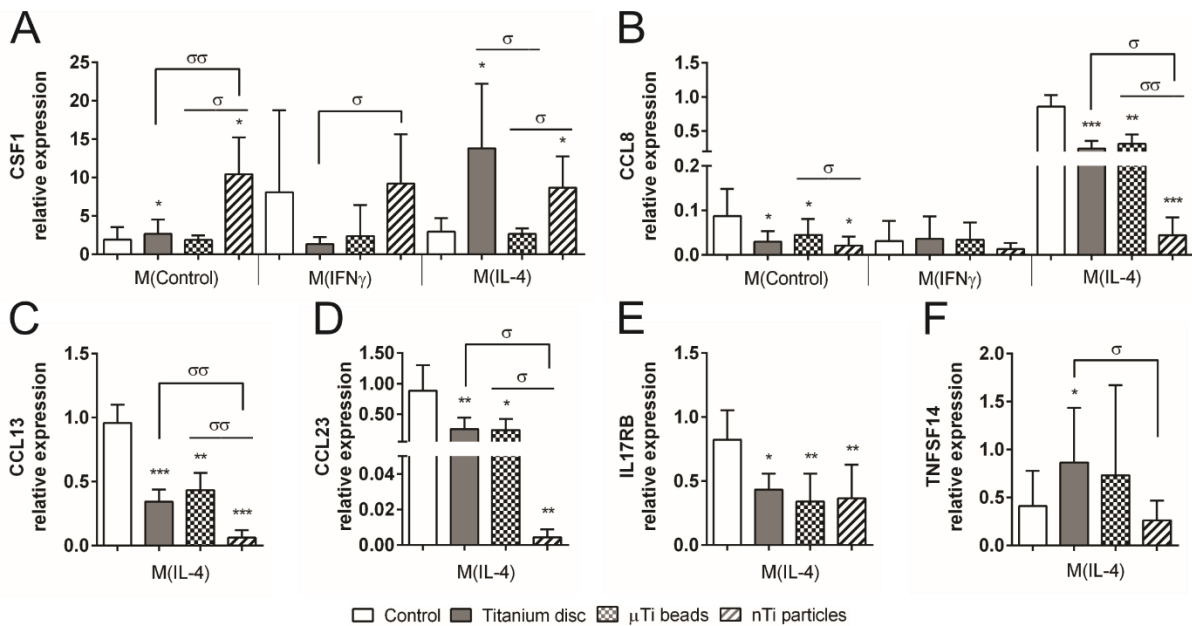

Figure 16. Comparison of gene expression from cytokine-cytokine receptor family in macrophages cultured on Ti discs, Ti microbeads and Ti nanoparticles. Gene expression was measured by RT-qPCR. **A.** CSF1 expression; **B.** CCL8 expression; **C.** CCL13 expression; **D.** CCL23 expression; **E.** IL17RB expression; **F.** TNFSF14 expression. All graphs represent mean values from 5 individual donors with standard deviations. In **C**, **D**, **E** and **F** only data for M(IL-4) is shown due to very low expression in other activation states (Ct > 40). For statistical analysis Student's paired T test was used. * denotes statistical significance between titanium and control of the respective activation state, while σ denotes statistical significance between different types of titanium (* $p < 0.05$; ** $p < 0.01$; *** $p < 0.001$; σ $p < 0.05$; σσ $p < 0.01$).

Similar results were obtained in the analysis of CCL13, CCL23 and IL17RB expression in M(IL-4), where all types of titanium down-regulated their expression compared to control (Figures 16C, 16D and 16E). The lowest expression of CCL13 and CCL23 was induced by nTi and was significantly lower than in Ti discs (CCL13 – 5.6 times; CCL23 – 59 times) and in µTi (CCL13 – 7 times; CCL23 – 55.8 times) (Figures 16C and 16D). TNFSF14 expression in M(IL-4) was up-regulated by Ti discs compared to control, with a similar tendency observed in µTi samples. Additionally, TNFSF14 expression induced by Ti discs was significantly higher than in nTi (3.3 times) (Figure 16F).

To verify if µTi and nTi in comparison to polished titanium discs differentially regulate the expression of other genes with potential implication in implant related complications, the expression of CHIT1, CHI3L1, MMP7 and MMP9 was analyzed by RT-qPCR (Figure 17). Expression of CHIT1 was significantly up-regulated compared to control only by nTi in both M(Control) and M(IFNγ), with no difference in expression in M(IL-4). In M(Control) nTi also induced higher levels of CHIT1 when compared with both Ti discs (12.4 times) and µTi (6.3 times), with similar findings in M(IFNγ) (compared to Ti discs – 8.3 times; to µTi – 5.4 times) (Figure 17A). Similar results were obtained in the analysis of CHI3L1 expression with nTi displaying highest levels of expression. In M(Control) both µTi and nTi induced up-regulation of CHI3L1 expression compared to Ti discs (µTi – 1.5 times; nTi – 4.6 times). In M(IL-4) only Ti discs and nTi

up-regulated CHI3L1 expression compared to control, with nTi displaying higher levels compared to both Ti discs (1.8 times) and µTi (3.1 times) (Figure 17B).
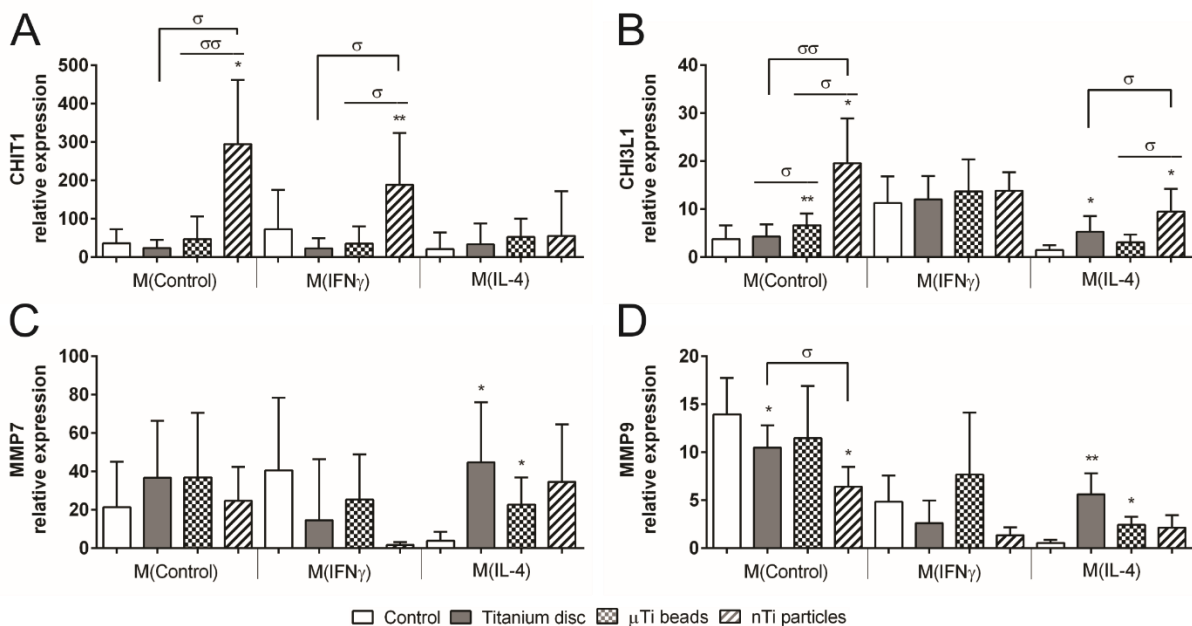

Figure 17. Comparison of CHIT1, CHI3L1, MMP7 and MMP9 gene expression in macrophages cultured on Ti discs, Ti microbeads and Ti nanoparticles. Gene expression was measured by RT-qPCR. **A.** CHIT1 expression; **B.** CHI3L1 expression; **C.** MMP7 expression; **D.** MMP9 expression. All graphs represent mean values from 5 individual donors with standard deviations. For statistical analysis Student's paired T test was used. * denotes statistical significance between titanium and control of the respective activation state, while σ denotes statistical significance between different types of titanium (* $p < 0.05$; ** $p < 0.01$; σ $p < 0.05$; σσ $p < 0.01$).

Previous results from the polished titanium experiment did not show significant changes in MMP8 expression (section 3.2.3). For this reason it was decided to focus on the analysis of MMP7 which showed up-regulation in polished titanium samples in the microarray data, although not statistically significant. MMP7 expression was significantly up-regulated in M(IL-4) by Ti discs and µTi, with nTi presenting the same tendency. However, no significant change in MMP7 between Ti types was observed regardless of the activation state (Figure 17C). In contrast, the size of titanium had an effect on the MMP9 expression. In M(Control) both Ti discs and nTi down-regulated MMP9 expression. Additionally, nTi displayed a significantly lower level of expression compared to Ti discs (1.6 times). In M(IL-4) a different scenario could be recognized, in which Ti discs and µTi up-regulated MMP9 expression, with nTi displaying the same tendency (Figure 17D).

In order to identify whether patterns of MMP-7 and MMP-9 gene expression correspond to the patterns of protein production, their secretion levels were analyzed by ELISA. MMP-7 partially confirmed the results from RT-qPCR with tendencies of up-regulation in M(IL-4) present in all Ti types. No significant difference was noted between the different types of Ti (Figure 18A). Secretion of MMP-9 was significantly up-regulated by Ti discs and nTi in M(IL-4) and the same tendency was noted for µTi as well, correlating with RT-qPCR data. However, no significant differences were observed between all Ti types in all activation states (Figure 18B).
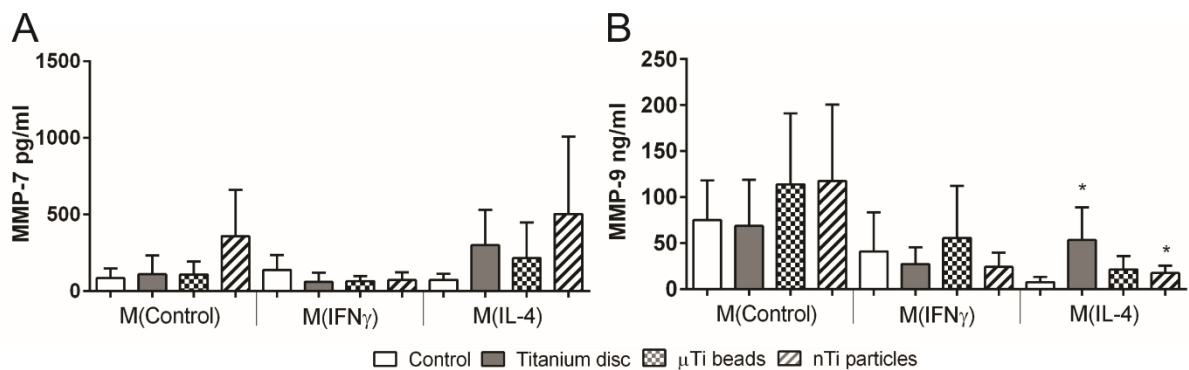
Figure 18. Effect of Ti discs, Ti microbeads and Ti nanoparticles on macrophage secretion of MMP-7 and MMP-9. MMP secretion was determined by ELISA. **A.** MMP-7 secretion; **B.** MMP-9 secretion. Both graphs represent mean values with standard deviation from 5 individual donors. For statistical analysis Student's paired T test was used. * denotes statistical significance between titanium and control of the respective activation state, while σ denotes statistical significance between different types of titanium (* $p < 0.05$; ** $p < 0.01$; σ $p < 0.05$).

The comparison of macrophage reactions to Ti discs, Ti microbeads and Ti nanoparticles revealed that all 3 types of titanium induce similar reactions in macrophages in terms of cytokine expression and production as well as in expression and secretion of matrix remodeling proteases. However, macrophages cultured with nTi generally displayed stronger reactions to the material, suggesting that nanoparticle phagocytosis enhances these reactions.

3.5 Analysis of the combined effects of bacteria and titanium on macrophage cytokine secretion

It is well established that biofilm formation is one of the reasons for implant failures[108]. To determine if bacteria found in orthopedic infections of titanium implants can influence the secretion of inflammatory cytokines by macrophage an experiment with Staphylococcus aureus and polished titanium was designed. For this purpose, heat killed Staphylococcus aureus (SA) was added to mature macrophages on day 6, and cells were cultured for additional 24h. The secretion of cytokines in response to SA stimulation was measured by ELISA. As pro-inflammatory cytokines TNFα, IL-1β, IL-6 and IL-8 were chosen, while CCL18 was selected as a cytokine that displays anti-inflammatory properties.
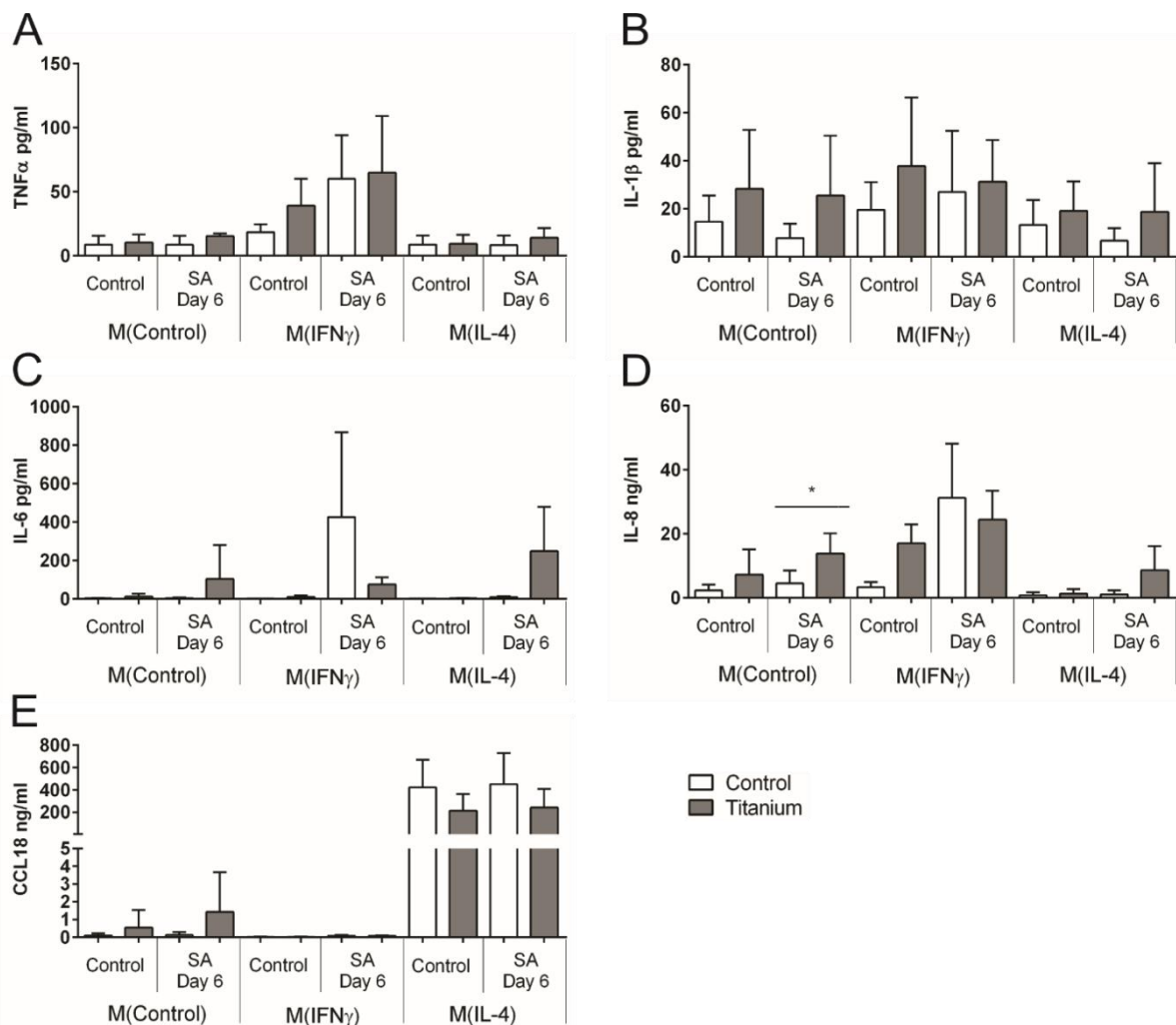
Figure 19. Cytokine secretion of mature macrophages upon stimulation with Staphylococcus aureus in the presence of titanium. SA was added to mature macrophages on day 6, and cells were cultured for additional 24h. Protein concentrations were measured by ELISA on day 7 of culture. **A.** TNFα secretion; **B.** IL-1β secretion; **C.** IL-6 secretion; **D.** IL-8 secretion; **E.** CCL18 secretion. All graphs represent mean values from 4 individual donors with standard deviations. For statistical analysis Student's paired T test was used (* $p < 0.05$; ** $p < 0.01$). SA – heat killed staphylococcus aureus; Control – macrophages without SA stimulation; SA Day 6 – macrophages stimulated with SA on day 6.

Figure 19A illustrates the secretion of TNFα by macrophages in response to polished titanium alone or in combination with SA. The highest levels of TNFα were

secreted in M(IFNγ) challenged with SA alone and in combination with polished titanium, however no significant difference in response to SA was observed in the presence of titanium (60.1 ± 33.9pg/ml vs 64.8 ± 44.4pg/ml). Similar results were obtained in the analysis of IL-1β secretion (Figure 19B). The highest levels of IL-6 secretion were in M(IFNγ) in SA alone, while in combination with titanium the levels of IL-6 were much lower (426.3 ± 441.1pg/ml vs 75 ± 38.3pg/ml). A different pattern was noted in M(IL-4) where the combination of SA and polished titanium induced higher levels of IL-6 when compared to SA alone (9.4 ± 4.9pg/ml vs 249.9 ± 229.3pg/ml) (Figure 19C). Secretion of IL-8 was significantly higher in M(IFNγ) in titanium samples when compared to control, as well as in SA alone and in SA in combination with titanium. A slight decrease was observed in SA in combination with titanium when compared to SA alone (31.2 ± 16.9ng/ml vs 24.5 ± 8.9ng/ml). In contrast, in M(Control) SA alone induced significantly lower production of IL-8 when compared to SA in combination with polished titanium discs (4.5 ± 4ng/ml vs 13.8 ± 6.3ng/ml) (Figure19D). The highest secretion levels for CCL18 were found in M(IL-4), while SA had no additional effect on CCL18 secretion in all types of macrophages. Titanium decreased CCL18 secretion in both control settings and when combined with SA (Figure 19E).

Infection and inflammation induce recruitment of monocytes into the tissue[109]. In order to examine if Staphylococcus aureus induces stronger reaction in naive monocytes during differentiation to mature macrophages, an experiment was designed with SA added on day 0 to naive monocytes cultured on titanium. Monocytes were differentiated in 3 subtypes of macrophages (M(Control), M(IFNγ), M(IL-4)), and on day 7 of culture the supernatants were analyzed by ELISA.

As expected, when SA was added to naive monocytes significantly higher cytokine levels were accumulated during the differentiation process. SA induced the highest levels of TNFα secretion in M(IFNγ). When combined with polished titanium, a tendency to inhibit TNFα secretion (34.6 ± 40ng/ml vs 27 ± 22.5ng/ml) was observed, however not statistically significant. In M(Control) and M(IL-4) no significant changes between SA alone and SA in combination with titanium were noted (Figure 20A). Similar results were obtained in the analysis of IL-1β secretion, where in all activation states SA alone induced the highest secretion levels. The most elevated levels were detected in M(IFNγ) in which SA alone induced a significantly higher secretion than when combined with polished titanium (1.3 ± 0.6ng/ml vs 0.9 ± 0.5ng/ml) (Figure 20B). IL-6 secretion was significantly up-regulated by SA in all activation states, with highest levels in M(Control) and M(IFNγ). Still, no significant difference was observed between SA alone and SA in combination with polished titanium (Figure 20C).

Similar results were noted in the analysis of IL-8 secretion. The highest levels were observed in M(IFNγ) and no significant difference was noted between SA alone and SA in combination with titanium (Figure 20D). In contrast to mature macrophages (Figure 19E), monocytes that underwent differentiation in the presence of SA alone in M(IL-4) secreted significantly higher levels of CCL18 (Figure 20E). When combined with polished titanium, CCL18 secretion was strongly inhibited, although not statistically significant (1253.4 ± 1040.3ng/ml vs 83.2 ± 64.9ng/ml) (Figure 20E).
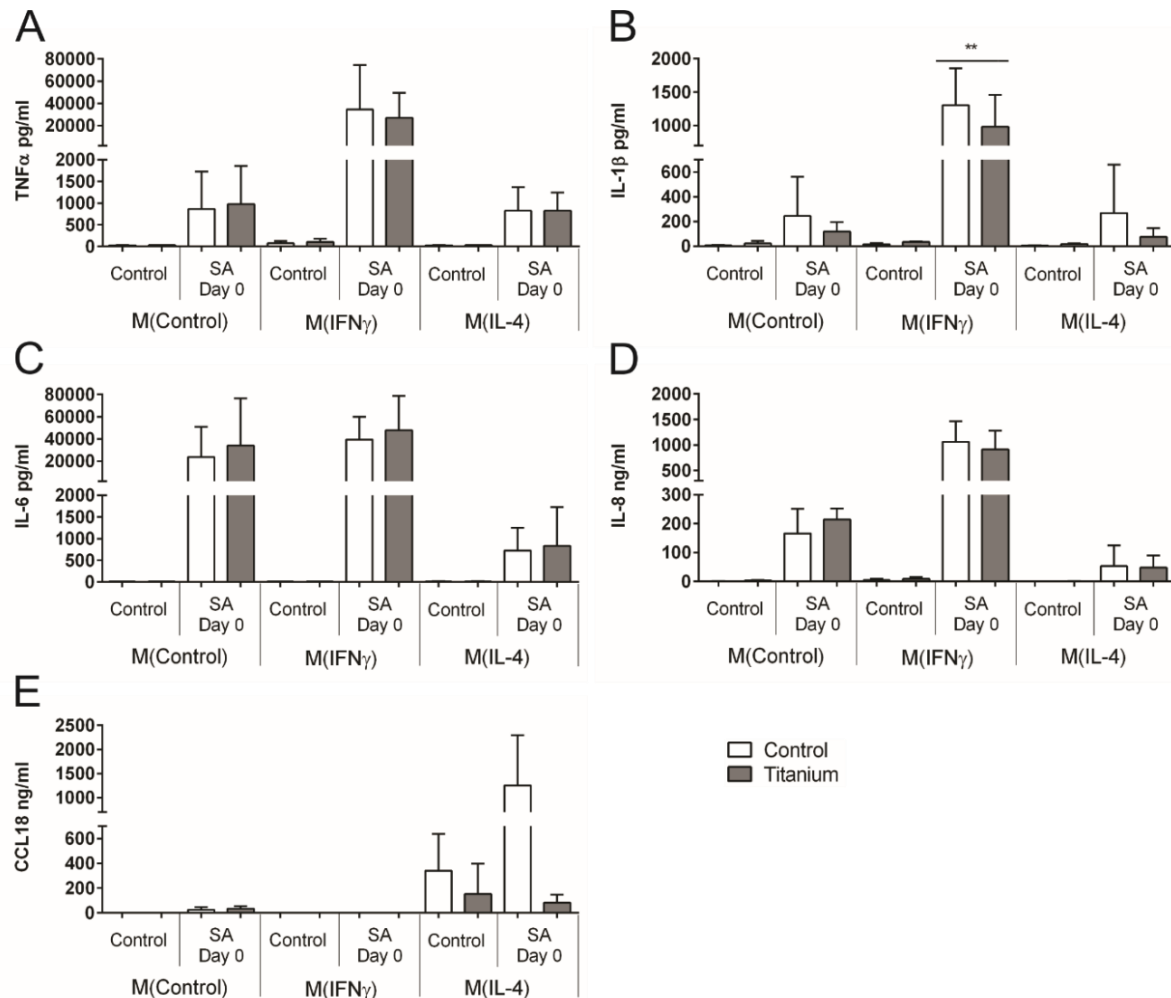
Figure 20. Cytokine secretion upon stimulation with Staphylococcus aureus on day 0.
SA was added to naive monocytes on day 0 and cells were differentiated and cultured for 7 days. Protein concentrations were measured by ELISA on day 7 of culture. **A.** TNFα secretion; **B.** IL-1β secretion; **C.** IL-6 secretion; **D.** IL-8 secretion; **E.** CCL18 secretion. All graphs represent mean values from 4 individual donors with standard deviations. For statistical analysis Student's paired T test was used (* p < 0.05; ** p < 0.01). SA – heat killed staphylococcus aureus; Control – macrophages without SA stimulation; SA Day 0 – macrophages stimulated with SA on day 0.

To analyze if SA stimulation can support secretion of matrix remodeling molecules, the secretion of MMP-7 and MMP-9 was measured by ELISA. SA was added to naive monocytes and mature macrophages (day 6) in the presence or absence of titanium and the concentration of MMP-7 and MMP-9 was measured on day 7 of culture (Figure 21). In mature macrophages SA stimulation alone did not influence the secretion of MMP-7 in any activation state. The highest levels of secretion were noted in M(IL-4). Although in SA stimulation in combination with polished titanium the levels of MMP-7 were higher than in polished titanium alone (16.4 ± 12.7ng/ml vs 7.9 ± 9.9ng/ml), the difference was not statistically significant (Figure 21A). In contrast, during monocyte to macrophage differentiation, SA stimulation alone strongly up-regulated the secretion of MMP-7 in M(Control) and in M(IL-4) when compared to control settings. Additionally, in M(IL-4), SA in combination with titanium induced significantly higher levels of MMP-7 than SA stimulation alone (69.5 ± 17.6ng/ml vs 28.9 ± 16.9ng/ml) (Figure 21B).
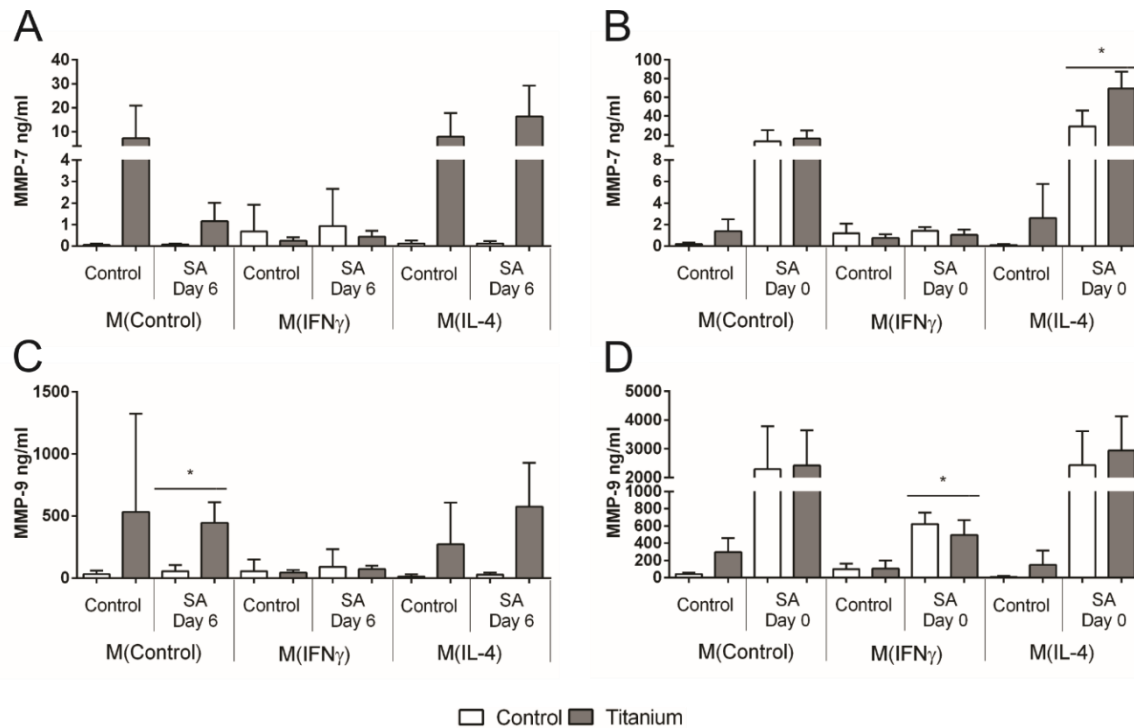
Figure 21. Secretion of MMP-7 and MMP-9 upon stimulation of naive monocytes and mature macrophages with Staphylococcus aureus. SA was added either on day 6 or on day 0 of cell culture and cells were further cultured for 24h or 7 days respectively. Protein concentrations were measured by ELISA on day 7 of culture. **A.** MMP-7 secretion with SA stimulation on day 6; **B.** MMP-7 secretion with SA stimulation on day 0; **C.** MMP-9 secretion with SA stimulation on day 6; **D.** MMP-9 secretion with SA stimulation on day 0. All graphs represent mean values from 4 individual donors with standard deviations. For statistical analysis Student's paired T test was used (* $p < 0.05$; ** $p < 0.01$). SA – heat killed staphylococcus aureus; Control – macrophages without SA stimulation; SA Day 6 – macrophages stimulated with SA on day 6; SA Day 0 – macrophages stimulated with SA on day 0.

The secretion pattern of MMP-9 in mature macrophages was similar to MMP-7, and SA stimulation alone did not induce additional changes in MMP-9 secretion. In M(Control) SA stimulation combined with titanium induced significantly higher levels of MMP-9 than SA alone (233 ± 164.8ng/ml vs 14.7 ± 16.6ng/ml). Similarly, in M(IL-4), SA stimulation in combination with polished titanium induced higher levels of MMP-9 than polished titanium alone (576.8 ± 352.3ng/ml vs 272.9 ± 336.6ng/ml), however the difference was not statistically significant (Figure 21C). Different results were obtained by the analysis of MMP-9 secretion when SA was added to naive monocytes. Stimulation with SA alone was able to up-regulate the secretion of MMP-9 in all activation states. SA in combination with polished titanium displayed lower levels of MMP-9 when compared to SA alone (479.7 ± 172.5ng/ml vs 621.9 ± 131.8ng/ml) in M(IFNγ), with no significant differences noted in other activation states (Figure 21D).

In summary these data demonstrate that the secretion of TNFα, IL-1β, IL-6, IL-8, CCL18, MMP-7 and MMP-9 is significantly altered only when SA is added to naive monocytes that undergo differentiation and not in case when SA is added to already maturated macrophages. Moreover, with the exception of MMP-7, titanium did not enhance the effects of SA both in mature macrophages and in naive monocytes.

3.6 Analysis of secretion of MMP-7 and MMP-9 by PBMC in response to polished titanium discs

Previous results have shown that titanium, regardless of its size, porosity and SA contamination, when compared to control generally stimulates a higher level of secretion of MMP-9 in M(Control) and M(IL-4) (Figures 9C, 10C, 18B, 21C and 21D). Likewise, a tendency for higher MMP-7 secretion induced by titanium in (M-IL4) has also been observed (Figures 18A, 21A and 21D). Both of these molecules are involved in matrix remodeling and thus possess a potential role in implant related complications. In order to investigate whether other immune cells can enhance or inhibit macrophage secretion of MMP-7 and MMP-9 in reaction to polished titanium, an experiment involving the whole fraction of peripheral blood mononuclear cells (PBMC) was designed. For this purpose, the previously described experimental design was employed (section 3.1) with the addition of PBMC and PBMC depleted of CD14+ monocytes (PBMC-CD14). Since no significant differences in MMP-7 and MMP-9 secretion patterns were previously observed in M(IFNγ), this stimulation was omitted.
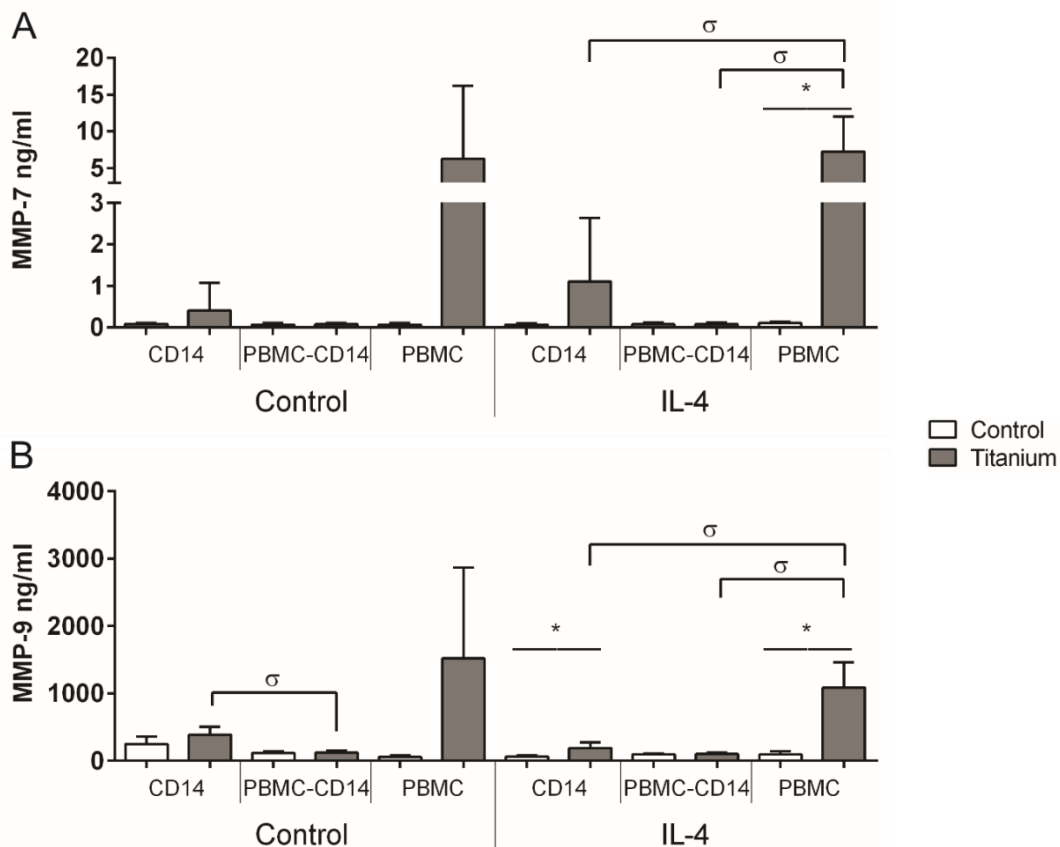

Figure 22. Secretion of MMP-7 and MMP-9 in macrophages, PBMC-CD14 and PBMC upon stimulation with polished titanium. Protein concentrations were measured by ELISA. **A.** MMP-7 secretion; **B.** MMP-9 secretion. Both graphs represent mean values from 5 individual donors with standard deviations. For statistical analysis Student's paired T test was used. * denotes statistical significance between titanium and control of the respective activation state, while σ denotes statistical significance between different types of cell populations (* $p < 0.05$; ** $p < 0.01$; σ $p < 0.05$).CD14 – macrophages; PBMC – peripheral blood mononuclear cells; PBMC-CD14 – PBMC depleted of CD14+ monocytes.

Figure 22A illustrates MMP-7 secretion in macrophages, PBMC-CD14 and PBMC upon stimulation with titanium. A tendency for higher levels of MMP-7 secretion in

macrophages stimulated with polished titanium was observed in both M(Control) and M(IL-4). However, the highest levels of secretion were observed in PBMC cultured on titanium in both Control and IL-4 stimulation. Without titanium in IL-4 stimulation, PBMC induced a minor increase in MMP-7 secretion compared to macrophages alone (0.11 ± 0.03ng/ml vs 0.07 ± 0.03ng/ml). Titanium induced higher levels of MMP-7 in PBMC when compared to macrophages (CD14) in both Control stimulation (6.3 ± 9.9ng/ml vs 0.4 ± 0.7ng/ml) as well as in IL-4 stimulation (7.3 ± 4.8ng/ml vs 1.1 ± 1.5ng/ml) Interestingly, only in PBMC-CD14, titanium did not induce any increase in MMP-7 secretion regardless of the stimulation (Control or IL-4) (Figure 22A). Similar results were obtained in the analysis of MMP-9 secretion. Titanium induced higher levels of MMP-9 in macrophages (CD14) and PBMC in both Control and IL-4 stimulations, while no reaction to titanium was observed in PBMC-CD14 population. Although without titanium PBMC secreted a low amount of MMP-9, when stimulated with titanium they produced the highest levels of MMP-9 in both Control and IL-4 stimulation. Additionally, titanium induced higher levels of MMP-9 in PBMC when compared to macrophages (CD14) in both Control (1519.3 ± 1350.6ng/ml vs 389.1 ± 118.3ng/ml) and IL-4 stimulation (1088.9 ± 371.9ng/ml vs 188.7 ± 87.1ng/ml) (Figure 22B).

Since MMPs are generally synthesized in their pro-form and require additional activation[110], the concentration of active MMP-7 and MMP-9 was also measured (Figure 23).
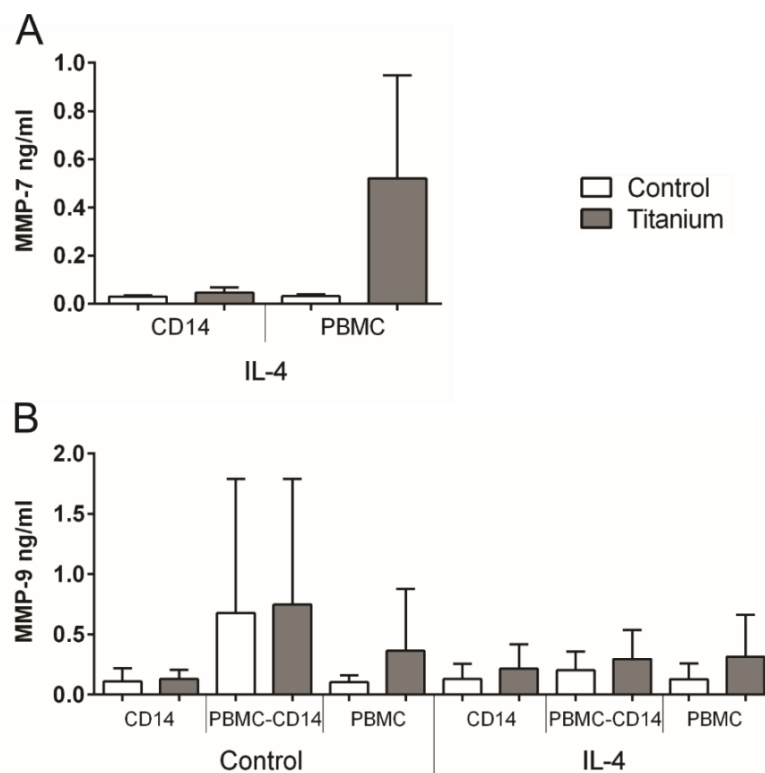

Figure 23. Analysis of the concentration of active MMP-7 and MMP-9 in supernatants from macrophages, PBMC-CD14 and PBMC stimulated with polished titanium. A. active MMP-7; **B.** active MMP-9. Graphs represent mean values with standard deviations from **A** – 3 and **B** – 5 individual donors. For statistical analysis Student's paired T test was used. CD14 – macrophages; PBMC – peripheral blood mononuclear cells; PBMC-CD14 – PBMC depleted of CD14+ monocytes.

The concentration of active MMP-7 was measured only in IL-4 stimulated CD14+ macrophages and in whole PBMC fraction where statistically significant differences

were identified for the total secreted MMP-7 levels (Figure 22A). PBMC-CD14 fraction was omitted due to very low levels of MMP-7 and absence of reaction to titanium. Concentration of active MMP-9 was measured in both Control and IL-4 stimulations in CD14+ macrophages, PBMC-CD14 and PBMC.

The concentration of active MMP-7 in macrophages (CD14) was not significantly changed by titanium. However, in PBMC stimulated with titanium a higher concentration of active MMP-7 was observed (0.5 ± 0.4ng/ml vs 0.03 ± 0.008ng/ml) although not statistically significant (Figure 23A). The concentration of active MMP-9 was not significantly changed by titanium in any stimulation (Control and IL-4) regardless of the cell population. Surprisingly the highest levels of active MMP-9 were observed in PBMC-CD14 fraction in Control stimulation. However, they were not statistically significantly higher than in other cell populations (Figure 23B).

Altogether these results show that PBMC greatly enhance macrophage reaction to titanium, increasing both MMP-7 and MMP-9 secretion. Furthermore, the results indicate that macrophages are essential for the recognition of titanium by PBMC, with no increase of MMP-7 and MMP-9 in response to titanium found in PBMC-CD14 fraction. The concentration of active MMP-7, but not of MMP-9, is also increased in PBMC cultured on titanium. However, the concentration of active MMPs in comparison with the total amounts of MMPs secreted by PBMC cultured on titanium is still less than 10%, suggesting that other cells in the periprosthetic tissue are responsible for their activation.

3.7 Analysis of the impact of macrophage–fibroblast interaction on the secretion of MMP-7 and MMP-9 on titanium surfaces

A major role in the deposition of extracellular matrix is attributed to fibroblasts. To determine if fibroblasts can inhibit or enhance macrophage secretion of MMP-7 and MMP-9 in reaction to polished titanium a macrophage-fibroblast co-culture system was employed. Fibroblasts were co-cultured with macrophages either in direct co-cultures (juxtacrine macrophage-fibroblast interaction, JMFI) or indirectly in transwells (paracrine macrophage-fibroblast interaction, PMFI). As a fibroblast model BJ fibroblasts were used.

MMP-7 secretion in M(Control) did not vary between direct and indirect fibroblast-macrophage culture conditions. In M(IFNγ) an increase in MMP-7 secretion was observed in PMFI when compared to JMFI (0.6 ± 0.8ng/ml vs 0.05 ± 0.02ng/ml), however it was not significantly higher than in macrophages in monoculture (0.5 ± 0.6ng/ml). Titanium was able to induce higher levels of MMP-7 secretion only in M(IL-4), although in all culture conditions. In M(IL-4), upon titanium stimulation, macrophages secreted higher levels of MMP-7 in comparison to control (0.5 ± 0.7ng/ml vs 0.06 ± 0.05ng/ml), however much lower than JMFI (2.9 ± 4.3ng/ml) and PFMI (2.2 ± 2.7ng/ml) with titanium stimulation (Figure 24A). Due to high variation between individual donors the differences between the culture conditions are not statistical significant. It is worth mentioning that in the presence of IL-4, fibroblasts alone secreted very low amounts of MMP-7 both without titanium (0.06 ± 0.009ng/ml) and with titanium (0.03 ± 0.007ng/ml) (data for fibroblasts alone are not shown).
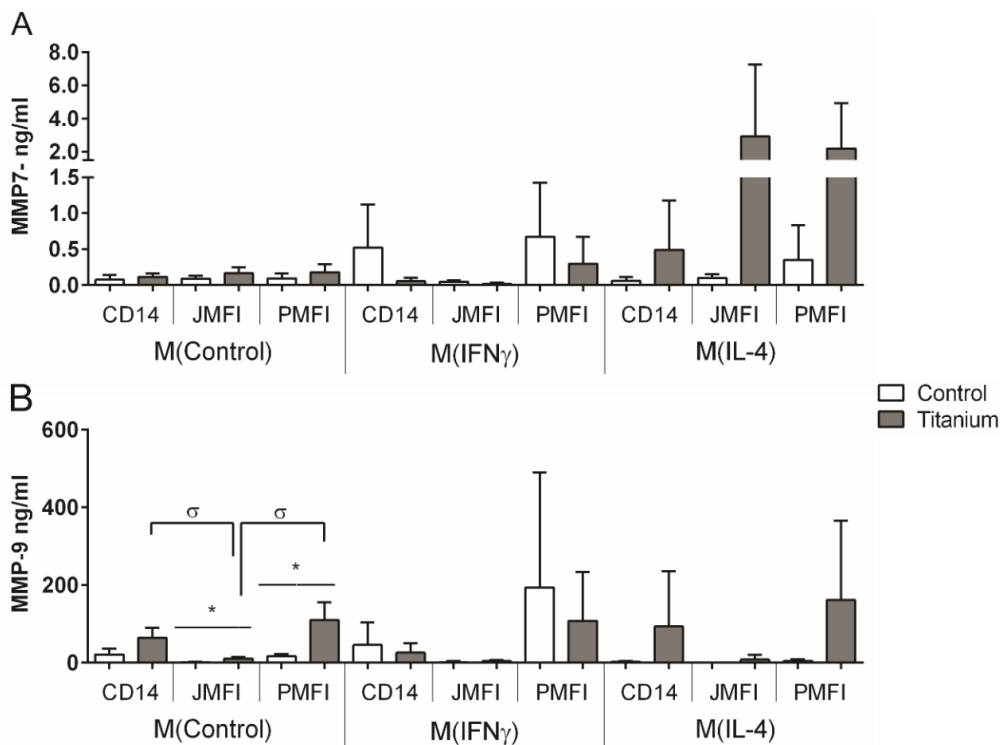

Figure 24. Secretion of MMP-7 and MMP-9 in macrophages co-cultured with fibroblasts upon stimulation with polished titanium. Protein concentrations were measured by ELISA. **A.** MMP-7 secretion; **B.** MMP-9 secretion. Both graphs represent mean values from 4 individual donors with standard deviations. For statistical analysis Student's paired T test was used. * denotes statistical significance between titanium and control of the respective activation state, while σ denotes statistical significance between different types of culture conditions (* p < 0.05; ** p < 0.01; σ p < 0.05). CD14 – macrophages alone; JFMI – juxtacrine macrophage-fibroblast interaction; PMFI – paracrine macrophage-fibroblast interaction.

A different secretion patter was identified in the analysis of MMP-9 secretion. Titanium up-regulated the secretion of MMP-9 in M(Control) and M(IL-4) in all culture conditions. In M(Control) PMFI when stimulated by titanium displayed higher levels of MMP-9 when compared to control (110 ± 45.7ng/ml vs 16.9 ± 5.3ng/ml) and to JMFI on titanium (110 ± 45.7ng/ml vs 10.6 ± 5ng/ml) (Figure 24B). Likewise, macrophage stimulated with titanium also secreted higher levels of MMP-9 when compared to JMFI on titanium (64.3 ± 26.6ng/ml vs 10.6 ± 5ng/ml). Similar results were noted in M(IL-4), where titanium stimulation in macrophages and in PMFI induced higher MMP-9 levels compared to JMFI (macrophages: 93.4 ± 143.1ng/ml; PMFI: 161.7 ± 204.5ng/ml; JMFI: 8.2 ± 11.7ng/ml). Interestingly, JMFI with and without titanium strongly inhibited the secretion of MMP-9 in all activation states. In M(IFNγ) titanium led to a reduction of MMP-9 in all culture conditions, however it was not statistically significant (Figure 24B). Fibroblasts alone did not secrete detectable levels of MMP-9 in any culture condition (data not shown).

In order to investigate whether fibroblasts are able to activate MMP-7 and MMP-9, the concentration of their active form was measured. Concentration of active MMP-7 was measured only in M(IL-4) where the differences between macrophage-fibroblast co-cultures and macrophages monocultures were the most evident (Figure 24A). Active MMP-9 concentration was measured only in M(Control) and M(IL-4) where titanium induced an increase in the secretion of MMP-9 (Figure 24B).
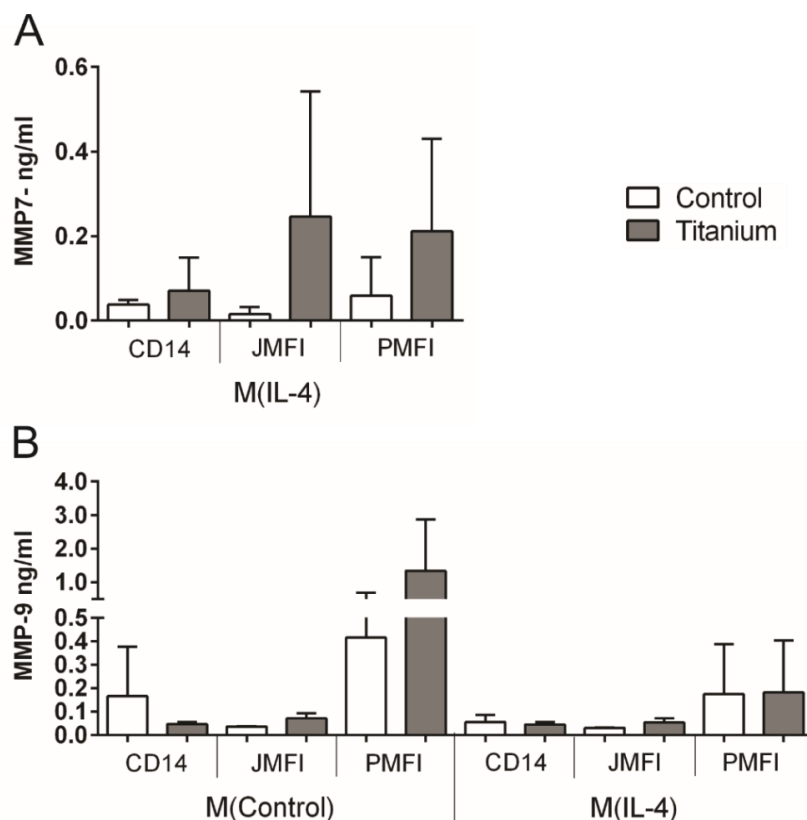

Figure 25. Analysis of active MMP-7 and MMP-9 secretion in macrophages co-cultured with fibroblasts upon stimulation with polished titanium discs. A. active MMP-7; **B.** active MMP-9. Graphs represent mean values with standard deviations from **A** – 4 donors, **B** – 3 donors. For statistical analysis Student's paired T test was used. CD14 – macrophages alone; JFMI – juxtacrine macrophage-fibroblast interaction; PMFI – paracrine macrophage-fibroblast interaction.

Figure 25A illustrates the concentration of active MMP-7 in macrophages co-cultured with fibroblasts in M(IL-4). Titanium generally increased the level of active

MMP-7 in all culture conditions. Upon titanium stimulation higher levels of active MMP-7 were observed in JMFI and PMFI in comparison to macrophages alone (JFMI: 0.25 ± 0.29ng/ml; PMFI: 0.2 ± 0.22ng/ml; macrophages: 0.07 ± 0.08ng/ml) (Figure 25A). A different pattern was observed in the analysis of active MMP-9 secretion. In M(IL-4), in all culture conditions no additional effect of titanium in up-regulation of active MMP-9 secretion was noted. In contrast to total MMP-9 secretion (Figure 24A), in M(Control), in macrophages cultured on titanium when compared to control a decrease in the concentration of active MMP-9 was detected (0.05 ± 0.01ng/ml vs 0.17 ± 0.21ng/ml). No significant difference between titanium and control was observed in JMFI group (0.07 ± 0.002ng/ml vs 0.04 ± 0.001ng/ml). The highest levels of active MMP-9 were detected in PMFI culture conditions, where a tendency for higher active MMP-9 secretion upon titanium stimulation in comparison to control was noted (1.3 ± 1.5ng/ml vs 0.4 ± 0.3ng/ml) (Figure 25B).

In summary, the analysis of macrophage-fibroblast interaction demonstrated that fibroblasts up-regulate MMP-7 secretion by macrophages cultured on titanium in both juxtacrine and paracrine interaction models. MMP-9 secretion was significantly inhibited in the juxtacrine interaction model, but not in the paracrine model, indicating that direct cell-cell contact is needed for MMP-9 inhibition. Still, in the macrophage-fibroblast interaction models the concentration of active molecules is less than 10% of the total amount, suggesting that fibroblasts do not significantly contribute to the activation of MMPs released by macrophages.

3.8 Analysis of individual responses to titanium

Analysis of cytokine secretion and gene expression in macrophages cultured on titanium revealed a broad spectrum of responses in individual donors. While implant failures do not happen in all patients, it is reasonable to assume that in patients with an elevated immune reaction to titanium there is a higher chance of implant failure. In order to better visualize individual responses to titanium a donor-specific gene expression profile, based on RT-qPCR data, was computed (Figure 26).
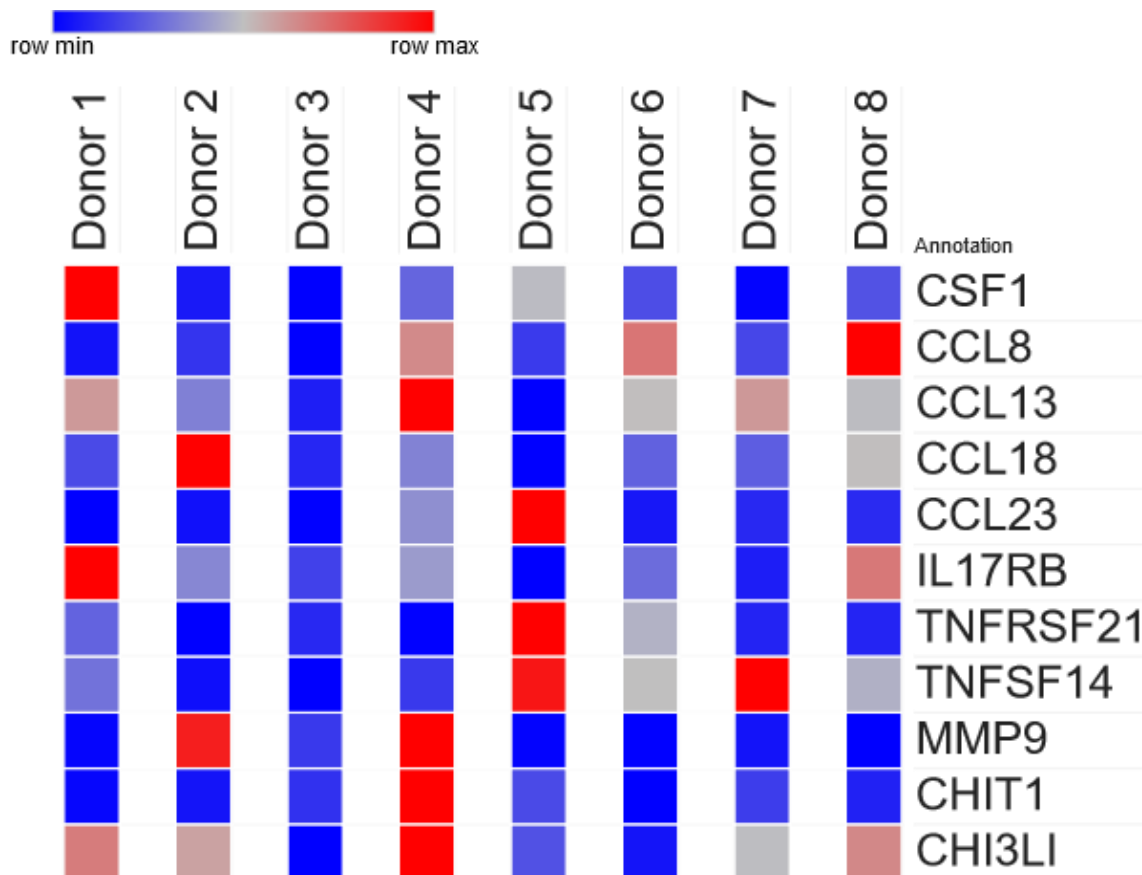

Figure 26. Donor profile of gene expression on polished titanium in M(IL-4). Each square represents the fold change of gene expression in M(IL-4) titanium versus M(IL-4) control. Red represents highest fold change while blue the smallest.

Since gene expression changes induced in titanium were more evident in M(IL-4), for the generation of the donor-specific gene expression profile only this activation state was used. In Figure 26 relative expression differences between titanium and control settings in M(IL-4) were graphically presented as colors. Red color indicates a bigger difference between titanium and control. For genes that are down-regulated by titanium (CCL8, CCL13, CCL18, CCL23 and IL17RB), the modulus of values was taken, in order to consistently represent the highest differences between titanium and control as red color. Thus donors with more red blocks present a higher reaction to titanium, while donors with more blue blocks present a milder reaction to titanium. This analysis suggests that Donor 4 (4 red blocks + 1 intermediate), 5 (3 red blocks + 1 intermediate) and 1 (2 red blocks + 2 intermediate) manifest highest reaction to titanium, while Donor 3 (0 red blocks) reacts mildly to titanium (Figure 26). These results indicate that a personalized approach for analysis of titanium-induced foreign body reactions is a promising tool for identification of patients for which titanium implants have to be avoided.

3.9 Analysis of inflammatory reactions of macrophages to biodegradable implant coating materials

Great mechanical properties and biocompatibility of titanium has made it the material of choice for implant manufacturing. However, due to the development of chronic inflammation at the implant-tissue interface, a part of implants is projected to fail[111]. One possible practical solution to overcome undesired immune reactions is to apply a surface coating to the titanium implant to increase its biocompatibility. For this purpose, synthetic polymers such as PLA, PLGA, PEG and PVA can be applied[93]. In this study 2 types of coatings were used: Polyarginine/Hyaluronic acid-based coating (PAR/HA) and polylactic acid-based coating (PLA).

3.9.1 Analysis of inflammatory reaction of macrophages to PAR/HA coating

Bacterial infection of implants represents a common reason for early implant failure[108]. In order to avoid bacterial contamination of implants antimicrobial coatings can be used. In this study a polyelectrolyte multilayer coating was used with polyarginine as polycation and hyaluronic acid as polyanion (PAR/HA). Since arginine is a common amino acid in the structure of antimicrobial peptides, it can be hypothesized that polyarginine also displays antimicrobial properties[112]. Polyelectrolyte multilayers can be used as delivery systems for biologically active molecules[113]. To increase the antimicrobial properties of the coating, PAR/HA coating was loaded with catestatin (PAR/HA+CAT), an antimicrobial peptide which exhibits activity against bacteria, yeast and fungi[114]. PAR/HA and PAR/HA+CAT coatings were provided by Dr. Philippe Lavalle from Strasbourg University. To analyze if PAR/HA and PAR/HA+CAT coatings can induce in macrophages the secretion of cytokines with inflammatory or anti-inflammatory properties, the secretion of TNFα and CCL18 on day 6 was measured by ELISA. Additionally, to identify individual reactions towards PAR/HA or PAR/HA+CAT coatings each donor was analyzed separately.
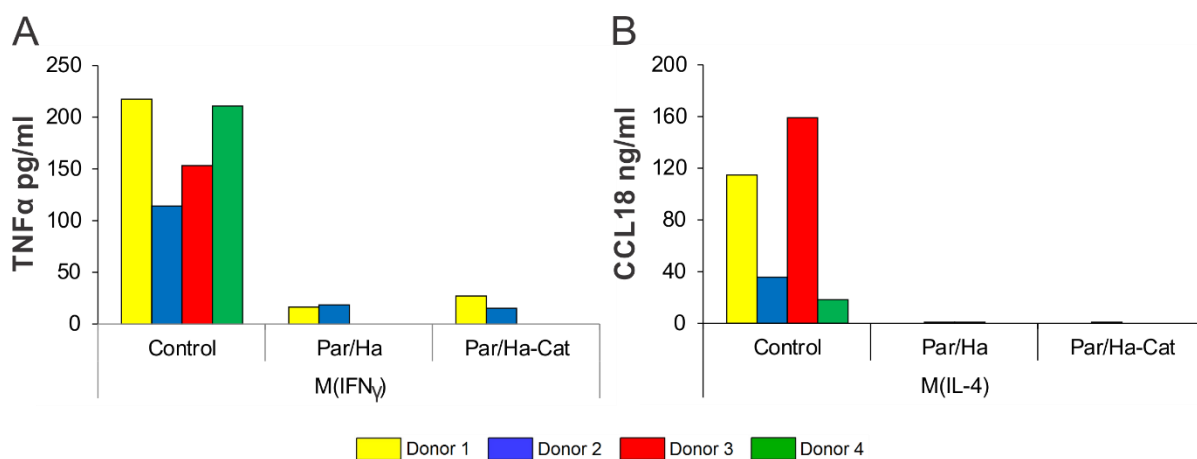

Figure 27. Secretion of TNFα and CCL18 by macrophages cultured on PAR/HA and PAR/HA+CAT coatings. A. TNFα secretion; **B**. CCL18 secretion. Both graphs represent values for each of the 4 individual donors separately. Due to very low secretion levels in other activation states in **A** only data for M(IFNγ) are shown, while in **B** only data for M(IL-4) are shown. PAR/HA – polyarginine/hyaluronic acid coating; PAR/HA+CAT – polyarginine/ hyaluronic acid coating loaded with catestatin.

The analysis of TNFα secretion by macrophages cultured on PAR/HA and PAR/HA+CAT coatings revealed that both coatings significantly inhibit its secretion in

M(IFNγ). For donor 1 the concentration of TNFα decreased from 217.2pg/ml in control to 16.2pg/ml on PAR/HA coating and 27.2pg/ml on PAR/HA+CAT coating. Similarly, for donor 2 the concentration of TNFα decreased from 113.5pg/ml in control to 18.6pg/ml on PAR/HA coating and 14.8pg/ml on PAR/HA+CAT coating. Macrophages from donor 3 and 4 did not secrete any detectable levels of TNFα on any of the coatings (Figure 27A). Similar results were obtained in the analysis of CCL18 secretion. Both PAR/HA and PAR/HA+CAT significantly suppressed the secretion of CCL18 in all donors. Minimal amounts of CCL18 were detected on PAR/HA in samples from donor 2 (0.23ng/ml) and 3 (0.16ng/ml), and on PAR/HA+CAT in samples from donor 2 (0.51ng/ml) (Figure 27B).

In summary, these data indicate that PAR/HA and PAR/HA+CAT coatings significantly inhibit the secretion of both TNFα and CCL18. Therefore, PAR/HA and PAR/HA+CAT are promising coating materials for titanium implants and can be used to avoid bacterial infection as well as local chronic inflammation.

3.9.2 Analysis of inflammatory reaction of macrophages to PLA coating

PLA as a material offers good mechanical properties, processability as well as high biocompatibility and is widely used in resorbable sutures, clips, screws and in drug delivery devices[115, 116]. Moreover, PLA can acquire additional properties by entrapment of biologically active molecules into its surface layer[117]. In the present study two types of PLA coatings were used: unmodified PLA films and PLA films embedded with Brilliant Green dye (BGD), which possesses antiseptic properties. PLA films were prepared and provided by Dr. Sergei I. Tverdokhlebov from Tomsk Polytechnic University. To analyze whether the PLA coatings alone (modified or unmodified) can induce inflammatory or anti-inflammatory reactions in macrophages, secretion of TNFα and CCL18 on day 6 of culture was measured by ELISA. The experimental design is depicted in Figure 28. In order to identify individual reactions to the coating material, both modified and unmodified PLA films were analyzed for each donor separately.
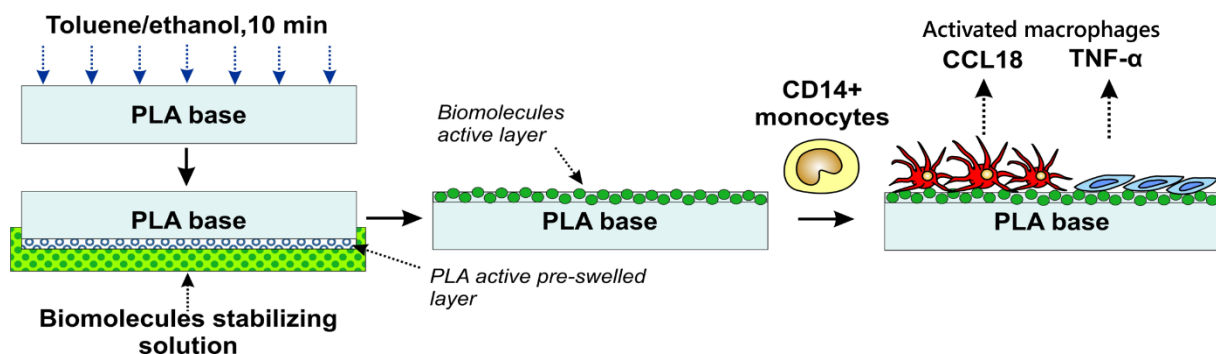

Figure 28. Experimental design for PLA coatings. PLA films were dipped into a toluene/ethanol miscible mixture (3:7 v/v) for 10min then rapidly transferred into a 0.001 M solution of BGD in ethanol/water mixture (1:1 v/v) (stabilizing solution). Films were incubated for 1, 2 or 3 hours, to enable different amounts of BGD to be embedded into the film. CD14 monocytes were seeded on top of the films and allowed to differentiate intro macrophages. M(IFNγ) and M(IL-4) macrophages have been generated by stimulating human monocytes with IFNγ and IL-4 respectively, for 6 days in serum-free medium. On day 6 TNFα and CCL18 were measured by ELISA. Adapted from Stankevich et al., Surface modification of biomaterials based on high-molecular polylactic acid and their effect on inflammatory reactions of primary human monocyte-derived macrophages: Perspective for personalized therapy, Copyright (2015), with permission from Elsevier.

Figure 29A illustrates the secretion of TNFα by macrophages cultured on PLA films. In M(IFNγ) unmodified PLA films did not increase TNFα secretion for all donors. However, all modified PLA films increased the secretion of TNFα in donor 5 from 105.4pg/ml in control to 163.3pg/ml on BGD1, 221.9pg/ml on BGD2 and 204.5pg/ml on BGD3. Similarly, macrophages from donor 7 secreted higher levels of TNFα on BGD1 (580.6pg/ml), BGD2 (694.2pg/ml) and BGD3 (661.2pg/ml) when compared to control (366.9pg/ml). For donor 9 BGD2 increased TNFα secretion (191.5pg/ml vs 99.8pg/ml in control), while for donors 6 and 8 the modified PLA films did not induce increased secretion of TNFα (Figure 29A).
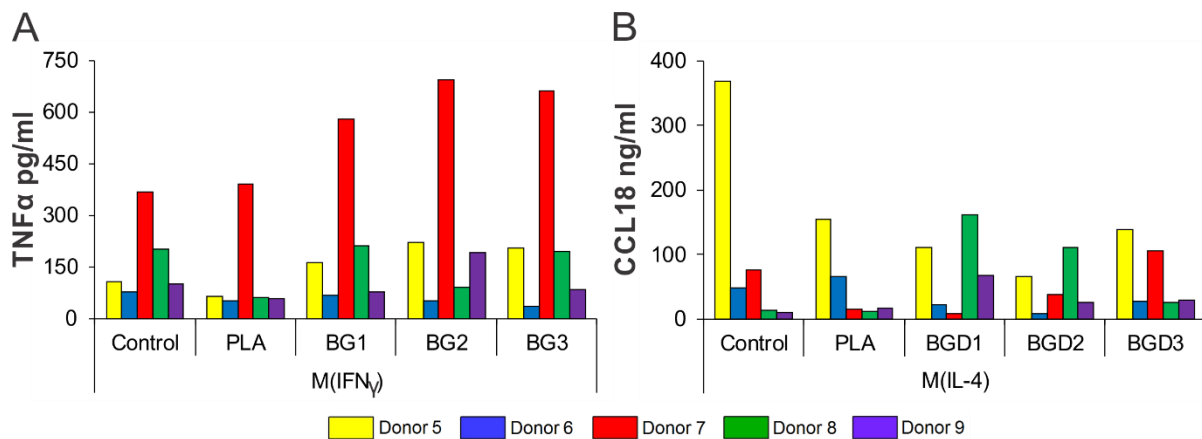

Figure 29. Secretion of TNFα and CCL18 by macrophages cultured on PLA films. A. TNFα secretion; **B.** CCL18 secretion. Both graphs represent values for each of the 5 individual donors separately. Due to very low secretion levels in other activation states in **A** only data for M(IFNγ) are shown, while in **B** only data for M(IL-4) are shown. PLA – polylactic acid film; BGD1 – PLA film treated with Brilliant Green dye for 1h; BGD2 – PLA film treated with Brilliant Green dye for 2h; BGD3 – PLA film treated with Brilliant Green dye for 3h.

A different secretion pattern was observed in the analysis of CCL18 in M(IL-4). Donor 5 showed a reduction of CCL18 secretion with both modified and unmodified PLA films in comparison to the control. The lowest values were observed on BGD2 (65.2ng/ml). Modified PLA films decreased the secretion of CCL18 in donor 6 from 47.6ng/ml in control to 21.1ng/ml on BGD1, 7.5ng/ml on BGD2 and 27.7ng/ml on BGD3 films, while unmodified PLA films increased CCL18 levels to 65.8ng/ml. In contrast, modified PLA films increased the secretion of CCL18 for donor 8 from 13.5ng/ml in control to 161.1ng/ml in BGD1, 110.8ng/ml in BGD2 and 24.9ng/ml in BGD3. For donor 7 a suppression of CCL18 secretion was observed on PLA (14.8ng/ml vs 76.3ng/ml), BGD1 (8.6ng/ml) and BGD2 (38.4ng/ml), while on BGD3 an increase of CCL18 was observed (106.7ng/ml). Compared to control all PLA films increased the secretion of CCL18 of donor 9, with highest levels observed in BGD1 (67.2ng/ml vs 9.6ng/ml) (Figure 29B).

These results show that modification of PLA material surface can change the inflammatory responses of macrophages. Additionally, a monocyte-based in-vitro system for testing individual responses to the implanted material and variants of coating can be useful for selecting a personalized implant.

4 DISCUSSION

4.1 Macrophage reaction to titanium

As an implantable material titanium offers many advantages, demonstrating good mechanical properties, outstanding corrosion resistance and high biocompatibility. However, adverse immune reactions to titanium can lead to the development of chronic inflammation and to implant rejection. In order to obtain long-lasting, failure-free titanium implants it is important to understand the immune mechanisms involved in the recognition and initiation of inflammatory reaction towards titanium. It is well established in the biomaterial community that macrophages are essential cells involved in the recognition of the implant material and initiation of the foreign body reaction[45, 53]. Therefore, a number of studies have attempted to elucidate macrophage reaction towards titanium. In comparison to other research groups, which have used RAW264.7 cells[67], THP-1 cells[68] and mouse bone-marrow derived macrophages[66], in this study human peripheral blood monocyte-derived macrophages were used. It was previously shown, that when mouse bone-marrow derived macrophages, THP-1 cells and human peripheral blood monocyte-derived macrophages are compared in parallel, a big difference in gene expression and cytokine production patterns among them can be observed[47, 118]. Thus, the model used in this study better reflects in vivo settings in human tissues.

Additionally, macrophages are known to display high phenotypic plasticity, adopting different phenotypes depending on microenvironmental cues. It is widely accepted that macrophages activated by IFNγ secrete more pro-inflammatory cytokines (TNFα, IL-1β, IL-6), while those activated by IL-4 secrete anti-inflammatory molecules (IL-1Ra, IL-10 and TGFβ)[46, 49]. Moreover, studies have shown that macrophages with different activation states exhibit diverse reactions towards biomaterials[119, 120]. In the present study, in order to simulate diverse activation states of macrophages, but also discriminate among their reactions to titanium, human peripheral blood-derived monocytes were brought to 3 distinct activation states: M(Control) (no additional stimulation), M(IFNγ) (stimulation with IFNγ) and M(IL-4) (stimulation with IL-4).

In order to simulate various interactions of macrophages with titanium implants, several types of titanium were used in this study. Polished titanium discs were used as a model of bulk titanium implants which are commonly employed in dental applications[121]. Furthermore, the smooth surface of polished titanium discs permitted to avoid interference from surface micro- or nanopatterns in the analysis of macrophage reactions to titanium as an implant material, with micro- and nanopatterns known to induce additional cell behaviors[89, 90]. Porous titanium discs were used to analyze whether porous titanium implants, which display promising results in terms of osseointegration[86], also display higher biocompatibility and consequently may reduce the foreign body reaction. These types of implants are currently applied for femoral and tracheal prosthesis[39, 122]. Additionally, implant debris has been implicated in periprosthetic osteolysis and induction of the production of pro-inflammatory cytokines in macrophages[123]. To simulate macrophage interaction with titanium implant debris, micro titanium beads of 125-200μm in diameter (μTi beads) and titanium nanoparticles of 15nm in diameter (nTi particles) were used.

4.1.1 Macrophage cytokine release in response to titanium

In this study, the first step was to analyze macrophage reaction on polished titanium discs. As foreign body reactions are characterized by a release of pro-inflammatory mediators[42], to determine if titanium is able to induce secretion of pro-inflammatory cytokines, supernatants from macrophages cultured on polished titanium discs were analyzed by ELISA. Pro-inflammatory cytokines TNFα, IL-1β and IL-6 were selected as a readout. Furthermore, to test whether titanium can promote or inhibit the secretion cytokines with anti-inflammatory properties, CCL18 secretion was also analyzed.

TNFα is secreted during the acute phase of inflammation and has a protective role against bacterial, viral and parasitic infections. However, it is widely recognized that it also plays a role in the pathophysiology of several chronic inflammatory diseases[124]. IL-1β is also a potent pro-inflammatory cytokine released in the acute phase of inflammation and involved in the innate immune response to infections and lesions. IL-1β promotes differentiation of CD4+ T cells into TH17 cells and takes part in neutrophil recruitment[125]. Additionally, higher levels of IL-1β were linked to several chronic inflammatory diseases such as rheumatoid arthritis, inflammatory bowel disease and psoriasis[126]. IL-6 is involved in a variety of biological activities. It promotes B cell differentiation, T cell differentiation and activation, proliferation of thymocytes and regulates bone homeostasis. Macrophages produce high amounts of IL-6 when stimulated with LPS, IFNγ, IL-1α, TNFα, and GM-CSF[125, 127]. IL-6 was also shown to play an important role in the pathophysiology of rheumatoid arthritis, Crohn's disease, juvenile idiopathic arthritis, Castleman's disease and systemic lupus erythematosus[128]. Thus all three selected pro-inflammatory cytokines (TNFα, IL-1β and IL-6) are involved in both acute phase of inflammation as well as chronic inflammation.

In contrast to TNFα, IL-1β or IL-6, CCL18 expression is induced in macrophages stimulated with IL-4/IL-13 and is suppressed in those stimulated with IFNγ[129]. Moreover, CCL18 is involved in activation of macrophages towards an anti-inflammatory phenotype, increasing the secretion of IL-10[130]. However, elevated levels of CCL18 were associated with various chronic inflammatory diseases[129], suggesting that higher levels of CCL18 are not necessarily beneficial in the long term.

In macrophages cultured on polished titanium discs higher levels of TNFα and IL-1β were observed in M(IFNγ) with no significant difference in other activation states. IL-6 secretion, on the other hand, was significantly elevated by titanium in all activation states. As a sensitive marker of inflammation TNFα was further selected as readout for macrophage reactions on porous titanium, μTi beads and nTi particles. It was found that porous titanium induced higher levels of TNFα in all activation states. This phenomenon was not observed on μTi beads and nTi particles. It can be explained by difference in sample size (11 monocyte donors in porous experiment, and 4 in μTi and nTi experiment) as well as high variation among the tested samples (in these experiments, macrophages from different donors were used). Although nTi particles did not increase the secretion of TNFα in macrophages, the results obtained on the titanium discs generally correlate with findings of other studies that showed elevated levels of TNFα, IL-1β and IL-6 in macrophages stimulated with titanium[66-68]. CCL18 secretion was slightly up-regulated by polished titanium in M(Control) and down-regulated in M(IFNγ). However, the amount of CCL18 in these activation states was negligible when compared to M(IL-4) in which polished titanium induced a slight inhibition of CCL18 secretion, although not statistically significant. In porous titanium this effect was even stronger, with titanium significantly inhibiting the secretion of CCL18 in M(IL-4). Additionally, both μTi and nTi inhibited the secretion of CCL18 in

M(IL-4), with nTi exerting the highest effect. Since CCL18 is known to promote an anti-inflammatory phenotype in macrophages[130], inhibition of CCL18 secretion upon stimulation with titanium can be regarded as a pro-inflammatory effect of titanium.

Collectively these results suggest that titanium promotes a pro-inflammatory cytokine profile secreted by macrophages that can have detrimental effects on different stages for implant integration in the tissues.

4.1.2 The analysis of gene expression in response to titanium using Affymetrix microarrays

Analysis of cytokine release in macrophages cultured on titanium offered limited insight into the extent of macrophage reactions towards titanium. In order to study these reactions in more detail, the effect of titanium on gene expression (whole transcriptome) in macrophages was analyzed. To accomplish this task microarray experiments were performed with polished and with porous titanium discs. Peripheral blood monocytes were cultured on polished or porous titanium discs and RNA from 6 (polished) or 8 (porous) donors was chosen (based on RNA integrity number and concentration) for microarray analysis. For each donor 6 different groups of macrophages were analyzed: M(Control), M(IFNγ), M(IL-4), M(Control) Ti, M(IFNγ) Ti and M(IL-4) Ti. The analysis of microarray data from both experiments displayed similar trends: the highest number of differences between titanium and control settings were found in M(IL-4) activation state, with 1452 genes up-or down-regulated in macrophages cultured on polished titanium discs and 3560 genes on porous titanium discs. In M(Control) there were 214 genes affected by polished titanium and 1244 genes by porous titanium. The lowest number of differences between titanium and control settings were found in M(IFNγ) activation state, where 150 genes were differentially regulated on polished titanium discs and 861 genes on porous titanium discs. Plotting the results on a 3D scatterplot confirmed these findings and showed that in both polished and porous titanium M(Control) and M(IFNγ) activation states have more homogeneous populations, when compared to M(IL-4). Consequently, these results demonstrate that macrophages in the M(IFNγ) activation state do not react as strongly to titanium as in M(IL-4) activation state. Furthermore, it can be hypothesized that IFNγ induces a pro-inflammatory gene expression profile similar to titanium and therefore can mask its effects.

Although the results from both microarray experiments (on polished and porous titanium) show a lot of similarities they contradict data presented by Pajarinen et al., where more genes were differentially regulated by titanium in macrophages from M(IFNγ) activation state (192 genes), followed by 63 genes in M(Control) and 59 genes in M(IL-4)[131]. When the results from both studies were compared only 40 genes from either polished titanium experiment or porous titanium experiment were also found in the results of Pajarinen et al., however the direction of change (up- or down-regulation) did not always match. The difference in number of genes up- or down-regulated by titanium in both studies can be explained by a different sample size (6 for polished titanium, 8 for porous titanium and 4 tested by Pajarinen et al.) as well as high variation among the tested samples. Additionally, the differences in culture conditions used by Pajarinen et al. (RPMI medium + 100ng/ml M-CSF + 10%FBS) compared to the culture conditions used in this study (Macrophage SFM medium + 1ng/ml M-CSF + 10^{-8}M Dexamethasone) as well as the titanium model employed (Ti microbeads vs Ti discs) introduce further variations in the study design and consequently lead to contrasting results. Moreover, the use of M-CSF at a concentration of 100ng/ml was shown to induce a macrophage phenotype very similar to the one obtained after IL-4 stimulation and, consequently, may interfere with the effects of IFNγ[132].

The surface of the material is known to influence cell behavior. Higher surface roughness promotes cell attachment and cell proliferation[89]. Macrophages cultured on materials with different topography acquire distinct activation states[90]. Additionally, materials designed to induce a specific shape to macrophages are also able to change macrophage polarization[133]. Different activation states of macrophages are characterized by distinct expression and secretion patterns of inflammatory cytokines[46, 49]. Surprisingly, when microarray data from the experiment with porous titanium is compared to data from polished titanium experiment, only small differences in the expression pattern of genes from cytokine-cytokine receptor family was noted. Although there were more gene members of this family affected by porous titanium (65 compared to 44; Tables 18, 19), the direction of change (up- or down-regulation) for the common genes was similar. For example, both types of titanium surfaces stimulated CSF1, IL1RN, TNFSF14 and suppressed CCL8 and CCL23 expression. However, the spectrum of inflammatory responses also displayed some stimulation specific differences: 1) in M(IFNγ) a significant down-regulation of INHBA, CXCL9 and CXCL10 was observed on porous titanium, while no effects were noted on polished titanium; 2) in M(IL-4) CCL13 was strongly down-regulated on porous titanium, but not on polished titanium. Down-regulation of CXCL9, CXCL10 and CCL13 in porous titanium is indicative for the suppression of specific inflammatory reactions, since all 3 genes are associated with adverse local tissue reaction[100]. Additionally, porous materials have been shown to promote osseointegration and capillary formation[87], however no significant differences in the expression of genes associated with wound healing and angiogenesis was noted between both types of titanium.

In order to identify which genes are regulated by titanium independently on the structure of the surface (polished vs porous) a comparison of the results obtained from microarray experiments was performed. A total of 1102 common genes were found differentially regulated by both types of titanium, with 135 genes in M(Control), 68 genes in M(IFNγ) and 899 genes in M(IL-4). Comparing the data according to the algorithm described in section 3.2.2 and filtering the gene list by genes involved in inflammation and in extracellular matrix degradation a list of 14 genes with potential implication in implant related complications can be identified (Table 19). Interestingly, all of the selected genes followed the same direction of change in both experiments.

Table 19. Comparison of microarray data from polished and porous titanium experiments. *(↑ - up-regulation > 2 fold; ↓ - down-regulation > 2 fold; ▲- up-regulation < 2 fold; ▼ - down-regulation < 2 fold; * - p > 0.05. M(IFNγ) was omitted due to the absence of any significant changes in the regulation of these genes)*

Gene Symbol	Polished Titanium (6 donors)		Porous titanium (8 donors)	
	M(Control)	M(IL-4)	M(Control)	M(IL-4)
CCL8	▼*	↓	not changed	↓
CCL23	not changed	↓	not changed	↓
CHI3L1	↑	↑	↑	↑
CHIT1	not changed	▲*	↑	↑
CSF1	▲*	↑	↑	↑
IL17RB	not changed	▼*	not changed	↓
IL1R2	▲*	↑*	▲*	↑
IL1RN	↑	↑*	↑	▲*
MMP7	▲*	↑*	↑	↑
MMP8	▲*	not changed	↑*	↑
MMP9	not changed	↑	not changed	↑
SPP1	↑	↑	↑	↑*
TNFRSF21	↑	↑	▲*	↑
TNFSF14	↑*	↑	↑	↑

The comparison of gene expression on polished and porous titanium discs revealed that titanium surface can induce some changes in gene expression. However, the differences are mainly in magnitude of change and not in the direction of change (up- or down-regulation) of gene expression. Thus, the reactions of macrophages to titanium as a material are stronger than those induced by the surface of titanium.

4.1.3 Validation of microarray results

Evaluation of microarray data from polished and porous titanium experiments revealed several gene families affected by titanium. For polished titanium these were: metallothioneins, matrix metalloproteinases, cytokine-cytokine receptors, zinc fingers C2-H2 type, immunoglobulin-like domain containing and endogenous ligands (Table 17). For porous titanium the most affected gene families were: metallothioneins, matrix metalloproteinases, cytokine-cytokine receptors, solute carrier family, chitinase-like proteins, integrins and purinergic receptors (Table 18). Thus three gene families were differentially regulated by both types of titanium (metallothioneins, matrix metalloproteinases, cytokine-cytokine receptors). Since genes from matrix metalloproteinases and cytokine-cytokine receptors families are more likely to be involved in implant related complications, several prominent members of these gene families were selected (based on microarray data) for RT-qPCR validation. The selected genes were: CSF1, CCL8, CCL13, CCL18, CCL23, IL17RB, TNFRSF21, TNFSF14, MMP8 and MMP9. Additionally, 2 members of the chitinase-like proteins (CHIT1 and CHI3L1) were also selected for RT-qPCR validation.

RT-qPCR analysis of gene expression generally validated the results from microarrays. As previously shown (sections 3.2.3 and 3.3.2), most of the genes were significantly differentially regulated in M(IL-4). Although there was a difference in magnitude of fold change between samples from polished and porous titanium, no difference was observed in the direction of change (up- or down-regulation) of gene expression, which also correlated with microarray data. RT-qPCR results revealed that titanium up-regulates CSF1, CHI3L1, CHIT1, MMP8, MMP9, TNFRSF21 and TNFSF14, and down-regulates CCL8, CCL13, CCL18, CCL23 and IL17RB.

CSF1 codes for macrophage colony-stimulating factor (M-CSF) which is an essential factor for the differentiation, migration and survival of macrophages and osteoclasts[134]. In macrophages cultured on polished titanium discs up-regulation of CSF1 was observed in M(Control) and M(IL-4) activation states. Similarly, on porous titanium CSF1 gene was up-regulated in M(Control), with the same tendency in M(IL-4). These results correlate with data from other studies in which an increase in M-CSF was noted in periprosthetic tissue in cases with aseptic loosening[135]. Thus, in the periprosthetic tissue macrophages in contact with titanium constitute a source of M-CSF, which can potentially lead to osteoclast activation and ultimately to aseptic loosening.

CCL8, CCL13, CCL18 and CCL23 are members of the chemokine family. CCL8 acts via CCR1, CCR2 and CCR5 and is chemotactic for lymphocytes, monocytes, basophils and eosinophils[136, 137]. CCL13 binds to CCR2 and CCR3 and along with CCL2, CCL3, CCL4, CCL5, CCL7 and CCL8 is chemotactic for monocytes and macrophages[57, 137]. Both polished and porous titanium discs down-regulated CCL8 and CCL13 in M(Control) and M(IL-4) macrophages, suggesting a decrease of the inflammatory reaction. In contrast, other studies have found that biomaterial adherent macrophages display an increased expression of CCL13 in vitro[138]. Moreover, in patients with adverse local tissue reaction, expression of CCL8 and CCL13 in the periprosthetic tissue is up-regulated when compared to patients with osteolysis[100]. This discrepancy between results may be explained by the use of different biomaterial for

assessing macrophage reactions (synthetic polymers) and by the presence of other cells, besides macrophages, in the periprosthetic tissue which alter the mRNA level of CCL8 and CCL13 in the tissue.

CCL18 operates through PITPNM3 and CCR8 and is chemotactic factor for T cells[137, 139]. As previously described, it is also involved in activation of macrophages towards an anti-inflammatory phenotype[130]. Macrophages in M(IL-4) activation state on both polished and porous titanium discs induced down-regulation of CCL18. However, in the periprosthetic tissue of patients with aseptic loosening, expression of CCL18 was up-regulated in comparison to patients with osteoarthritis, suggesting that other cellular components of the periprosthetic tissue may alter the mRNA level of CCL18 in vivo[101]. Elevated levels of CCL18 were also associated with various chronic inflammatory diseases[129]. Thus, the role of CCL18 in inflammatory processes and in implant related complications is still controversial.

CCL23 acts via CCR1 and FPR2 and is chemotactic for T cells, monocytes and neutrophils[137, 140]. Moreover, CCL23 was found to be involved in chemotaxis and differentiation of osteoclast precursors, suggesting a role in osteolysis[141]. Thus, the decrease in CCL23 expression in M(Control) and M(IL-4) macrophages observed on both polished and porous titanium discs represents an anti-inflammatory reaction, which may potentially inhibit osteolysis. Additionally, it is worth mentioning that all of the down-regulated chemokines are localized in close proximity on the chromosome, with CCL8, CCL13, CCL18 and CCL23 located in the 17q11.2 and 17q12 loci, suggesting that these genes are co-regulated.

IL17RB and TNFRSF21 code for cytokine receptors, which upon interaction with their binding partners (IL-25 and TRADD respectively) are able to induce the activation of NF-κB[102, 142], and consequently can lead to an increase in inflammatory response and apoptosis. IL17RB was down-regulated by polished and porous titanium in M(IL-4) macrophages, an effect which can be considered favorable in light of published studies[102]. On the other hand, TNFRSF21 was up-regulated in M(Control) by polished titanium, suggesting potential exacerbation of an inflammatory reaction.

TNFSF14, also known as LIGHT, is a member of tumor necrosis factor superfamily and has been shown to be involved in bone resorption by promoting RANKL-mediated osteoclastogenesis[143]. Polished titanium induced up-regulation of TNFSF14 in M(IL-4), with a similar tendency also observed on the protein level. Comparable results, although not statistically significant, were obtained on porous titanium, suggesting that titanium through up-regulation of TNFSF14 and M-CSF may promote osteoclastogenesis.

MMPs are a family of proteolytic enzymes that have an essential role in maintaining the physiological human tissue homeostasis[144]. Additionally, they have been found to be involved in the activation of various cytokines, chemokines and growth factors[145]. Thus deregulated expression of MMPs can lead to several pathological processes[146]. In implantation, MMP8 has been linked to peri-implantitis and periodontitis[105], while MMP9 to an early implant failure[147]. In the present study up-regulation of MMP8 was observed in M(IL-4) macrophages cultured on porous titanium, with similar tendency on polished titanium. MMP9 expression was up-regulated in M(IL-4) macrophages by both polished and porous titanium. Moreover, on protein level, up-regulation of MMP-9 secretion by macrophages cultured on polished titanium was also noted. It can be hypothesized that in the periprosthetic tissue macrophages in contact with titanium constitute a major source of MMP8 and MMP9, which can lead to peri-implantitis and implant failure.

CHIT1 and CHI3L1 are members of the chitinase-like proteins family and their up-regulation has been linked to various chronic inflammatory diseases[103]. In this study,

CHIT1 (chitotriosidase) was up-regulated by porous titanium in all activation states, while polished titanium induced up-regulation only in M(IL-4), although this effect was not statistically significant. On the other hand, CHI3L1 was up-regulated by polished titanium in all activation states and by porous titanium in M(Control) and M(IL-4). Furthermore, similar patterns of CHIT1 and CHI3L1 expression were also detected on protein level in macrophages cultured on polished titanium discs. Up-regulation of CHIT1 was associated with aseptic loosening in total knee arthroplasty[106], while elevated levels of CHI3L1 were noted in the periprosthetic tissue of patients with titanium implants[148]. Thus, titanium-induced up-regulation of CHIT1 and CHI3L1 may lead to chronic inflammation and aseptic loosening. Moreover, it is worth taking into consideration that both CHIT1 and CHI3L1 share a locus on the chromosome (1q32.1), suggesting that these genes are co-regulated.

A summary of microarray results validation by RT-qPCR in both polished and porous experiments is presented in Table 20.

Table 20. Summary of microarray validation results. RT-qPCR data; in **bold** – p < 0.05; in *italic* – p > 0.05; positive values denote up-regulation, while negative values denote down-regulation by titanium; N/A – not available; * 9 donors analyzed; ** 10 donors analyzed.

Gene Symbol	Fold change in Polished Ti vs control			Fold change in Porous Ti vs control		
	M(Control) (8 donors)	M(IFNγ) (8 donors)	M(IL-4) (8 donors)	M(Control) (11 donors)	M(IFNγ) (11 donors)	M(IL-4) (11 donors)
CSF1	**3.5**	*2.8*	**8.0**	**4.2**	no change	*1.9*
CCL8	**-3.3**	*1.1*	**-4.8**	**-2.6**	*-1.3*	**-9.7**
CCL13	**-1.7**	*1.6*	**-3.5**	*-1.2*	*18.2*	**-8.7**
CCL18	*1.5*	*1.8*	**-3.6**	*-1.1 **	*1.9 **	**-5.8 ***
CCL23	N/A	N/A	**-3.1**	N/A	N/A	**-38.9**
CHI3L1	**1.9**	**1.8**	**3.3**	**3.5**	*1.8*	**2.5**
CHIT1	*-1.1*	*1.2*	**3.9**	**4.0**	**1.4**	**4.4**
IL17RB	N/A	N/A	**-2.5**	N/A	N/A	**-32.6 ***
MMP8	*1.4*	N/A	*3.1*	*2.3*	N/A	**4.7**
MMP9	*1.1*	*2.1*	**5.1**	*1.3*	*1.8*	**3.0**
TNFRSF21	**2.5**	*-1.9*	*1.6*	*1.1*	*1.2*	*1.1*
TNFSF14	N/A	N/A	**2.3**	N/A	N/A	*2.4*

These results share many similarities with data published by other authors, in which gene expression in the periprosthetic tissue of titanium implants was analyzed. It was shown that titanium implants induced up-regulation of MMP8, MMP9, CHIT1 and CHI3L1 in the periprosthetic tissue[148] that correlates with data from the present study. Thus, the model used in this study for analyzing the inflammatory reactions of macrophages to titanium reflects several findings made in vivo. However, CCL18 was found to be up-regulated in the periprosthetic tissue[148], while in this study it was down-regulated by titanium, indicating that the overall reaction to titanium in vivo is more complex.

In summary these results suggest that titanium induces a specific activation state in macrophages with rather pro-inflammatory properties. Additionally, the activation state of macrophages plays a role in the extent of reaction towards titanium. The pro-inflammatory effects of titanium are most strongly pronounced in M(IL-4) that model functional subtype of healing macrophages. Thus, microenvironmental cues in the periprosthetic tissue are expected to significantly influence the development of the foreign body reaction towards titanium.

4.1.4 Comparison of macrophages reactions to Ti discs, Ti microbeads and Ti nanoparticles

Studies on THP-1 cells have demonstrated that cells react differently to titanium particles in comparison to titanium discs. THP-1 cells cultured on discs secreted significantly higher levels of TNFα, CCL2, CCL3 and IL-1Ra[82]. In the present study, when human monocyte-derived macrophages were cultured with polished Ti discs, Ti microbeads (µTi) and Ti nanoparticles (nTi) no difference was observed in the secretion of TNFα, while a slight inhibition of CCL18 secretion was observed in nTi when compared to µTi, but not with Ti discs. In order to investigate whether macrophages cultured with µTi and nTi can induce different cytokine expression patterns compared to Ti discs on the mRNA level, expression of several genes was analyzed by RT-qPCR. The genes analyzed by RT-qPCR were: CSF1, CCL8, CCL13, CCL23, IL17RB, TNFSF14, MMP7, MMP9, CHIT1 and CHI3L1. MMP7 was added to the gene list as a substitute for MMP8, since previous results from the polished titanium experiment did not show significant changes in MMP8 expression.

The comparison of macrophage reactions to Ti discs, Ti microbeads and Ti nanoparticles revealed that all 3 types of titanium induce similar reactions in macrophages in terms of cytokine expression and production as well as in expression and secretion of matrix remodeling proteases. Apart from CSF1 and CHI3L1 expression there was virtually no difference between macrophage reactions to Ti discs and µTi. However, macrophages cultured with nTi generally displayed stronger reactions to the material inducing significantly stronger up-regulation of CSF1, CHIT1 and CHI3L1 and stronger down-regulation of CCL8, CCL13, CCL18 and CCL23 in comparison to Ti discs and µTi. In this study Ti discs were used as a model of bulk titanium implants, while µTi with a diameter of 125-200µm as a model of non-phagocytosable implant debris and nTi with a diameter of 15nm as a model of phagocytosable implant debris. The stronger macrophage reactions to nTi suggest that nanoparticle phagocytosis enhances these reactions. Indeed, other authors also report that phagocytosable particles, in comparison to bigger particles, induce stronger inflammatory reaction in macrophages, which consequently secrete higher levels of TNFα, IL-1β, IL-6 and PGE2[149]. Furthermore, the size of the particles also influences macrophage response, with smaller phagocytosable particles causing more severe inflammatory reactions[150]. In a bone resorption model, only macrophages challenged with phagocytosable particles were able to increase their bone-resorbing activity[151]. Thus enhanced inflammatory response of macrophages to nTi could result in osteolysis and aseptic loosening.

Collectively these results indicate that macrophages do not respond equally to titanium of different sizes. The difference in response can be explained by phagocytosis of the material which takes place when the particles are smaller than 10µm[57]. However, these reactions differ only in their magnitude and are influenced by the initial activation state of macrophages. Therefore, in vivo, in the periprosthetic tissue both the size of wear particles and the microenvironmental signals will modulate the foreign body response.

4.2 Bacterial influence on cytokine secretion of macrophage in contact with titanium

Titanium implants are used in many medical applications with great success. Nevertheless, due to the development of various complications (Table 8) a part of titanium implants fail. Studies report a failure rate of 3,4% to 6,5% in total knee arthroplasty and up to 9% in total hip arthroplasty[152, 153]. It is well established that biofilm formation is one of the reasons for implant failures. A biofilm can be defined as a "structured consortium of bacteria encased in a self-produced matrix", which consists of exopolysaccharides, proteins, teichoic acids and extracellular DNA[108]. The formation of biofilm on the surface of implants presents additional difficulties in the treatment of infection, particularly because it provides resistance to antibiotics and host defense mechanisms[154]. One of the most common pathogens involved in metallic implant failures both in orthopedics and dentistry is Staphylococcus aureus[108, 154, 155]. To model a bacterial infection of titanium implants and to analyze its effects on macrophage cytokine secretion an experiment with Staphylococcus aureus and polished titanium was designed. Additionally, it is widely accepted that monocytes are constantly recruited into the tissue during infection and inflammation[109]. To model differentiation of naive monocytes in the proximity of an infected implant, an experiment with SA and naive monocytes cultured on titanium was also designed.

The experiments in this study have shown that SA stimulation induces a minor response in mature macrophages with TNFα and IL-6 expressions only marginally elevated in M(IFNγ), while the expression of IL-1β and CCL18 were unchanged in all activation states. The only cytokine significantly up-regulated in response to SA stimulation on day 6 was IL-8 in M(IFNγ). Moreover, when titanium was taken into consideration (together with SA) no increase in the secretion of TNFα, IL-1β and CCL18 was determined, with only slightly elevated levels of IL-8 observed in M(Control) and of IL-6 in M(IL-4).

In contrast, when SA was added to naive monocytes a stronger reaction was observed. The reaction was up to 100 times higher than when SA was added to already matured macrophages, with up-regulation of CCL18 secretion in M(IL-4) and of TNFα, IL-1β, IL-6 and IL-8 secretion in all activation states. Titanium did not enhance cytokine secretion when SA was added to naive monocytes and, on the contrary, inhibited the secretion of IL-1β and CCL18. Furthermore, SA induced significantly higher levels of matrix remodeling proteinases MMP-7 and MMP-9 when added to naive monocytes, but not to the mature macrophages. Additionally, titanium synergistically up-regulated the secretion of MMP-7 in naive monocytes stimulated with IL-4. However, this phenomenon was not observed in MMP-9 secretion.

An important role in the recognition of Staphylococcus aureus by immune cells is attributed to Toll-like receptor 2 (TLR2)[156]. Since monocytes and macrophages display different amounts of TLR2 on their surface, it is reasonable to assume that they present distinct reactions to Staphylococcus aureus[157]. Moreover, TNFα, IL-1β, IL-6, IL-8 and MMP-9 expression is dependent on the activation of TLR2[156, 158]. Thus, higher expression of TLR2 on naive monocytes in comparison to mature macrophages may explain the strong up-regulation of these cytokines when naive monocytes are challenged by SA. Furthermore, it was reported that immune cells recognize Staphylococcus aureus through the interaction of TLR2 with TLR1, TLR6, CD14 and CD36[156]. However, in order to fully elucidate the mechanisms of interaction of the receptors involved in titanium and SA recognition more research is needed.

In summary, it can be hypothesized that in vivo, an infection with Staphylococcus aureus induces not only an up-regulation of pro-inflammatory cytokines and

chemokines, but also of matrix remodeling proteins, which constitutes a possible mechanism for implant failures. Moreover, the immune reaction against Staphylococcus aureus infection is not dependent on titanium. Thus, implants made of different materials are also subjected to failure when an infection with Staphylococcus aureus occurs.

4.3 Macrophages, PBMC and fibroblasts in implant settings.

The results of this study have shown that macrophage response to titanium implants is very complex and is determined not only by titanium surface and size but also by macrophage activation state. Previous data also indicated that two members of the matrix metalloproteinases family, namely MMP7 and MMP9, are up-regulated in macrophages in response to titanium on gene and protein level. MMPs are generally considered major factors involved in extracellular matrix remodeling, osteolysis and periprosthetic loosening[107]. Both MMP-7 and MMP-9 have been shown to be involved in osteoclastogenesis and consequently in osteolysis[159, 160]. Moreover, elevated levels of MMP-7 and MMP-9 were detected in periprosthetic tissue of patients with loose artificial hip joints[161]. The results from the current study generally correlate with data obtained from the analysis of periprosthetic tissue of patients with titanium implants. However, some discrepancies were still observed (for example: down-regulation of CCL18 on titanium vs up-regulation of CCL18 in periprosthetic tissue), suggesting that other cellular components of the periprosthetic tissue influence the overall reaction to titanium. In order to study whether other cells in the periprosthetic tissue can modulate macrophage secretion of MMP-7 and MMP-9 in response to titanium, co-culture systems with peripheral blood mononuclear cells (PBMC) and fibroblasts were employed.

In order to distinguish which cells from the PMBC fraction are able to alter the secretion of MMP-7 and MMP-9 upon recognition of titanium or if the interaction of PBMC cells can enhance this effect, monocytes (CD14+ cells), PBMC depleted of CD14+ cells (PBMC-CD14) and whole PBMC were cultured on polished titanium discs. The experiments have shown that titanium does not induce increased levels of MMP-7 and MMP-9 in PBMC-CD14 fraction. However, the whole fraction of PBMC secreted significantly higher levels of MMP-7 and MMP-9 in response to titanium than macrophages alone. PBMC are comprised mainly of 2 types of cells: lymphocytes (B cells, T cells and NK cells) and monocytes. Studies have shown that lymphocytes also have the ability to react to metals and have been used as a diagnostic tool for type IV hypersensitivity to metals in the form of a lymphocytes transformation test (LTT)[162]. Moreover, the results presented in the current study correlate with data published by other authors which show that lymphocytes in both paracrine and juxtacrine manner are able to enhance macrophage reactions to foreign bodies[163]. Still, the lack of reaction towards titanium by the PBMC-CD14 fraction reinforces the widely accepted concept that macrophages are the key immune cells involved in foreign body recognition.

Fibroblasts represent one of the main cell types involved in the deposition of extracellular matrix. When stimulated with titanium wear particles fibroblasts were shown to increase the expression of pro-inflammatory factors such as IL-1β, IL-6, IL-8, CCL2 and MMP-1[65]. To determine if fibroblasts influence macrophage secretion of MMP-7 and MMP-9 in reaction to polished titanium a macrophage-fibroblast co-culture system was employed. In order to discriminate whether direct cell-cell interaction (juxtacrine macrophage-fibroblast interaction, JMFI) or secretion of soluble factors

(paracrine macrophage-fibroblast interaction, PMFI) influence macrophage response to titanium a transwell system was also used. The analysis of MMP-7 and MMP-9 secretion from macrophage-fibroblast co-culture experiments revealed that fibroblasts are able to significantly alter the secretion of these matrix metalloproteinases in response to titanium. In IL-4 stimulated cultures MMP-7 secretion was up-regulated in macrophage-fibroblast co-cultures on titanium in both paracrine and juxtacrine interaction models. In contrast, the secretion of MMP-9 was significantly inhibited in the juxtacrine interaction model, while no significant change was observed in the paracrine interaction model. Thus direct cell-cell contact is needed for the inhibition of MMP-9. This comes in contradiction to data presented by other authors which show that in a macrophage-fibroblast co-culture model the levels of MMP-9 were up-regulated in comparison to macrophage or fibroblast monoculture[164]. The discrepancy in the results can be explained by the use of different experimental settings (in this study MMP-9 levels were measured after 6 days of culture, while Zhu et al. after 24h). It is worth mentioning that fibroblasts alone did not present any changes in the secretion of MMP-7 and MMP-9 in response to titanium (data not shown), indicating that the primary source of these proteinases are macrophages, while fibroblasts can modulate their secretion.

MMPs are secreted in a proenzyme form requiring additional activation to exert their proteolytic activity[110]. Furthermore, it was shown that MMPs can also be activated by cells not directly involved in their secretion[165]. To analyze whether PBMC or fibroblasts are able to activate MMP-7 and/or MMP-9 the concentration of their active forms was also measured. Although the total concentration (pro- and active form) of both MMP-7 and MMP-9 was significantly changed by PBMC and fibroblast when co-cultured with macrophages on titanium, the concentration of their active form did not change substantially. These data suggest that MMP-7 and MMP-9 can be activated by other cells in the periprosthetic tissue.

Collectively these results indicate that in the periprosthetic tissue macrophages represent major producers of MMP-7 and MMP-9. Moreover, both PBMC and fibroblasts are able to significantly alter macrophage response to titanium. The activation of MMP-7 and MMP-9 is however performed by other cellular components of the periprosthetic tissue. Although both MMP-7 and MMP-9 were linked to implant complications[161], it is worth mentioning, that elevated levels of MMP-7 and MMP-9 in the periprosthetic tissue of titanium implants also correlated with osseointegration[166]. Thus the biological role of the metalloproteinases in the context of implants is ambiguous and probably dependent on the overall microenvironmental state.

4.4 Individual response to titanium

Previous experiments revealed that titanium induces specific changes in the regulation of several genes involved in modulation of inflammation and matrix remodeling (up-regulation of CSF1, CHI3L1, CHIT1, MMP8, MMP9, TNFRSF21 and TNFSF14; and down-regulation of CCL8, CCL13, CCL18, CCL23 and IL17RB). On the other hand, a high variation in expression of some genes between individual donors was observed, suggesting that not all donors react to titanium in the same way. Studies have shown that implant failure does not happen in all patients. The failure rate of orthopedic implants lies between 3.4% and 9%, while a 5.4% failure rate was reported for dental implants [152, 153, 167]. Aseptic loosening, characterized by a subtle, progressive destruction of the periprosthetic tissue as a result of foreign body response, constitutes a major factor in implant failure[60]. It is therefore reasonable to assume that in patients with higher reaction towards titanium there is a higher chance of implant failure. In this study a donor-specific gene expression profile (based on RT-qPCR data) was used to assess individual responses to titanium. By analyzing the differences induced by titanium in the expression of 11 genes it was possible to distinguish between donors with a high and low reaction to titanium. The results suggest that a macrophage-based approach for the identification of foreign body reaction towards titanium can be used to predict patients which react strongly to titanium and consequently have a higher chance of implant failure. However, in order for this method to be more sensitive and applicable in clinical settings, larger studies have to be conducted with samples from patients with both successful and failed implants. Additionally, to account for intrinsic interindividual variation multiple samples from the same individual at certain time intervals have to be taken for analysis[168].

4.5 Macrophage reactions to biodegradable implant coatings

The widespread use of titanium in biomedical applications is due to its superior biocompatibility and excellent mechanical properties. Still, due to various complications up to 9% of implants fail[153]. Two main causes of implant failure are aseptic loosening and infection[60, 108]. In order to enhance implant biocompatibility and minimize the chance of biofilm formation on the surface of implants, implant coatings can be applied. The use of coatings gives the advantage of increasing certain surface characteristics of the implant, such as biocompatibility and antimicrobial properties, without altering the bulk mechanical properties of the implant material[42].

In this study two types of coatings have been used: polyarginine/hyaluronic acid-based coatings (PAR/HA) and polylactic acid-based coatings (PLA). The coating made of polyarginine and hyaluronic acid was produced in the form of a polyelectrolyte multilayer film with polyarginine as polycation and hyaluronic acid as polyanion. Both components were chosen for their antimicrobial properties. Arginine is a common amino acid in the structure of antimicrobial peptides[112], while hyaluronic acid has been shown to inhibit bacterial adhesion[169]. Additionally, polyelectrolyte multilayer films can be used as delivery systems for biologically active molecules[113]. Therefore, to enhance the bactericidal properties of PAR/HA coatings, these were loaded with catestatin (PAR/HA+CAT). Catestatin is an antimicrobial peptide which demonstrates activity against bacteria, yeast and fungi[114]. Thus both PAR/HA and PAR/HA+CAT coatings are able to provide protection against a variety of infectious agents.

Polylactic acid is a synthetic biodegradable polymer commonly used in medical applications for the production of resorbable sutures, clips, screws and in drug delivery

devices[116]. The use of polylactic acid in biomedical applications is determined by its good mechanical properties, processability as well as high biocompatibility[115]. Moreover, through entrapment of biologically active molecules into its surface layer PLA can acquire additional properties[117]. In the present study two types of PLA coatings were used: unmodified PLA films and PLA films embedded with Brilliant Green dye (BGD), which possesses antiseptic properties.

To determine how macrophages react to both PAR/HA-based coatings and to PLA-based coatings the secretion of TNFα and CCL18 was analyzed by ELISA. Elevated levels of TNFα and CCL18 were associated with various chronic inflammatory diseases[124, 129]. The analysis revealed that PAR/HA and PAR/HA+CAT coatings significantly inhibited the secretion of TNFα and CCL18, suggesting that these types of coatings are able to inhibit the development of chronic inflammation. Unmodified PLA films were generally able to decrease the secretion of TNFα and CCL18. However, the PLA films modified with BGD induced TNFα and CCL18 secretion in a donor-specific way. These results demonstrated that surface modification of PLA films can be used to change inflammatory reactions of macrophages to the material. Thus embedding PLA-based coatings with antiseptic or immunomodulatory molecules can be used in implantation for the reduction of implant failure rate.

In vivo, the coating of the implant rather than the main implant material will interact with immune cells. Thus, analyzing macrophage reactions to implant surface coatings, as well as to the main implant material, is important for the determination of the overall foreign body reaction towards the implant. Moreover, evaluation of individual responses to implant coatings represents a promising approach for the selection of an optimal implant coating in a personalized way.

5 SUMMARY

Nowadays implants and medical devices are seen as efficient and practical solutions for a multitude of health associated problems. Titanium and titanium alloys have been successfully used in orthopedics, dentistry, cardiology and otorhinolaryngology. Superior mechanical properties, excellent corrosion resistance, low magnetic susceptibility and high biocompatibility have been the reason for choosing titanium for implantation. Still, up to 9% of implants fail due to the development of various complications. A major cause of implant failure is aseptic loosening, characterized by a progressive destruction of the periprosthetic tissue as a result of foreign body response. Macrophages are essential cells involved in the recognition of the foreign body and in the initiation and coordination of the foreign body response. In order to investigate the extent of macrophage reaction to titanium, human peripheral blood monocyte-derived macrophages were cultured with polished and porous titanium discs. To simulate different macrophage activation states and to discriminate among their reactions to titanium, macrophages were brought to 3 distinct activation states: M(Control), M(IFNγ) and M(IL-4). ELISA analysis revealed that both polished and porous titanium discs induce similar inflammatory cytokine profiles in macrophages. Affymetrix microarray analysis revealed a total of 1690 genes were differentially regulated by polished titanium and 4648 genes were differentially regulated by porous titanium. In both experiments, the highest number of differences between titanium and control settings were found in M(IL-4). Microarray analysis showed that both polished and porous titanium affected several genes involved in inflammation and matrix remodeling. RT-qPCR analysis confirmed that polished titanium up-regulates CSF1, TNFSF14, CHI3L1 and MMP9 and down-regulates CCL8, CCL13, CCL18, CCL23 and IL17RB in M(IL-4) macrophages. Likewise, porous titanium up-regulates the expression of CHIT1, CHI3L1, MMP8 and MMP9 and suppresses CCL8, CCL13, CCL18, CCL23 and IL17RB in M(IL-4) macrophages. Additionally, in order to model wear debris, titanium microbeads and nanoparticles were used. RT-qPCR analysis demonstrated that nanoparticles induce stronger up-regulation of CSF1, CHIT1 and CHI3L1 and stronger down-regulation of CCL8, CCL13, CCL18, and CCL23 when compared to polished titanium discs or to titanium microbeads. In summary, it was demonstrated that titanium induces pro-inflammatory and tissue-remodeling responses first of all in M(IL-4) macrophages, that model healing macrophages. This can explain failure of implants on later stages of implant integration.

In order to simulate a bacterial infection of titanium implants, heat killed Staphylococcus Aureus were added to mature macrophages and naive monocytes cultured with polished titanium discs. Cytokine release analysis revealed that when Staphylococcus Aureus is added to naive monocytes higher levels of TNFα, IL-1β, IL-6, IL-8, CCL18, MMP-7 and MMP-9 are secreted. However, the reaction to Staphylococcus Aureus is not affected by titanium.

In order to examine the effect of peripheral blood mononuclear cells and fibroblasts on the secretion of MMP-7 and MMP-9 by macrophages in response to titanium, co-culture models were established. MMP-7 and MMP-9 secretion levels were increased when the whole fraction of peripheral blood mononuclear cells was exposed to titanium. However, depletion of CD14+ monocytes abrogated this effect. Similarly, fibroblasts stimulated the secretion of MMP-7 in both juxtacrine and paracrine macrophage-fibroblast interaction models. In contrast, MMP-9 secretion was inhibited by fibroblasts in the juxtacrine interaction model. Still, neither peripheral blood mononuclear cells nor

fibroblasts were able to substantially increase the concentration of active MMP-7 and MMP-9 in response to titanium.

To increase implant biocompatibility implant coatings can be applied. In this study two types of coatings have been used: polyarginine/hyaluronic acid-based coatings and polylactic acid-based coatings. To test macrophage reaction to these coatings the secretion of TNFα and CCL18 was analyzed. Polyarginine/hyaluronic acid-based coatings inhibited the secretion of TNFα and CCL18 in all donors analyzed. In contrast, the reaction of macrophages to polylactic acid-based coatings was donor-dependent.

Collectively the results of this study indicate that macrophage reaction to titanium implants is determined by several factors: 1) macrophage activation state; 2) titanium surface; 3) titanium size; 4) other cellular components of the periprosthetic tissue; 5) donor-specific factors. However, macrophage reaction to Staphylococcus Aureus is independent of titanium. Furthermore, analysis of macrophage responses to the main implant material as well as to coating materials in a donor-specific way represents a promising approach for the selection of optimal personalized implant materials.

6   BIBLIOGRAPHY

1. Kirkup, JR: The history and evolution of surgical instruments. I. Introduction. *Ann R Coll Surg Engl,* 63**:** 279-285, 1981.
2. Thurston, AJ: Pare and prosthetics: the early history of artificial limbs. *ANZ J Surg,* 77**:** 1114-1119, 2007.
3. Abraham, CM: A brief historical perspective on dental implants, their surface coatings and treatments. *Open Dent J,* 8**:** 50-55, 2014.
4. EC: Directive 2007/47/EC of the European Parliament and of the Council of 5 September 2007 amending Council Directive 90/385/EEC on the approximation of the laws of the Member States relating to active implantable medical devices, Council Directive 93/42/EEC concerning medical devices and Directive 98/8/EC concerning the placing of biocidal products on the market. *Official Journal of the European Union,* 50**:** 21–55, 2007.
5. EEC: Council Directive 93/42/EEC of 14 June 1993 concerning medical devices. *Official Journal of the European Union,* 36**:** 1-43, 1993.
6. Eurostat: Population by type of disability, sex, age and marital status. Table hlth_dp060. Retrieved from http://ec.europa.eu/eurostat/web/health/. 2011.
7. Eurostat: Surgical operations and procedures performed in hospitals by ICD-9-CM. Table hlth_co_proc2. Retrieved from http://ec.europa.eu/eurostat/web/health/. 2014.
8. French-Mowat, E, Burnett, J: How are medical devices regulated in the European Union? *J R Soc Med,* 105 Suppl 1**:** S22-28, 2012.
9. Domb, AJ, Khan, W: *Focal controlled drug delivery,* New York, Springer, 2014.
10. Falcone, T, Hurd, WW, Ohio Library and Information Network: Clinical reproductive medicine and surgery a practical guide. 2nd ed ed. New York, Springer,, 2013 pp 1 online resource (x, 340 p.).
11. Wong, JY, Bronzino, JD, Peterson, DR: *Biomaterials : principles and practices,* Boca Raton, FL, CRC Press, 2013.
12. Soffer, EE: Gastric electrical stimulation for gastroparesis. *J Neurogastroenterol Motil,* 18**:** 131-137, 2012.
13. Bonavina, L, Saino, G, Lipham, JC, Demeester, TR: LINX((R)) Reflux Management System in chronic gastroesophageal reflux: a novel effective technology for restoring the natural barrier to reflux. *Therap Adv Gastroenterol,* 6**:** 261-268, 2013.
14. Park, JB, Lakes, RS: *Biomaterials : an introduction,* New York, NY, Springer, 2007.
15. Williams, DF, ebrary Inc.: The Williams dictionary of biomaterials. Liverpool, Liverpool University Press,, 1999 pp xvii, 343 p.
16. Thorne, C, Grabb, WC, Smith, JW: *Grabb and Smith's plastic surgery,* Philadelphia, Wolters Kluwer Health/Lippincott Williams & Wilkins, 2007.
17. Ratner, BD: *Biomaterials science : an introduction to materials in medicine,* Amsterdam ; Boston, Elsevier Academic Press, 2004.
18. Ghosh, M, Chatterjee, S: Diffusion bonded transition joints of titanium to stainless steel with improved properties. *Materials Science and Engineering: A,* 358**:** 152-158, 2003.
19. Halka, M, Nordstrom, B: *Transition metals,* New York, NY, Facts on File, 2011.
20. Moore, JJ, Moore, JJ, Boyce, EA: *Chemical metallurgy,* London etc., Butterworths, 1990.
21. Greenwood, NN, Earnshaw, A: *Chemistry of the elements,* Oxford, Butterworth-Heinemann, 1998.

22. Bourikas, K, Kordulis, C, Lycourghiotis, A: Titanium dioxide (anatase and rutile): surface chemistry, liquid-solid interface chemistry, and scientific synthesis of supported catalysts. *Chem Rev,* 114**:** 9754-9823, 2014.

23. Christensen, PA, Dilks, A, Egerton, TA, Temperley, J: Infrared spectroscopic evaluation of the photodegradation of paint Part I The UV degradation of acrylic films pigmented with titanium dioxide. *Journal of Materials Science,* 34**:** 5689-5700, 1999.

24. Newman, MD, Stotland, M, Ellis, JI: The safety of nanosized particles in titanium dioxide- and zinc oxide-based sunscreens. *J Am Acad Dermatol,* 61**:** 685-692, 2009.

25. Fujishima, A, Kohayakawa, K, Honda, K: Hydrogen Production under Sunlight with an Electrochemical Photocell. *Journal of The Electrochemical Society,* 122**:** 1487-1489, 1975.

26. Gaya, UI, Abdullah, AH: Heterogeneous photocatalytic degradation of organic contaminants over titanium dioxide: A review of fundamentals, progress and problems. *Journal of Photochemistry and Photobiology C: Photochemistry Reviews,* 9**:** 1-12, 2008.

27. Teh, CM, Mohamed, AR: Roles of titanium dioxide and ion-doped titanium dioxide on photocatalytic degradation of organic pollutants (phenolic compounds and dyes) in aqueous solutions: A review. *Journal of Alloys and Compounds,* 509**:** 1648-1660, 2011.

28. Boyer, RR: International Symposium on Metallurgy and Technology of Titanium AlloysAn overview on the use of titanium in the aerospace industry. *Materials Science and Engineering: A,* 213**:** 103-114, 1996.

29. hexagonal close-packed structure: common metallic crystal structures. [Illustration]. . *In Encyclopædia Britannica.* Retrieved from https://www.britannica.com/science/body-centred-cubic-structure/images-videos/The-commonest-metallic-crystal-structures/1527, 2011.

30. Elias, CN, Lima, JHC, Valiev, R, Meyers, MA: Biomedical applications of titanium and its alloys. *JOM,* 60**:** 46-49, 2008.

31. Rack, HJ, Qazi, JI: Titanium alloys for biomedical applications. *Materials Science and Engineering: C,* 26**:** 1269-1277, 2006.

32. Li, Y, Yang, C, Zhao, H, Qu, S, Li, X, Li, Y: New Developments of Ti-Based Alloys for Biomedical Applications. *Materials,* 7**:** 1709, 2014.

33. Head, WC, Bauk, DJ, Emerson, RHJ: Titanium As the Material of Choice for Cementless Femoral Components in Total Hip Arthroplasty. *Clinical Orthopaedics and Related Research,* 311**:** 85-90, 1995.

34. Huiskes, R, Weinans, H, van Rietbergen, B: The relationship between stress shielding and bone resorption around total hip stems and the effects of flexible materials. *Clin Orthop Relat Res***:** 124-134, 1992.

35. Geetha, M, Singh, A, Asokamani, R, Gogia, A: Ti based biomaterials, the ultimate choice for orthopaedic implants–a review. *Progress in Materials science,* 54**:** 397-425, 2009.

36. Nakai, M, Niinomi, M, Zhao, X, Zhao, X: Self-adjustment of Young's modulus in biomedical titanium alloys during orthopaedic operation. *Materials Letters,* 65**:** 688-690, 2011.

37. Brunette, DM: *Titanium in medicine : material science, surface science, engineering, biological responses, and medical applications,* Berlin ; New York, Springer, 2001.

38. Calin, M, Gebert, A, Ghinea, AC, Gostin, PF, Abdi, S, Mickel, C, Eckert, J: Designing biocompatible Ti-based metallic glasses for implant applications. *Materials Science and Engineering: C,* 33**:** 875-883, 2013.

39. Debry, C, Dupret–Bories, A, Vrana, NE, Hemar, P, Lavalle, P, Schultz, P: Laryngeal replacement with an artificial larynx after total laryngectomy: The possibility of restoring larynx functionality in the future. *Head & Neck,* 36**:** 1669-1673, 2014.

40. Daneshi, A, Mohammadi, S, Javadi, M, Hassannia, F: Repair of large nasal septal perforation with titanium membrane:: report of 10 cases. *American Journal of Otolaryngology,* 31**:** 387-389, 2010.

41. Lee, B, Zubair, MN, Marquez, YD, Lee, DM, Kalayjian, LA, Heck, CN, Liu, CY: A Single-Center Experience with the NeuroPace RNS System: A Review of Techniques and Potential Problems. *World Neurosurg,* 84**:** 719-726, 2015.

42. Kzhyshkowska, J, Gudima, A, Riabov, V, Dollinger, C, Lavalle, P, Vrana, NE: Macrophage responses to implants: prospects for personalized medicine. *J Leukoc Biol,* 98**:** 953-962, 2015.

43. Mosby Inc.: *Mosby's medical dictionary,* St. Louis, MO, Mosby, 2009.

44. Ambe, P, Weber, SA, Schauer, M, Knoefel, WT: Swallowed foreign bodies in adults. *Deutsches Arzteblatt international,* 109**:** 869-875, 2012.

45. Vrana, NE, Iniewski, K: *Cell and material interface : advances in tissue engineering, biosensor, implant, and imaging technologies,* Boca Raton, CRC Press, 2016.

46. Gordon, S, Martinez, FO: Alternative activation of macrophages: mechanism and functions. *Immunity,* 32**:** 593-604, 2010.

47. Spiller, KL, Wrona, EA, Romero-Torres, S, Pallotta, I, Graney, PL, Witherel, CE, Panicker, LM, Feldman, RA, Urbanska, AM, Santambrogio, L, Vunjak-Novakovic, G, Freytes, DO: Differential gene expression in human, murine, and cell line-derived macrophages upon polarization. *Experimental Cell Research,* 347**:** 1-13, 2016.

48. Ginhoux, F, Schultze, JL, Murray, PJ, Ochando, J, Biswas, SK: New insights into the multidimensional concept of macrophage ontogeny, activation and function. *Nature immunology,* 17**:** 34-40, 2016.

49. Martinez, FO, Sica, A, Mantovani, A, Locati, M: Macrophage activation and polarization. *Frontiers in bioscience : a journal and virtual library,* 13**:** 453-461, 2008.

50. Gratchev, A, Kzhyshkowska, J, Kothe, K, Muller-Molinet, I, Kannookadan, S, Utikal, J, Goerdt, S: Mphi1 and Mphi2 can be re-polarized by Th2 or Th1 cytokines, respectively, and respond to exogenous danger signals. *Immunobiology,* 211**:** 473-486, 2006.

51. Xue, J, Schmidt, SV, Sander, J, Draffehn, A, Krebs, W, Quester, I, De Nardo, D, Gohel, TD, Emde, M, Schmidleithner, L, Ganesan, H, Nino-Castro, A, Mallmann, MR, Labzin, L, Theis, H, Kraut, M, Beyer, M, Latz, E, Freeman, TC, Ulas, T, Schultze, JL: Transcriptome-based network analysis reveals a spectrum model of human macrophage activation. *Immunity,* 40**:** 274-288, 2014.

52. Murray, PJ, Allen, JE, Biswas, SK, Fisher, EA, Gilroy, DW, Goerdt, S, Gordon, S, Hamilton, JA, Ivashkiv, LB, Lawrence, T, Locati, M, Mantovani, A, Martinez, FO, Mege, J-L, Mosser, DM, Natoli, G, Saeij, JP, Schultze, JL, Shirey, KA, Sica, A, Suttles, J, Udalova, I, van Ginderachter, JA, Vogel, SN, Wynn, TA: Macrophage activation and polarization: nomenclature and experimental guidelines. *Immunity,* 41**:** 14-20, 2014.

53. Love, RJ, Jones, KS: The recognition of biomaterials: pattern recognition of medical polymers and their adsorbed biomolecules. *J Biomed Mater Res A,* 101**:** 2740-2752, 2013.

54. Lin, TH, Tamaki, Y, Pajarinen, J, Waters, HA, Woo, DK, Yao, Z, Goodman, SB: Chronic inflammation in biomaterial-induced periprosthetic osteolysis: NF-kappaB as a therapeutic target. *Acta Biomater,* 10**:** 1-10, 2014.

55. Revell, PA: The combined role of wear particles, macrophages and lymphocytes in the loosening of total joint prostheses. *Journal of the Royal Society, Interface / the Royal Society,* 5**:** 1263-1278, 2008.

56. Landgraeber, S, Jager, M, Jacobs, JJ, Hallab, NJ: The pathology of orthopedic implant failure is mediated by innate immune system cytokines. *Mediators Inflamm,* 2014**:** 185150, 2014.

57. Anderson, JM, Rodriguez, A, Chang, DT: Foreign body reaction to biomaterials. *Semin Immunol,* 20**:** 86-100, 2008.

58. Alfarsi, MA, Hamlet, SM, Ivanovski, S: The Effect of Platelet Proteins Released in Response to Titanium Implant Surfaces on Macrophage Pro-Inflammatory Cytokine Gene Expression. *Clin Implant Dent Relat Res,* 17**:** 1036-1047, 2015.

59. Rakshit, DS, Ly, K, Sengupta, TK, Nestor, BJ, Sculco, TP, Ivashkiv, LB, Purdue, PE: Wear debris inhibition of anti-osteoclastogenic signaling by interleukin-6 and interferon-gamma. Mechanistic insights and implications for periprosthetic osteolysis. *J Bone Joint Surg Am,* 88**:** 788-799, 2006.

60. Abu-Amer, Y, Darwech, I, Clohisy, JC: Aseptic loosening of total joint replacements: mechanisms underlying osteolysis and potential therapies. *Arthritis Res Ther,* 9 Suppl 1**:** S6, 2007.

61. Tanaka, Y, Nakayamada, S, Okada, Y: Osteoblasts and osteoclasts in bone remodeling and inflammation. *Current drug targets Inflammation and allergy,* 4**:** 325-328, 2005.

62. Pioletti, DP, Kottelat, A: The influence of wear particles in the expression of osteoclastogenesis factors by osteoblasts. *Biomaterials,* 25**:** 5803-5808, 2004.

63. O'Neill, SC, Queally, JM, Devitt, BM, Doran, PP, O'Byrne, JM: The role of osteoblasts in peri-prosthetic osteolysis. *The bone & joint journal,* 95-b**:** 1022-1026, 2013.

64. Lochner, K, Fritsche, A, Jonitz, A, Hansmann, D, Mueller, P, Mueller-Hilke, B, Bader, R: The potential role of human osteoblasts for periprosthetic osteolysis following exposure to wear particles. *International journal of molecular medicine,* 28**:** 1055-1063, 2011.

65. Koreny, T, Tunyogi-Csapo, M, Gal, I, Vermes, C, Jacobs, JJ, Glant, TT: The role of fibroblasts and fibroblast-derived factors in periprosthetic osteolysis. *Arthritis and rheumatism,* 54**:** 3221-3232, 2006.

66. Beidelschies, MA, Huang, H, McMullen, MR, Smith, MV, Islam, AS, Goldberg, VM, Chen, X, Nagy, LE, Greenfield, EM: Stimulation of macrophage TNFalpha production by orthopaedic wear particles requires activation of the ERK1/2/Egr-1 and NF-kappaB pathways but is independent of p38 and JNK. *J Cell Physiol,* 217**:** 652-666, 2008.

67. Minematsu, H, Shin, MJ, Celil Aydemir, AB, Seo, SW, Kim, DW, Blaine, TA, Macian, F, Yang, J, Lee, FY: Orthopedic implant particle-induced tumor necrosis factor-alpha production in macrophage-monocyte lineage cells is mediated by nuclear factor of activated T cells. *Ann N Y Acad Sci,* 1117**:** 143-150, 2007.

68. Valles, G, Gonzalez-Melendi, P, Gonzalez-Carrasco, JL, Saldana, L, Sanchez-Sabate, E, Munuera, L, Vilaboa, N: Differential inflammatory macrophage response to rutile and titanium particles. *Biomaterials,* 27**:** 5199-5211, 2006.

69. Mao, X, Pan, X, Peng, X, Cheng, T, Zhang, X: Inhibition of titanium particle-induced inflammation by the proteasome inhibitor bortezomib in murine macrophage-like RAW 264.7 cells. *Inflammation,* 35**:** 1411-1418, 2012.

70. Naganuma, Y, Takakubo, Y, Hirayama, T, Tamaki, Y, Pajarinen, J, Sasaki, K, Goodman, SB, Takagi, M: Lipoteichoic acid modulates inflammatory response in macrophages after phagocytosis of titanium particles through Toll-like receptor 2 cascade and inflammasomes. *J Biomed Mater Res A,* 104**:** 435-444, 2016.

71. Ruiz, PA, Moron, B, Becker, HM, Lang, S, Atrott, K, Spalinger, MR, Scharl, M, Wojtal, KA, Fischbeck-Terhalle, A, Frey-Wagner, I, Hausmann, M, Kraemer, T, Rogler, G: Titanium dioxide nanoparticles exacerbate DSS-induced colitis: role of the NLRP3 inflammasome. *Gut*, 2016.

72. Luo, G, Li, Z, Wang, Y, Wang, H, Zhang, Z, Chen, W, Zhang, Y, Xiao, Y, Li, C, Guo, Y, Sheng, P: Resveratrol Protects against Titanium Particle-Induced Aseptic Loosening Through Reduction of Oxidative Stress and Inactivation of NF-kappaB. *Inflammation*, 2016.

73. Lee, NK, Choi, YG, Baik, JY, Han, SY, Jeong, DW, Bae, YS, Kim, N, Lee, SY: A crucial role for reactive oxygen species in RANKL-induced osteoclast differentiation. *Blood,* 106**:** 852-859, 2005.

74. Yang, H, Xu, Y, Zhu, M, Gu, Y, Zhang, W, Shao, H, Wang, Y, Ping, Z, Hu, X, Wang, L, Geng, D: Inhibition of titanium-particle-induced inflammatory osteolysis after local administration of dopamine and suppression of osteoclastogenesis via D2-like receptor signaling pathway. *Biomaterials,* 80**:** 1-10, 2016.

75. Sang, X, Zheng, L, Sun, Q, Li, N, Cui, Y, Hu, R, Gao, G, Cheng, Z, Cheng, J, Gui, S, Liu, H, Zhang, Z, Hong, F: The chronic spleen injury of mice following long-term exposure to titanium dioxide nanoparticles. *J Biomed Mater Res A,* 100**:** 894-902, 2012.

76. Warme, BA, Epstein, NJ, Trindade, MC, Miyanishi, K, Ma, T, Saket, RR, Regula, D, Goodman, SB, Smith, RL: Proinflammatory mediator expression in a novel murine model of titanium-particle-induced intramedullary inflammation. *J Biomed Mater Res B Appl Biomater,* 71**:** 360-366, 2004.

77. Yazdi, AS, Guarda, G, Riteau, N, Drexler, SK, Tardivel, A, Couillin, I, Tschopp, J: Nanoparticles activate the NLR pyrin domain containing 3 (Nlrp3) inflammasome and cause pulmonary inflammation through release of IL-1alpha and IL-1beta. *Proc Natl Acad Sci U S A,* 107**:** 19449-19454, 2010.

78. Huang, KT, Wu, CT, Huang, KH, Lin, WC, Chen, CM, Guan, SS, Chiang, CK, Liu, SH: Titanium nanoparticle inhalation induces renal fibrosis in mice via an oxidative stress upregulated transforming growth factor-beta pathway. *Chem Res Toxicol,* 28**:** 354-364, 2015.

79. Jiang, Y, Jia, T, Gong, W, Wooley, PH, Yang, SY: Titanium particle-challenged osteoblasts promote osteoclastogenesis and osteolysis in a murine model of periprosthestic osteolysis. *Acta Biomater,* 9**:** 7564-7572, 2013.

80. Clohisy, JC, Frazier, E, Hirayama, T, Abu-Amer, Y: RANKL is an essential cytokine mediator of polymethylmethacrylate particle-induced osteoclastogenesis. *J Orthop Res,* 21**:** 202-212, 2003.

81. Cadosch, D, Gautschi, OP, Chan, E, Simmen, HP, Filgueira, L: Titanium induced production of chemokines CCL17/TARC and CCL22/MDC in human osteoclasts and osteoblasts. *J Biomed Mater Res A,* 92**:** 475-483, 2010.

82. Kim, DH, Novak, MT, Wilkins, J, Kim, M, Sawyer, A, Reichert, WM: Response of monocytes exposed to phagocytosable particles and discs of comparable surface roughness. *Biomaterials,* 28**:** 4231-4239, 2007.

83. Alfarsi, MA, Hamlet, SM, Ivanovski, S: Titanium surface hydrophilicity modulates the human macrophage inflammatory cytokine response. *J Biomed Mater Res A,* 102**:** 60-67, 2014.

84. Hotchkiss, KM, Reddy, GB, Hyzy, SL, Schwartz, Z, Boyan, BD, Olivares-Navarrete, R: Titanium surface characteristics, including topography and wettability, alter macrophage activation. *Acta Biomater,* 31**:** 425-434, 2016.

85. Hyzy, SL, Olivares-Navarrete, R, Hutton, DL, Tan, C, Boyan, BD, Schwartz, Z: Microstructured titanium regulates interleukin production by osteoblasts, an effect modulated by exogenous BMP-2. *Acta Biomater,* 9**:** 5821-5829, 2013.

86. Kujala, S, Ryhänen, J, Danilov, A, Tuukkanen, J: Effect of porosity on the osteointegration and bone ingrowth of a weight-bearing nickel–titanium bone graft substitute. *Biomaterials,* 24**:** 4691-4697, 2003.

87. Karageorgiou, V, Kaplan, D: Porosity of 3D biomaterial scaffolds and osteogenesis. *Biomaterials,* 26**:** 5474-5491, 2005.

88. Liu, X, Chu, PK, Ding, C: Surface modification of titanium, titanium alloys, and related materials for biomedical applications. *Materials Science and Engineering: R: Reports,* 47**:** 49-121, 2004.

89. Deligianni, DD, Katsala, N, Ladas, S, Sotiropoulou, D, Amedee, J, Missirlis, YF: Effect of surface roughness of the titanium alloy Ti-6Al-4V on human bone marrow cell response and on protein adsorption. *Biomaterials,* 22**:** 1241-1251, 2001.

90. Bartneck, M, Schulte, VA, Paul, NE, Diez, M, Lensen, MC, Zwadlo-Klarwasser, G: Induction of specific macrophage subtypes by defined micro-patterned structures. *Acta Biomater,* 6**:** 3864-3872, 2010.

91. Gittens, RA, Scheideler, L, Rupp, F, Hyzy, SL, Geis-Gerstorfer, J, Schwartz, Z, Boyan, BD: A review on the wettability of dental implant surfaces II: Biological and clinical aspects. *Acta Biomater,* 10**:** 2907-2918, 2014.

92. Rostam, HM, Singh, S, Vrana, NE, Alexander, MR, Ghaemmaghami, AM: Impact of surface chemistry and topography on the function of antigen presenting cells. *Biomater Sci,* 3**:** 424-441, 2015.

93. Morais, JM, Papadimitrakopoulos, F, Burgess, DJ: Biomaterials/tissue interactions: possible solutions to overcome foreign body response. *The AAPS journal,* 12**:** 188-196, 2010.

94. Gao, G, Lange, D, Hilpert, K, Kindrachuk, J, Zou, Y, Cheng, JTJ, Kazemzadeh-Narbat, M, Yu, K, Wang, R, Straus, SK, Brooks, DE, Chew, BH, Hancock, REW, Kizhakkedathu, JN: The biocompatibility and biofilm resistance of implant coatings based on hydrophilic polymer brushes conjugated with antimicrobial peptides. *Biomaterials,* 32**:** 3899-3909, 2011.

95. Wolf, MT, Dearth, CL, Ranallo, CA, LoPresti, ST, Carey, LE, Daly, KA, Brown, BN, Badylak, SF: Macrophage polarization in response to ECM coated polypropylene mesh. *Biomaterials,* 35**:** 6838-6849, 2014.

96. Vrana, N, Erdemli, O, Francius, G, Fahs, A, Rabineau, M, Debry, C, Tezcaner, A, Keskin, D, Lavalle, P: Double entrapment of growth factors by nanoparticles loaded into polyelectrolyte multilayer films. *Journal of Materials Chemistry B,* 2**:** 999-1008, 2014.

97. Ozcelik, H, Vrana, NE, Gudima, A, Riabov, V, Gratchev, A, Haikel, Y, Metz-Boutigue, MH, Carrado, A, Faerber, J, Roland, T, Kluter, H, Kzhyshkowska, J, Schaaf, P, Lavalle, P: Harnessing the multifunctionality in nature: a bioactive agent release system with self-antimicrobial and immunomodulatory properties. *Advanced healthcare materials,* 4**:** 2026-2036, 2015.

98. Dai, M, Wang, P, Boyd, AD, Kostov, G, Athey, B, Jones, EG, Bunney, WE, Myers, RM, Speed, TP, Akil, H, Watson, SJ, Meng, F: Evolving gene/transcript definitions significantly alter the interpretation of GeneChip data. *Nucleic acids research,* 33**:** e175, 2005.

99. Tarca, AL, Romero, R, Draghici, S: Analysis of microarray experiments of gene expression profiling. *American journal of obstetrics and gynecology,* 195**:** 373-388, 2006.
100. Kolatat, K, Perino, G, Wilner, G, Kaplowitz, E, Ricciardi, BF, Boettner, F, Westrich, GH, Jerabek, SA, Goldring, SR, Purdue, PE: Adverse local tissue reaction (ALTR) associated with corrosion products in metal-on-metal and dual modular neck total hip replacements is associated with upregulation of interferon gamma-mediated chemokine signaling. *J Orthop Res,* 33**:** 1487-1497, 2015.
101. Koulouvaris, P, Ly, K, Ivashkiv, LB, Bostrom, MP, Nestor, BJ, Sculco, TP, Purdue, PE: Expression profiling reveals alternative macrophage activation and impaired osteogenesis in periprosthetic osteolysis. *J Orthop Res,* 26**:** 106-116, 2008.
102. Lavorgna, A, Matsuoka, M, Harhaj, EW: A Critical Role for IL-17RB Signaling in HTLV-1 Tax-Induced NF-κB Activation and T-Cell Transformation. *PLOS Pathogens,* 10**:** e1004418, 2014.
103. Lee, CG, Da Silva, CA, Dela Cruz, CS, Ahangari, F, Ma, B, Kang, M-J, He, C-H, Takyar, S, Elias, JA: Role of Chitin and Chitinase/Chitinase-Like Proteins in Inflammation, Tissue Remodeling, and Injury. *Annual review of physiology,* 73**:** 10.1146/annurev-physiol-012110-142250, 2011.
104. Page-McCaw, A, Ewald, AJ, Werb, Z: Matrix metalloproteinases and the regulation of tissue remodelling. *Nature reviews Molecular cell biology,* 8**:** 221-233, 2007.
105. Kivela-Rajamaki, MJ, Teronen, OP, Maisi, P, Husa, V, Tervahartiala, TI, Pirila, EM, Salo, TA, Mellanen, L, Sorsa, TA: Laminin-5 gamma2-chain and collagenase-2 (MMP-8) in human peri-implant sulcular fluid. *Clin Oral Implants Res,* 14**:** 158-165, 2003.
106. Tomankova, T, Kriegova, E, Fillerova, R, Luzna, P, Ehrmann, J, Gallo, J: Comparison of periprosthetic tissues in knee and hip joints: differential expression of CCL3 and DC-STAMP in total knee and hip arthroplasty and similar cytokine profiles in primary knee and hip osteoarthritis. *Osteoarthritis Cartilage,* 22**:** 1851-1860, 2014.
107. Syggelos, SA, Aletras, AJ, Smirlaki, I, Skandalis, SS: Extracellular Matrix Degradation and Tissue Remodeling in Periprosthetic Loosening and Osteolysis: Focus on Matrix Metalloproteinases, Their Endogenous Tissue Inhibitors, and the Proteasome. *BioMed Research International,* 2013**:** 230805, 2013.
108. Arciola, CR, Campoccia, D, Speziale, P, Montanaro, L, Costerton, JW: Biofilm formation in Staphylococcus implant infections. A review of molecular mechanisms and implications for biofilm-resistant materials. *Biomaterials,* 33**:** 5967-5982, 2012.
109. Shi, C, Pamer, EG: Monocyte recruitment during infection and inflammation. *Nature reviews Immunology,* 11**:** 762-774, 2011.
110. Löffek, S, Schilling, O, Franzke, C-W: Biological role of matrix metalloproteinases: a critical balance. *European Respiratory Journal,* 38**:** 191-208, 2011.
111. Kurtz, S, Ong, K, Lau, E, Mowat, F, Halpern, M: Projections of primary and revision hip and knee arthroplasty in the United States from 2005 to 2030. *J Bone Joint Surg Am,* 89**:** 780-785, 2007.
112. Chan, DI, Prenner, EJ, Vogel, HJ: Tryptophan- and arginine-rich antimicrobial peptides: structures and mechanisms of action. *Biochim Biophys Acta,* 1758**:** 1184-1202, 2006.

113. Barthes, J, Mertz, D, Bach, C, Metz-Boutigue, MH, Senger, B, Voegel, JC, Schaaf, P, Lavalle, P: Stretch-induced biodegradation of polyelectrolyte multilayer films for drug release. *Langmuir : the ACS journal of surfaces and colloids,* 28**:** 13550-13554, 2012.

114. Radek, KA, Lopez-Garcia, B, Hupe, M, Niesman, IR, Elias, PM, Taupenot, L, Mahata, SK, O'Connor, DT, Gallo, RL: The neuroendocrine peptide catestatin is a cutaneous antimicrobial and induced in the skin after injury. *The Journal of investigative dermatology,* 128**:** 1525-1534, 2008.

115. Stankevich, KS, Gudima, A, Filimonov, VD, Kluter, H, Mamontova, EM, Tverdokhlebov, SI, Kzhyshkowska, J: Surface modification of biomaterials based on high-molecular polylactic acid and their effect on inflammatory reactions of primary human monocyte-derived macrophages: perspective for personalized therapy. *Materials science & engineering C, Materials for biological applications,* 51**:** 117-126, 2015.

116. Ruozi, B, Belletti, D, Manfredini, G, Tonelli, M, Sena, P, Vandelli, MA, Forni, F, Tosi, G: Biodegradable device applied in flatfoot surgery: Comparative studies between clinical and technological aspects of removed screws. *Materials Science and Engineering: C,* 33**:** 1773-1782, 2013.

117. Rasal, RM, Janorkar, AV, Hirt, DE: Poly(lactic acid) modifications. *Progress in Polymer Science,* 35**:** 338-356, 2010.

118. Heil, TL, Volkmann, KR, Wataha, JC, Lockwood, PE: Human peripheral blood monocytes versus THP-1 monocytes for in vitro biocompatibility testing of dental material components. *Journal of oral rehabilitation,* 29**:** 401-407, 2002.

119. Spiller, KL, Anfang, RR, Spiller, KJ, Ng, J, Nakazawa, KR, Daulton, JW, Vunjak-Novakovic, G: The role of macrophage phenotype in vascularization of tissue engineering scaffolds. *Biomaterials,* 35**:** 4477-4488, 2014.

120. Brown, BN, Londono, R, Tottey, S, Zhang, L, Kukla, KA, Wolf, MT, Daly, KA, Reing, JE, Badylak, SF: Macrophage phenotype as a predictor of constructive remodeling following the implantation of biologically derived surgical mesh materials. *Acta Biomater,* 8**:** 978-987, 2012.

121. Cochran, DL: A comparison of endosseous dental implant surfaces. *Journal of periodontology,* 70**:** 1523-1539, 1999.

122. Mantelli, P, Fioruzzi, A, Bisogno, L, Fioruzzi, C, Fusco, U, Olivieri, M, Lisanti, M: Short femoral stem and porous titanium: winning combination? *Acta bio-medica : Atenei Parmensis,* 85 Suppl 2**:** 71-74, 2014.

123. Noordin, S, Masri, B: Periprosthetic osteolysis: genetics, mechanisms and potential therapeutic interventions. *Canadian journal of surgery Journal canadien de chirurgie,* 55**:** 408-417, 2012.

124. Bradley, JR: TNF-mediated inflammatory disease. *The Journal of pathology,* 214**:** 149-160, 2008.

125. Akdis, M, Burgler, S, Crameri, R, Eiwegger, T, Fujita, H, Gomez, E, Klunker, S, Meyer, N, O'Mahony, L, Palomares, O, Rhyner, C, Ouaked, N, Schaffartzik, A, Van De Veen, W, Zeller, S, Zimmermann, M, Akdis, CA: Interleukins, from 1 to 37, and interferon-gamma: receptors, functions, and roles in diseases. *The Journal of allergy and clinical immunology,* 127**:** 701-721.e701-770, 2011.

126. Turner, MD, Nedjai, B, Hurst, T, Pennington, DJ: Cytokines and chemokines: At the crossroads of cell signalling and inflammatory disease. *Biochim Biophys Acta,* 1843**:** 2563-2582, 2014.

127. Arango Duque, G, Descoteaux, A: Macrophage cytokines: involvement in immunity and infectious diseases. *Frontiers in immunology,* 5**:** 491, 2014.

128. Tanaka, T, Kishimoto, T: The biology and medical implications of interleukin-6. *Cancer immunology research,* 2**:** 288-294, 2014.

129. Schutyser, E, Richmond, A, Van Damme, J: Involvement of CC chemokine ligand 18 (CCL18) in normal and pathological processes. *J Leukoc Biol,* 78**:** 14-26, 2005.

130. Schraufstatter, IU, Zhao, M, Khaldoyanidi, SK, Discipio, RG: The chemokine CCL18 causes maturation of cultured monocytes to macrophages in the M2 spectrum. *Immunology,* 135**:** 287-298, 2012.

131. Pajarinen, J, Kouri, VP, Jamsen, E, Li, TF, Mandelin, J, Konttinen, YT: The response of macrophages to titanium particles is determined by macrophage polarization. *Acta Biomater,* 9**:** 9229-9240, 2013.

132. Martinez, FO, Gordon, S, Locati, M, Mantovani, A: Transcriptional profiling of the human monocyte-to-macrophage differentiation and polarization: new molecules and patterns of gene expression. *J Immunol,* 177**:** 7303-7311, 2006.

133. McWhorter, FY, Wang, T, Nguyen, P, Chung, T, Liu, WF: Modulation of macrophage phenotype by cell shape. *Proc Natl Acad Sci U S A,* 110**:** 17253-17258, 2013.

134. Hume, DA, MacDonald, KPA: Therapeutic applications of macrophage colony-stimulating factor-1 (CSF-1) and antagonists of CSF-1 receptor (CSF-1R) signaling. *Blood,* 119**:** 1810-1820, 2012.

135. Xu, JW, Konttinen, YT, Waris, V, Patiala, H, Sorsa, T, Santavirta, S: Macrophage-colony stimulating factor (M-CSF) is increased in the synovial-like membrane of the periprosthetic tissues in the aseptic loosening of total hip replacement (THR). *Clinical rheumatology,* 16**:** 243-248, 1997.

136. Proost, P, Wuyts, A, Van Damme, J: Human monocyte chemotactic proteins-2 and -3: structural and functional comparison with MCP-1. *J Leukoc Biol,* 59**:** 67-74, 1996.

137. Zlotnik, A, Yoshie, O: The Chemokine Superfamily Revisited. *Immunity,* 36**:** 705-716, 2012.

138. Jones, JA, Chang, DT, Meyerson, H, Colton, E, Kwon, IK, Matsuda, T, Anderson, JM: Proteomic analysis and quantification of cytokines and chemokines from biomaterial surface-adherent macrophages and foreign body giant cells. *J Biomed Mater Res A,* 83**:** 585-596, 2007.

139. Islam, SA, Ling, MF, Leung, J, Shreffler, WG, Luster, AD: Identification of human CCR8 as a CCL18 receptor. *The Journal of Experimental Medicine,* 210**:** 1889-1898, 2013.

140. Patel, VP, Kreider, BL, Li, Y, Li, H, Leung, K, Salcedo, T, Nardelli, B, Pippalla, V, Gentz, S, Thotakura, R, Parmelee, D, Gentz, R, Garotta, G: Molecular and functional characterization of two novel human C-C chemokines as inhibitors of two distinct classes of myeloid progenitors. *J Exp Med,* 185**:** 1163-1172, 1997.

141. Votta, BJ, White, JR, Dodds, RA, James, IE, Connor, JR, Elizabeth, Lee, R, Eichman, CF, Kumar, S, Lark, MW, Gowen, M: CKβ-8 [CCL23], a novel CC chemokine, is chemotactic for human osteoclast precursors and is expressed in bone tissues. *Journal of Cellular Physiology,* 183**:** 196-207, 2000.

142. Pan, G, Bauer, JH, Haridas, V, Wang, S, Liu, D, Yu, G, Vincenz, C, Aggarwal, BB, Ni, J, Dixit, VM: Identification and functional characterization of DR6, a novel death domain-containing TNF receptor. *FEBS Letters,* 431**:** 351-356, 1998.

143. Edwards, JR, Sun, SG, Locklin, R, Shipman, CM, Adamopoulos, IE, Athanasou, NA, Sabokbar, A: LIGHT (TNFSF14), a novel mediator of bone resorption, is elevated in rheumatoid arthritis. *Arthritis and rheumatism,* 54**:** 1451-1462, 2006.

144. Gaffney, J, Solomonov, I, Zehorai, E, Sagi, I: Multilevel regulation of matrix metalloproteinases in tissue homeostasis indicates their molecular specificity in vivo. *Matrix Biol,* 44-46**:** 191-199, 2015.
145. Nissinen, L, Kahari, VM: Matrix metalloproteinases in inflammation. *Biochim Biophys Acta,* 1840**:** 2571-2580, 2014.
146. Sbardella, D, Fasciglione, GF, Gioia, M, Ciaccio, C, Tundo, GR, Marini, S, Coletta, M: Human matrix metalloproteinases: an ubiquitarian class of enzymes involved in several pathological processes. *Mol Aspects Med,* 33**:** 119-208, 2012.
147. Santos, MC, Campos, MI, Souza, AP, Trevilatto, PC, Line, SR: Analysis of MMP-1 and MMP-9 promoter polymorphisms in early osseointegrated implant failure. *Int J Oral Maxillofac Implants,* 19**:** 38-43, 2004.
148. Thalji, GN, Nares, S, Cooper, LF: Early molecular assessment of osseointegration in humans. *Clin Oral Implants Res,* 25**:** 1273-1285, 2014.
149. Matthews, JB, Besong, AA, Green, TR, Stone, MH, Wroblewski, BM, Fisher, J, Ingham, E: Evaluation of the response of primary human peripheral blood mononuclear phagocytes to challenge with in vitro generated clinically relevant UHMWPE particles of known size and dose. *Journal of biomedical materials research,* 52**:** 296-307, 2000.
150. Kusaka, T, Nakayama, M, Nakamura, K, Ishimiya, M, Furusawa, E, Ogasawara, K: Effect of Silica Particle Size on Macrophage Inflammatory Responses. *PLOS ONE,* 9**:** e92634, 2014.
151. Glant, TT, Jacobs, JJ, Molnar, G, Shanbhag, AS, Valyon, M, Galante, JO: Bone resorption activity of particulate-stimulated macrophages. *Journal of bone and mineral research : the official journal of the American Society for Bone and Mineral Research,* 8**:** 1071-1079, 1993.
152. Beckmann, NA, Mueller, S, Gondan, M, Jaeger, S, Reiner, T, Bitsch, RG: Treatment of severe bone defects during revision total knee arthroplasty with structural allografts and porous metal cones-a systematic review. *J Arthroplasty,* 30**:** 249-253, 2015.
153. Makela, KT, Matilainen, M, Pulkkinen, P, Fenstad, AM, Havelin, L, Engesaeter, L, Furnes, O, Pedersen, AB, Overgaard, S, Karrholm, J, Malchau, H, Garellick, G, Ranstam, J, Eskelinen, A: Failure rate of cemented and uncemented total hip replacements: register study of combined Nordic database of four nations. *BMJ,* 348**:** f7592, 2014.
154. Ribeiro, M, Monteiro, FJ, Ferraz, MP: Infection of orthopedic implants with emphasis on bacterial adhesion process and techniques used in studying bacterial-material interactions. *Biomatter,* 2**:** 176-194, 2012.
155. Pye, AD, Lockhart, DE, Dawson, MP, Murray, CA, Smith, AJ: A review of dental implants and infection. *The Journal of hospital infection,* 72**:** 104-110, 2009.
156. Fournier, B, Philpott, DJ: Recognition of Staphylococcus aureus by the innate immune system. *Clinical microbiology reviews,* 18**:** 521-540, 2005.
157. Juarez, E, Nunez, C, Sada, E, Ellner, JJ, Schwander, SK, Torres, M: Differential expression of Toll-like receptors on human alveolar macrophages and autologous peripheral monocytes. *Respiratory research,* 11**:** 2, 2010.
158. Gebbia, JA, Coleman, JL, Benach, JL: Selective induction of matrix metalloproteinases by Borrelia burgdorferi via toll-like receptor 2 in monocytes. *The Journal of infectious diseases,* 189**:** 113-119, 2004.
159. Franco, GC, Kajiya, M, Nakanishi, T, Ohta, K, Rosalen, PL, Groppo, FC, Ernst, CW, Boyesen, JL, Bartlett, JD, Stashenko, P, Taubman, MA, Kawai, T: Inhibition of matrix metalloproteinase-9 activity by doxycycline ameliorates

RANK ligand-induced osteoclast differentiation in vitro and in vivo. *Exp Cell Res,* 317**:** 1454-1464, 2011.

160. Lynch, CC, Hikosaka, A, Acuff, HB, Martin, MD, Kawai, N, Singh, RK, Vargo-Gogola, TC, Begtrup, JL, Peterson, TE, Fingleton, B, Shirai, T, Matrisian, LM, Futakuchi, M: MMP-7 promotes prostate cancer-induced osteolysis via the solubilization of RANKL. *Cancer cell,* 7**:** 485-496, 2005.

161. Takei, I, Takagi, M, Santavirta, S, Ida, H, Ishii, M, Ogino, T, Ainola, M, Konttinen, YT: Messenger ribonucleic acid expression of 16 matrix metalloproteinases in bone-implant interface tissues of loose artificial hip joints. *Journal of biomedical materials research,* 52**:** 613-620, 2000.

162. Valentine-Thon, E, Muller, K, Guzzi, G, Kreisel, S, Ohnsorge, P, Sandkamp, M: LTT-MELISA is clinically relevant for detecting and monitoring metal sensitivity. *Neuro endocrinology letters,* 27 Suppl 1**:** 17-24, 2006.

163. Chang, DT, Colton, E, Anderson, JM: Paracrine and juxtacrine lymphocyte enhancement of adherent macrophage and foreign body giant cell activation. *J Biomed Mater Res A,* 89**:** 490-498, 2009.

164. Zhu, P, Ding, J, Zhou, J, Dong, W-J, Fan, C-M, Chen, Z-N: Expression of CD147 on monocytes/macrophages in rheumatoid arthritis: its potential role in monocyte accumulation and matrix metalloproteinase production. *Arthritis Research & Therapy,* 7**:** R1023-R1033, 2005.

165. Dreier, R, Wallace, S, Fuchs, S, Bruckner, P, Grassel, S: Paracrine interactions of chondrocytes and macrophages in cartilage degradation: articular chondrocytes provide factors that activate macrophage-derived pro-gelatinase B (pro-MMP-9). *Journal of cell science,* 114**:** 3813-3822, 2001.

166. Shubayev, VI, Branemark, R, Steinauer, J, Myers, RR: Titanium implants induce expression of matrix metalloproteinases in bone during osseointegration. *Journal of rehabilitation research and development,* 41**:** 757-766, 2004.

167. Moraschini, V, Poubel, LA, Ferreira, VF, Barboza Edos, S: Evaluation of survival and success rates of dental implants reported in longitudinal studies with a follow-up period of at least 10 years: a systematic review. *International journal of oral and maxillofacial surgery,* 44**:** 377-388, 2015.

168. Whitney, AR, Diehn, M, Popper, SJ, Alizadeh, AA, Boldrick, JC, Relman, DA, Brown, PO: Individuality and variation in gene expression patterns in human blood. *Proc Natl Acad Sci U S A,* 100**:** 1896-1901, 2003.

169. Cassinelli, C, Morra, M, Pavesio, A, Renier, D: Evaluation of interfacial properties of hyaluronan coated poly(methylmethacrylate) intraocular lenses. *Journal of biomaterials science Polymer edition,* 11**:** 961-977, 2000.

7 CURRICULUM VITAE

PERSONAL DETAILS

Name and Surname:	Alexandru Gudima
Date of birth:	27.09.1986
Place of birth:	Chișinău, Republic of Moldova
Family status:	Married
Father:	Alexandru Gudima
Mother:	Elena Gudima

EDUCATIONAL BACKGROUND

(1997) – (2005)	"Mircea Eliade" lyceum, Chişinău,
(07.06.2005)	Degree: Diploma of Baccalaureate. Grade: 9.25.

UNIVERSITY BACKGROUND

2005 – 2011	Study at the State Medical and Pharmaceutical University "Nicolae Testemițanu" of the Republic of Moldova, faculty of General Medicine
11.06.11	Diploma of Higher Education
2011 – 2012	Internship in the Oncology Department at the State University of Medicine and Pharmacy "Nicolae Testemițanu" of the Republic of Moldova
2012 – 2013	Ruprecht–Karls University of Heidelberg, Germany Medical Faculty Mannheim Major: Translational medical research
04.09.13	Degree: Master of Science. Grade: 1.3.
2013 – present	Post-graduate study at Ruprecht–Karls University of Heidelberg, Germany Medical Faculty Mannheim

8   ACKNOWLEDGEMENTS